Volume 25, Number 6, 2025 ISSN 1562-8353

NONLINEAR DYNAMICS AND SYSTEMS THEORY
An International Journal of Research and Surveys

Volume 25 Number 6 2025

CONTENTS

 ISSN 1562-8353 Printed in Ukraine
To receive contents and abstracts by e-mail, visit our Website at: **http://www.e-ndst.kiev.ua**

NONLINEAR DYNAMICS & SYSTEMS THEORY

Volume 25, No. 6, 2025

Nonlinear Dynamics and Systems Theory

An International Journal of Research and Surveys

InforMath Publishing Group
http://www.e-ndst.kiev.ua

Nonlinear Dynamics and Systems Theory

An International Journal of Research and Surveys

INSTRUCTIONS FOR CONTRIBUTORS

(1) General. Nonlinear Dynamics and Systems Theory (ND&ST) is an international journal devoted to publishing peer-refereed, high quality, original papers, brief notes and review articles focusing on nonlinear dynamics and systems theory and their practical applications in engineering, physical and life sciences. Submission of a manuscript is a representation that the submission has been approved by all of the authors and by the institution where the work was carried out. It also represents that the manuscript has not been previously published, has not been copyrighted, is not being submitted for publication elsewhere, and that the authors have agreed that the copyright in the article shall be assigned exclusively to InforMath Publishing Group by signing a transfer of copyright form. Before submission, the authors should visit the website:

http://www.e-ndst.kiev.ua

for information on the preparation of accepted manuscripts. Please download the archive Sample_NDST.zip containing example of article file (you can edit only the file Samplefilename.tex).

(2) Manuscript and Correspondence. Manuscripts should be in English and must meet common standards of usage and grammar. To submit a paper, send by e-mail a file in PDF format directly to

Professor A.A. Martynyuk, Institute of Mechanics,
Nesterov str.3, 03057, Kiev-57, Ukraine
e-mail: journalndst@gmail.com

or to one of the Regional Editors or to a member of the Editorial Board. Final version of the manuscript must typeset using LaTex program which is prepared in accordance with the style file of the Journal. Manuscript texts should contain the title of the article, name(s) of the author(s) and complete affiliations. Each article requires an abstract not exceeding 150 words. Formulas and citations should not be included in the abstract. AMS subject classifications and key words must be included in all accepted papers. Each article requires a running head (abbreviated form of the title) of no more than 30 characters. The sizes for regular papers, survey articles, brief notes, letters to editors and book reviews are: (i) 10-14 pages for regular papers, (ii) up to 24 pages for survey articles, and (iii) 2-3 pages for brief notes, letters to the editor and book reviews.

(3) Tables, Graphs and Illustrations. Each figure must be of a quality suitable for direct reproduction and must include a caption. Drawings should include all relevant details and should be drawn professionally in black ink on plain white drawing paper. In addition to a hard copy of the artwork, it is necessary to attach the electronic file of the artwork (preferably in PCX format).

(4) References. Each entry must be cited in the text by author(s) and number or by number alone. All references should be listed in their alphabetic order. Use please the following style:

Journal: [1] H. Poincare, Title of the article. *Title of the Journal* **volume** (issue) (year) pages. [Language]

Book: [2] A.M. Lyapunov, *Title of the Book.* Name of the Publishers, Town, year.

Proceeding: [3] R. Bellman, Title of the article. In: *Title of the Book.* (Eds.). Name of the Publishers, Town, year, pages. [Language]

(5) Proofs and Sample Copy. Proofs sent to authors should be returned to the Editorial Office with corrections within three days after receipt. The corresponding author will receive a sample copy of the issue of the Journal for which his/her paper is published.

(6) Editorial Policy. Every submission will undergo a stringent peer review process. An editor will be assigned to handle the review process of the paper. He/she will secure at least two reviewers' reports. The decision on acceptance, rejection or acceptance subject to revision will be made based on these reviewers' reports and the editor's own reading of the paper.

NONLINEAR DYNAMICS AND SYSTEMS THEORY
An International Journal of Research and Surveys
Published by InforMath Publishing Group since 2001

Volume 25 Number 6 2025

CONTENTS

Founded by A.A. Martynyuk in 2001.
Registered in Ukraine Number: KB No 5267 / 04.07.2001.

NONLINEAR DYNAMICS AND SYSTEMS THEORY

An International Journal of Research and Surveys

Impact Factor from SCOPUS for 2024: SJR – 0.262, SNIP – 1.098 and CiteScore – 1.5

Nonlinear Dynamics and Systems Theory (ISSN 1562–8353 (Print), ISSN 1813–7385 (Online)) is an international journal published under the auspices of the S.P. Timoshenko Institute of Mechanics of National Academy of Sciences of Ukraine and Curtin University of Technology (Perth, Australia). It aims to publish high quality original scientific papers and surveys in areas of nonlinear dynamics and systems theory and their real world applications.

AIMS AND SCOPE

Nonlinear Dynamics and Systems Theory is a multidisciplinary journal. It publishes papers focusing on proofs of important theorems as well as papers presenting new ideas and new theory, conjectures, numerical algorithms and physical experiments in areas related to nonlinear dynamics and systems theory. Papers that deal with theoretical aspects of nonlinear dynamics and/or systems theory should contain significant mathematical results with an indication of their possible applications. Papers that emphasize applications should contain new mathematical models of real world phenomena and/or description of engineering problems. They should include rigorous analysis of data used and results obtained. Papers that integrate and interrelate ideas and methods of nonlinear dynamics and systems theory will be particularly welcomed.

PUBLICATION AND SUBSCRIPTION INFORMATION

Nonlinear Dynamics and Systems Theory will have 6 issues in 2025, printed in hard copy (ISSN 1562–8353) and available online (ISSN 1813–7385), by InforMath Publishing Group, Nesterov str., 3, Institute of Mechanics, Kiev, MSP 680, Ukraine, 03057. Subscription prices are available upon request from the Publisher, EBSCO Information Services (`mailto:journals@ebsco.com`), or website of the Journal: `http://e-ndst.kiev.ua`. Subscriptions are accepted on a calendar year basis. Issues are sent by airmail to all countries of the world. Claims for missing issues should be made within six months of the date of dispatch.

ABSTRACTING AND INDEXING SERVICES

Papers published in this journal are indexed or abstracted in: Mathematical Reviews / MathSciNet, Zentralblatt MATH / Mathematics Abstracts, PASCAL database (INIST–CNRS) and SCOPUS.

Nonlinear Dynamics and Systems Theory, **25** (6) (2025) 585–595

Solvability of Functional Equations' Classes Arising in Dynamic Programming Using Fixed-Point Technique

Ahlem Achichi [1], Iqbal M. Batiha [2,3,*], Leila Benaoua [1], Taki-Eddine Oussaeif [1], Nidal Anakira [4] and Tala Sasa [5]

[1] *Department of Mathematics and Informatics, Dynamic and Control Systems Laboratory, Oum El Bouaghi University, Algeria.*
[2] *Department of Mathematics, Al Zaytoonah University of Jordan, Amman 11733, Jordan.*
[3] *Nonlinear Dynamics Research Center (NDRC), Ajman University, Ajman 346, UAE.*
[4] *Faculty of Education and Arts, Sohar University, Sohar 3111, Oman.*
[5] *Applied Science Research Center, Applied Science Private University, Amman, Jordan.*

Received: February 6, 2025; Revised: November 2, 2025

Abstract: This paper is devoted to the existence, uniqueness, and iterative approximation of solutions for the classes of functional equations arising in dynamic programming of multistage decision processes. The findings presented here extend and integrate several results from the existing literature. Illustrative examples are also provided to emphasize the significance of the main results. The approach is based on fixed point techniques applied in suitable function spaces. Furthermore, our results unify a variety of known theorems within a broader and more flexible framework.

Keywords: *functional equations; dynamic programming; fixed point; iterative approximation.*

Mathematics Subject Classification (2020): 70K20, 70K30, 93C10.

1 Introduction

In 1922, Banach [1] proved his celebrated fixed point theorem, commonly known as the Banach contraction principle. Bellman [2, 3] introduced and explored the existence of solutions for a class of functional equations arising in dynamic programming. Since then, many researchers (see [4–11]) have studied the existence and uniqueness of solutions to functional equations by modifying the conditions of Bellman's equations in the context of multistage decision processes.

* Corresponding author: mailto:i.batiha@zuj.edu.jo

Recent advances in the study of functional equations, fractional differential models, and fixed point theory have led to significant developments in both theory and applications across various mathematical and engineering domains. In particular, methods for solving Volterra-type and fractional integro-differential equations have been extensively developed using novel decomposition and numerical strategies [12–14]. Parallel to this, fixed point techniques in generalized metric spaces have emerged as powerful tools for addressing nonlinear problems in functional analysis and dynamic systems [15–17]. These tools have found fruitful applications in the analysis of reaction-diffusion systems, blow-up phenomena, and inverse problems under integral constraints [18–24]. Building on this growing body of work, our paper aims to explore the solvability of functional equations arising in dynamic programming by applying fixed point techniques in suitable function spaces.

In this work, we present and analyze the existence, uniqueness, and iterative approximation of solutions for the following classes of functional equations and systems of functional equations arising in dynamic programming:

$$f(x) = \operatorname{opt}_{y\in D} \left\{u(x, y) + \operatorname{opt} \left\{p_i(x, y) + A_i(x, y, f(a_i(x, y))) : i = 1, 2, 3\right\}\right\}, \tag{1}$$

$$\begin{aligned} f(x) = \operatorname{opt}_{y\in D}\big\{&u(x, y) + r(x, y)f(c(x, y)) + \operatorname{opt}\{p_i(x, y)f(s(x, y)),\\ &t_i(x, y) + q_i(x, y)A_i(x, y, f(a_i(x, y))) : i = 1, 2, 3\}\big\}, \end{aligned} \tag{2}$$

$$f(x) = \operatorname{opt}_{y\in D} \left\{p(x, y) + \operatorname{opt} \left\{u_i(x, y) + A_i(x, y, g(a_i(x, y))) : i = 1, 2, 3\right\}\right\}, \tag{3a}$$

$$f(x) = \operatorname{opt}_{y\in D} \left\{q(x, y) + \operatorname{opt} \left\{v_i(x, y) + B_i(x, y, f(b_i(x, y))) : i = 1, 2, 3\right\}\right\}. \tag{3b}$$

Here, opt denotes either sup or inf. The variables x and y represent the state and decision vectors, respectively. The mappings s, c, and a_i $(i = 1, 2, 3)$ denote process transformations, and the functions $f(x)$ and $g(x)$ represent the optimal return functions with initial state x.

The structure of this paper is as follows. In Section 2, we introduce basic concepts, notations, and useful lemmas. In Section 3, we establish the existence, uniqueness, and iterative approximation of solutions to functional equation (1) in the spaces $BC(S)$ and $B(S)$.

2 Preliminaries

In this section, we introduce notations, definitions, and some preliminary results that will be used in the remainder of the paper. Let $\mathbb{R} = (-\infty, +\infty)$, $\mathbb{R}^+ = [0, \infty)$, and $\mathbb{R}^- = (-\infty, 0]$. For every $t \in \mathbb{R}$, let $[t]$ denote the greatest integer less than or equal to t. Let $(X, \|\cdot\|)$ and $(Y, \|\cdot\|')$ be real Banach spaces. Let $S \subseteq X$ denote the state space and $D \subseteq Y$ denote the decision space. We define the following function classes:

$$\begin{aligned}
\Phi_1 &= \left\{\varphi : \mathbb{R}^+ \to \mathbb{R}^+ \mid \varphi \text{ is right-continuous at } t = 0\right\},\\
\Phi_2 &= \left\{\varphi : \mathbb{R}^+ \to \mathbb{R}^+ \mid \varphi \text{ is non-decreasing}\right\},\\
\Phi_3 &= \left\{\varphi \in \Phi_1 \mid \varphi(0) = 0\right\},\\
\Phi_4 &= \left\{\varphi \in \Phi_1 \cap \Phi_2 \mid \varphi(t) < t \text{ for all } t > 0\right\},\\
\Phi_5 &= \left\{\varphi \in \Phi_2 \mid \varphi(t) < t \text{ for all } t > 0\right\}.
\end{aligned}$$

We also define the following function spaces:

$$\begin{aligned} B(S) &= \{f : S \to \mathbb{R} \mid f \text{ is bounded}\}, \\ BC(S) &= \{f \in B(S) \mid f \text{ is continuous}\}, \\ BB(S) &= \{f : S \to \mathbb{R} \mid f \text{ is bounded on bounded subsets of } S\}. \end{aligned}$$

It is easy to verify that both $(B(S), \|\cdot\|_1)$ and $(BC(S), \|\cdot\|_1)$ are Banach spaces under the supremum norm $\|f\|_1 = \sup_{x\in S} |f(x)|$. For every positive integer k and for $f, g \in BB(S)$, define the pseudometric

$$d_k(f, g) = \sup\left\{|f(x) - g(x)| : x \in \overline{B}(0, k)\right\},$$

where $\overline{B}(0, k) = \{x \in S : \|x\| \le k\}$. We then define a complete metric d on $BB(S)$ by

$$d(f, g) = \sum_{k=1}^{\infty} \frac{1}{2^k} \cdot \frac{d_k(f, g)}{1 + d_k(f, g)}.$$

The collection $\{d_k\}_{k\ge1}$ forms a countable family of pseudometrics on $BB(S)$. A sequence $\{f_n\} \subseteq BB(S)$ is said to converge to $f \in BB(S)$ if for every $k \in \mathbb{N}$, we have $d_k(f_n, f_m) \to 0$ as $n, m \to \infty$. Therefore, $(BB(S), d)$ is a complete metric space.

Definition 2.1 A metric space (M, ρ) is said to be *metrically convex* if for any $x, y \in M$, there exists $z \in M$, with $z \neq x, y$, such that $\rho(x, y) = \rho(x, z) + \rho(z, y)$. Intuitively, every Banach space is metrically convex.

Lemma 2.1 (Menger [5]) *If M is a complete metrically convex metric space, then for every $\alpha \in (0, 1)$ and for any $x, y \in M$, there exists $z \in M$ such that $\rho(x, z) = \alpha\rho(x, y)$ and $\rho(z, y) = (1 - \alpha)\rho(x, y)$.*

Lemma 2.2 ([5]) *Assume that M is a complete metrically convex metric space and that $f : M \to M$ is a mapping satisfying*

$$\rho(fx, fy) \le K\rho(x, y) \tag{4}$$

for some constant $K < \infty$. Define the function $\phi : [0, b) \to [0, b)$ by

$$\phi(t) = \sup\{\rho(fx, fy) : x, y \in M,\ \rho(x, y) = t\}.$$

Then we have

(a) ϕ is subadditive; that is, for all $s, t > 0$ such that $s + t < b$, we have

$$\phi(s + t) \le \phi(s) + \phi(t).$$

(b) ϕ is upper semicontinuous from the right on $[0, b)$.

Proof. (a) Let $x, y \in M$ with $\rho(x, y) = s + t$. Since M is metrically convex, there exists $z \in M$ such that $\rho(x, z) = s$ and $\rho(z, y) = t$. Then

$$\rho(fx, fy) \le \rho(fx, fz) + \rho(fz, fy) \le \phi(s) + \phi(t). \quad \Diamond$$

Taking the supremum over all such $x, y \in M$ with $\rho(x,y) = s+t$ gives the result in (a).

(b) From part (a), for $t > t_0$ and $t - t_0 < b$, we have

$$\phi(t) \leq \phi(t-t_0) + \phi(t_0) \leq K(t-t_0) + \phi(t_0)$$

since $\phi(t-t_0) \leq K(t-t_0)$ by the assumption in equation (4). Therefore,

$$\limsup_{t \to t_0^+} \phi(t) \leq \phi(t_0),$$

proving that ϕ is upper semicontinuous from the right at t_0.

Lemma 2.3 *Let M be a complete metric space, and let $f : M \to M$ be a mapping satisfying*

$$\rho(fx, fy) \leq \varphi\left(\rho(x,y)\right), \tag{5}$$

where $\varphi : \overline{P} \to \mathbb{R}^+$ is upper semicontinuous from the right on $\overline{P}$ and satisfies $\varphi(t) < t$ for all $t \in \overline{P} \setminus \{0\}$. Then f has a unique fixed point $x_0 \in M$, and for all $x \in M$, the sequence $f^n x \to x_0$ as $n \to \infty$.

Proof. Fix $x \in M$ and define $c_n = \rho(f^n x, f^{n-1}x)$. From the contractive condition, we have

$$c_{n+1} = \rho(f^{n+1}x, f^n x) = \rho(f(f^n x), f(f^{n-1}x)) \leq \varphi(c_n),$$

which implies that $\{c_n\}$ is a decreasing sequence. Since $\varphi(t) < t$ for all $t > 0$, the sequence must converge to a limit $c \geq 0$. Assume, by contradiction, that $c > 0$. Then, taking limits, we get

$$c = \lim_{n \to \infty} c_n \leq \limsup_{t \to c^+} \varphi(t) \leq \varphi(c),$$

which contradicts $\varphi(c) < c$. Therefore, $c = 0$. Next, we show that $\{f^n x\}$ is a Cauchy sequence. Suppose not. Then there exist $\varepsilon > 0$ and sequences $\{m_k\}$, $\{n_k\}$ with $m_k > n_k \geq k$ such that

$$d_k := \rho(f^{m_k}x, f^{n_k}x) \geq \varepsilon \quad \text{for all } k \in \mathbb{N}.$$

Choose m_k as the smallest index greater than n_k such that this holds. Since $c_n \to 0$, we may assume

$$\rho(f^{m_k - 1}x, f^{n_k}x) < \varepsilon.$$

Then

$$d_k \leq \rho(f^{m_k}x, f^{m_k-1}x) + \rho(f^{m_k-1}x, f^{n_k}x) \leq c_{m_k} + \varepsilon.$$

Thus, $d_k \to \varepsilon^+$ as $k \to \infty$. However, consider

$$\begin{aligned} d_k &= \rho(f^{m_k}x, f^{n_k}x) \\ &\leq \rho(f^{m_k}x, f^{m_k+1}x) + \rho(f^{m_k+1}x, f^{n_k+1}x) + \rho(f^{n_k+1}x, f^{n_k}x) \\ &\leq c_{m_k+1} + c_{n_k+1} + \varphi(d_k) \leq 2c_k + \varphi(d_k). \end{aligned}$$

Taking the limit as $k \to \infty$, we obtain

$$\varepsilon \leq \varphi(\varepsilon),$$

which contradicts $\varphi(\varepsilon) < \varepsilon$ for $\varepsilon > 0$. Hence, $\{f^n x\}$ is a Cauchy sequence. By the completeness of M, there exists a limit point $x_0 \in M$ such that $f^n x \to x_0$. Since f is continuous (implied by the inequality and structure of the argument), we have

$$fx_0 = \lim_{n\to\infty} f(f^n x) = \lim_{n\to\infty} f^{n+1}x = x_0,$$

so x_0 is a fixed point of f. To prove uniqueness, suppose x_0 and x_1 are both fixed points. Then

$$\rho(x_0, x_1) = \rho(fx_0, fx_1) \le \varphi(\rho(x_0, x_1)) < \rho(x_0, x_1),$$

which is a contradiction unless $\rho(x_0, x_1) = 0$, hence $x_0 = x_1$.

Lemma 2.4 ([5]) *Let (M, ρ) be a complete metrically convex metric space, and let $f : M \to M$ be a mapping satisfying*

$$\rho(fx, fy) \le \varphi\left(\rho(x, y)\right) \quad \textit{for all } x, y \in M, \tag{6}$$

where $\varphi : \overline{P} \to \mathbb{R}^+$ is a function such that $\varphi(t) < t$ for all $t \in \overline{P} \setminus \{0\}$, with $P = \{\rho(x, y) : x, y \in M\}$ and $\overline{P}$ being its closure. Then f has a unique fixed point $u \in M$, and for every $x \in M$, we have

$$\lim_{n\to\infty} f^n(x) = u.$$

Proof. Let $\phi : [0, b) \to [0, b)$ be defined as in Lemma 2.2:

$$\phi(t) = \sup\{\rho(fx, fy) : x, y \in M,\ \rho(x, y) = t\}.$$

By Lemma 2.2, ϕ is upper semicontinuous from the right on $[0, b)$. Furthermore, for all $t \in [0, b)$,

$$\phi(t) \le \varphi(t).$$

If $P = [0, b]$ with $b < \infty$, we extend ϕ by defining $\phi(b) := \varphi(b)$. Then we have

$$\rho(fx, fy) \le \phi\left(\rho(x, y)\right) \quad \text{for all } x, y \in M.$$

Now, since ϕ is upper semicontinuous from the right and satisfies $\phi(t) < t$ for $t > 0$, the conditions of Lemma 2.1 (the generalized fixed point theorem) are satisfied for ϕ. Hence, f has a unique fixed point $u \in M$, and the sequence $\{f^n(x)\}$ converges to u for every $x \in M$.

Lemma 2.5 ([8]) *Let $\{a_i, b_i : 1 \le i \le n\} \subseteq \mathbb{R}$. Then*

$$|\text{opt}\{a_i : 1 \le i \le n\} - \text{opt}\{b_i : 1 \le i \le n\}| \le \max\left\{|a_i - b_i| : 1 \le i \le n\right\}. \tag{$*$}$$

Here, opt *denotes either the supremum or infimum.*

Proof. The inequality clearly holds for $n = 1$. Assume that $(*)$ holds for some $n \in \mathbb{N}$. Consider the case $n + 1$:

$$\text{opt}\{a_i : 1 \le i \le n+1\} = \text{opt}\left\{\text{opt}\{a_i : 1 \le i \le n\},\ a_{n+1}\right\},$$

and similarly for the b_i's. Using the inductive hypothesis and Lemma 2.1 from [9], we obtain

$$\begin{aligned}
&|\text{opt}\{a_i : 1 \le i \le n+1\} - \text{opt}\{b_i : 1 \le i \le n+1\}| \\
&\quad \le \max\left\{|\text{opt}\{a_i : 1 \le i \le n\} - \text{opt}\{b_i : 1 \le i \le n\}|, |a_{n+1} - b_{n+1}|\right\} \\
&\quad \le \max\left\{|a_i - b_i| : 1 \le i \le n+1\right\}.
\end{aligned}$$

Hence, by induction, the inequality holds for all $n \in \mathbb{N}$.

Lemma 2.6 *Let $a_i, b_i \in \mathbb{R}$ for $i = 1, 2, 3$. Then*

$$\max\{|a_i + b_i| : i = 1, 2, 3\} \leq \max\{|a_i| : i = 1, 2, 3\} + \max\{|b_i| : i = 1, 2, 3\}.$$

Proof. By the triangle inequality, we have for each $i = 1, 2, 3$:

$$|a_i + b_i| \leq |a_i| + |b_i|.$$

Taking the maximum over i, we obtain

$$\max\{|a_i + b_i| : i = 1, 2, 3\} \leq \max\{|a_i| + |b_i| : i = 1, 2, 3\}.$$

Finally, since for each i,

$$|a_i| + |b_i| \leq \max\{|a_i| : i = 1, 2, 3\} + \max\{|b_i| : i = 1, 2, 3\},$$

we conclude

$$\max\{|a_i + b_i| : i = 1, 2, 3\} \leq \max\{|a_i| : i = 1, 2, 3\} + \max\{|b_i| : i = 1, 2, 3\}.$$

Lemma 2.7 *[8]*

(i) Let $A : S \times D \to \mathbb{R}$ be a mapping such that $\mathrm{opt}_{y\in D} A(x_0, y)$ is bounded for some $x_0 \in S$. Then

$$\left|\mathrm{opt}_{y\in D} A(x_0, y)\right| \leq \sup_{y\in D} |A(x_0, y)|.$$

(ii) Let $A, B : S \times D \to \mathbb{R}$ be mappings such that both $\mathrm{opt}_{y\in D} A(x_1, y)$ and $\mathrm{opt}_{y\in D} B(x_2, y)$ are bounded for some $x_1, x_2 \in S$. Then

$$\left|\mathrm{opt}_{y\in D} A(x_1, y) - \mathrm{opt}_{y\in D} B(x_2, y)\right| \leq \sup_{y\in D} |A(x_1, y) - B(x_2, y)|.$$

Proof. **(i)** If $\sup_{y\in D} |A(x_0, y)| = +\infty$, the inequality holds trivially. Otherwise, assume $\sup_{y\in D} |A(x_0, y)| < \infty$. Then, for all $y \in D$,

$$-|A(x_0, y)| \leq A(x_0, y) \leq |A(x_0, y)|.$$

Taking the infimum and supremum over $y \in D$, we obtain

$$\inf_{y\in D} A(x_0, y) \geq -\sup_{y\in D} |A(x_0, y)|, \quad \sup_{y\in D} A(x_0, y) \leq \sup_{y\in D} |A(x_0, y)|.$$

Hence,

$$\left|\mathrm{opt}_{y\in D} A(x_0, y)\right| \leq \sup_{y\in D} |A(x_0, y)|.$$

(ii) If $\sup_{y\in D} |A(x_1, y) - B(x_2, y)| = +\infty$, the inequality holds trivially. Otherwise, for all $y \in D$,

$$|A(x_1, y) - B(x_2, y)| \leq \sup_{y\in D} |A(x_1, y) - B(x_2, y)|.$$

Thus,

$$B(x_2, y) - \sup_{y\in D} |A(x_1, y) - B(x_2, y)| \leq A(x_1, y) \leq B(x_2, y) + \sup_{y\in D} |A(x_1, y) - B(x_2, y)|.$$

Taking $\mathrm{opt}_{y\in D}$ on both sides yields

$$\left|\mathrm{opt}_{y\in D} A(x_1, y) - \mathrm{opt}_{y\in D} B(x_2, y)\right| \leq \sup_{y\in D} |A(x_1, y) - B(x_2, y)|.$$

3 Existence and Uniqueness of Solutions in $BC(S)$ and $B(S)$

We now discuss the existence and uniqueness of solutions to the functional equation (1) in the spaces $BC(S)$ and $B(S)$.

Theorem 3.1 *Let $u, p_i : S \times D \to \mathbb{R}$, $a_i : S \times D \to S$, and $A_i : S \times D \times \mathbb{R} \to \mathbb{R}$ for $i = 1, 2, 3$ be given mappings. Let $\varphi \in \Phi_3$ and $\psi \in \Phi_4$. Assume the following conditions hold:*

(C1) *The mappings u, p_i, and A_i are bounded for each $i = 1, 2, 3$.*

(C2) *For every $x_0 \in S$, the limits*

$$u(x, y) \to u(x_0, y), \quad p_i(x, y) \to p_i(x_0, y), \quad a_i(x, y) \to a_i(x_0, y)$$

hold uniformly for $y \in D$ as $x \to x_0$, for all $i = 1, 2, 3$.

(C3) *For all $x, x_0 \in S$, $y \in D$, and $z \in \mathbb{R}$,*

$$\max\left\{|A_i(x, y, z) - A_i(x_0, y, z)| : i = 1, 2, 3\right\} \le \varphi\left(\|x - x_0\|\right).$$

(C4) *For all $x \in S$, $y \in D$, and $z, z_0 \in \mathbb{R}$,*

$$\max\left\{|A_i(x, y, z) - A_i(x, y, z_0)| : i = 1, 2, 3\right\} \le \psi\left(\|z - z_0\|\right).$$

Then the functional equation (1) admits a unique solution $w \in BC(S)$, and for every $h \in BC(S)$, the sequence $\{H^n h\}_{n\ge1}$ converges to w, where the operator $H : BC(S) \to BC(S)$ is defined by

$$Hh(x) = \mathrm{opt}_{y\in D}\left\{u(x, y) + \mathrm{opt}\left\{p_i(x, y) + A_i(x, y, h(a_i(x, y))) : i = 1, 2, 3\right\}\right\}, \; x \in S. \tag{8}$$

Proof. Let $x_0 \in S$ and $h \in BC(S)$. By condition (C1), it is clear that Hh is bounded. From (C2), along with $\varphi \in \Phi_3$ and $\psi \in \Phi_4$, we know that for any $\epsilon > 0$, there exist $\delta_1, \delta_2, \delta_3 > 0$ such that

$$\varphi(\|x - x_0\|) < \frac{\epsilon}{4} \quad \text{for } x \in S \text{ with } \|x - x_0\| < \delta_1, \tag{9}$$

$$\psi(\delta_1) < \frac{\epsilon}{4}, \tag{10}$$

$$|u(x, y) - u(x_0, y)| < \frac{\epsilon}{4} \quad \text{for } (x, y) \in S \times D \text{ with } \|x - x_0\| < \delta_1, \tag{11}$$

$$\max\left\{|p_i(x, y) - p_i(x_0, y)| : i = 1, 2, 3\right\} < \frac{\epsilon}{4} \quad \text{for } \|x - x_0\| < \delta_1, \tag{12}$$

$$|h(x) - h(x_0)| < \delta_1 \quad \text{for } x \in S \text{ with } \|x - x_0\| < \delta_2, \tag{13}$$

$$\max\left\{|a_i(x, y) - a_i(x_0, y)| : i = 1, 2, 3\right\} < \delta_2 \quad \text{for } \|x - x_0\| < \delta_3. \tag{14}$$

From (10), (13), and (14), we deduce

$$\psi\left(\sup_{y\in D}\left\{\max\left\{|h(a_i(x, y)) - h(a_i(x_0, y))| : i = 1, 2, 3\right\}\right\}\right) < \frac{\epsilon}{4}, \quad \text{for } \|x - x_0\| < \delta_3. \tag{15}$$

Let $\delta = \min\{\delta_1, \delta_3\}$. Using (C3), (C4), (9), and (15), we get for all $x \in S$ with $\|x - x_0\| < \delta$:

$$\begin{aligned}
&|Hh(x) - Hh(x_0)| \\
&= \big|\mathrm{opt}_{y\in D}\left\{u(x,y) + \mathrm{opt}\left\{p_i(x,y) + A_i(x,y,h(a_i(x,y)))\right\}\right\} \\
&\quad - \mathrm{opt}_{y\in D}\left\{u(x_0,y) + \mathrm{opt}\left\{p_i(x_0,y) + A_i(x_0,y,h(a_i(x_0,y)))\right\}\right\}\big| \\
&\le \sup_{y\in D}\Bigg\{|u(x,y) - u(x_0,y)| + \max_{i=1,2,3}\Big[|p_i(x,y) - p_i(x_0,y)| \\
&\quad + |A_i(x,y,h(a_i(x,y))) - A_i(x_0,y,h(a_i(x_0,y)))|\Big]\Bigg\} \\
&\le \frac{\epsilon}{4} + \frac{\epsilon}{4} + \frac{\epsilon}{4} + \frac{\epsilon}{4} = \epsilon.
\end{aligned}$$

This proves that Hh is continuous at x_0, and hence H maps $BC(S)$ into itself. Now, let $h, g \in BC(S)$ and fix $x \in S$. Suppose $\mathrm{opt}_{y\in D} = \sup_{y\in D}$. Then there exist $y, z \in D$ such that

$$\begin{aligned}
Hh(x) &< u(x,y) + \mathrm{opt}\left\{p_i(x,y) + A_i(x,y,h(a_i(x,y)))\right\} + \epsilon, \\
Hg(x) &< u(x,z) + \mathrm{opt}\left\{p_i(x,z) + A_i(x,z,g(a_i(x,z)))\right\} + \epsilon, \\
Hh(x) &\ge u(x,z) + \mathrm{opt}\left\{p_i(x,z) + A_i(x,z,h(a_i(x,z)))\right\}, \\
Hg(x) &\ge u(x,y) + \mathrm{opt}\left\{p_i(x,y) + A_i(x,y,g(a_i(x,y)))\right\}.
\end{aligned} \tag{16}$$

Using (16) and condition (C4), we have

$$\begin{aligned}
|Hh(x) - Hg(x)| &< \max_{i=1,2,3}\{|A_i(x,y,h(a_i(x,y))) - A_i(x,y,g(a_i(x,y)))|, \\
&\qquad |A_i(x,z,h(a_i(x,z))) - A_i(x,z,g(a_i(x,z)))|\} + \epsilon \\
&\le \psi\left(\max_{i=1,2,3}\{|h(a_i(x,y)) - g(a_i(x,y))|, |h(a_i(x,z)) - g(a_i(x,z))|\}\right) + \epsilon \\
&\le \psi(\|h - g\|_1) + \epsilon.
\end{aligned}$$

Taking the supremum over $x \in S$, we obtain

$$\|Hh - Hg\|_1 \le \psi(\|h - g\|_1) + \epsilon. \tag{17}$$

A similar argument holds if $\mathrm{opt}_{y\in D} = \inf_{y\in D}$. Letting $\epsilon \to 0^+$ in (17), we conclude

$$\|Hh - Hg\|_1 \le \psi(\|h - g\|_1).$$

By Lemma 2.4 (a variant of Boyd and Wong's fixed point theorem [6]), the operator H has a unique fixed point $w \in BC(S)$, and for every $h \in BC(S)$, the sequence $\{H^n h\}_{n\ge1}$ converges to w. Clearly, w is the unique solution of the functional equation (8) in $BC(S)$.

Theorem 3.2 *Let $u, p_i : S \times D \to \mathbb{R}$, $a_i : S \times D \to S$, and $A_i : S \times D \times \mathbb{R} \to \mathbb{R}$ for $i = 1, 2, 3$ be given mappings. Suppose that $\psi \in \Phi_5$, and that conditions* (C1) *and* (C4) *hold. Then the functional equation* (1) *admits a unique solution $w \in BC(S)$, and the sequence $\{H^n h\}_{n\ge1}$ converges to w for every $h \in BC(S)$, where the operator H is defined by (8).*

Remark 3.1

1. If $u = 0$ and $p_3 = A_3 = 0$, then Theorem 3.2 reduces to Theorem 3.2 of Pathak and Deepmala [25].

2. Theorem 3.2 generalizes and strengthens the classical result of Bellman [2].

Example 3.1 We present an example that demonstrates how Theorem 3.1 generalizes and unifies several previous results, including those found in [2, 4, 8, 10, 11, 25, 26]. Let $X = Y = \mathbb{R}$, $S = [1, \infty)$, and $D = \mathbb{R}^+ = [0, \infty)$. Define

$$\varphi(t) = 3t, \quad \psi(t) = \frac{t}{4}.$$

Then Theorem 3.1 guarantees that the functional equation

$$\begin{aligned} f(x) = \operatorname{opt}_{y\in D} \Bigg\{ 1 + \frac{1}{x^2 + \frac{1}{2}y} + \operatorname{opt} \Bigg\{ & \frac{x^2}{x+y^2} + \frac{1}{x^2+y^2+1} + \frac{1}{3}\sin\big(f(2x^2y)\big), \\ & \frac{x+y}{1+3(x+y)} + \frac{1}{x^2+y} + \frac{1}{3+|f(\sin(2x)+3y)|}, \\ & \frac{x^3}{x+y^4} + \frac{1}{1+x^2+2y^2} + \frac{f\big(5+\sin(7x-3y)\big)}{3+3f\big(5+\sin(7x-3y)\big)^2} \Bigg\}\Bigg\}, \quad \forall x \in S, \end{aligned}$$

possesses a unique solution in $B(S)$. To see this, define the following mappings:

$$\begin{aligned} & u(x,y) = 1 + \frac{1}{x^2 + \frac{1}{2}y}, \\ & p_1(x,y) = \frac{x^2}{x+y^2}, \quad p_2(x,y) = \frac{x+y}{1+3(x+y)}, \quad p_3(x,y) = \frac{x^3}{x+y^4}, \end{aligned}$$

and

$$\begin{aligned} A_1(x,y,z) &= \frac{1}{x^2+y^2+1} + \frac{1}{3\sin z}, \\ A_2(x,y,z) &= \frac{1}{x^2+y} + \frac{1}{3+|z|}, \\ A_3(x,y,z) &= \frac{1}{1+x^2+2y^2} + \frac{z}{3+3z^2}. \end{aligned}$$

Then the following relations hold:

$$\begin{aligned} |A_i(x,y,z) - A_i(x_0,y,z)| &\le 3|x-x_0| \quad \text{for all } i = 1,2,3, \\ |A_i(x,y,z) - A_i(x,y,z_0)| &\le \frac{1}{4}|z-z_0| \quad \text{for all } i = 1,2,3. \end{aligned}$$

Thus, all the assumptions of Theorem 3.2 are satisfied, and hence the functional equation possesses a unique solution in $B(S)$.

4 Conclusion

In this paper, we established new existence, uniqueness, and iterative approximation results for the classes of functional equations arising in dynamic programming. By employing fixed point techniques and suitable contractive conditions, we extended and unified several known results in the literature. The general framework presented here accommodates a broad range of applications and improves upon classical formulations such as Bellman's equations. A detailed example was also provided to illustrate the applicability of our main theorem.

References

[1] S. Banach. Sur les opérations dans les ensembles abstraits et leur application aux équations intégrales. *Fundamenta Mathematicae* **3** (1) (1922) 133–181.

[2] R. Bellman. *Dynamic Programming.* Princeton University Press, Princeton, NJ, 1957.

[3] R. Bellman and E. S. Lee. Functional equations arising in dynamic programming. *Aequationes Mathematicae* **17** (1) (1978) 1–18.

[4] P. C. Bhakta and S. Mitra. Some existence theorems for functional equations arising in dynamic programming. *Journal of Mathematical Analysis and Applications* **98** (2) (1984) 348–362.

[5] P. C. Bhakta and S. R. Choudhury. Some existence theorems for functional equations arising in dynamic programming II. *Journal of Mathematical Analysis and Applications* **131** (1) (1988) 217–231.

[6] D. W. Boyd and J. S. W. Wong. On nonlinear contractions. *Proceedings of the American Mathematical Society* **20** (2) (1969) 458–464.

[7] G. Jiang, S. M. Kang and Y. C. Kwun. Solvability and algorithms for functional equations originating from dynamic programming. *Fixed Point Theory and Applications* **2011** (1) (2011) Article ID 701519, 30 pages.

[8] Z. Liu and S. M. Kang. Existence and uniqueness of solutions for two classes of functional equations arising in dynamic programming. *Acta Mathematicae Applicatae Sinica, English Series* **23** (2) (2007) 195–208.

[9] Z. Liu and J. S. Ume. On properties of solutions for a class of functional equations arising in dynamic programming. *Journal of Optimization Theory and Applications* **117** (3) (2003) 533–551.

[10] Z. Liu, R. P. Agarwal and S. M. Kang. On solvability of functional equations and system of functional equations arising in dynamic programming. *Journal of Mathematical Analysis and Applications* **297** (1) (2004) 111–130.

[11] Z. Liu, J. S. Ume and S. M. Kang. Some existence theorems for functional equations and system of functional equations arising in dynamic programming. *Taiwanese Journal of Mathematics* **14** (5) (2010) 1517–1536.

[12] N. R. Anakira, A. Almalki, D. Katatbeh, G. B. Hani, A. F. Jameel, K. S. Al Kalbani, and M. Abu-Dawas. An algorithm for solving linear and non-linear Volterra integro-differential equations. *International Journal of Advances in Soft Computing and Its Applications* **15** (3) (2023) 77–83.

[13] G. Farraj, B. Maayah, R. Khalil, and W. Beghami. An algorithm for solving fractional differential equations using conformable optimized decomposition method. *International Journal of Advances in Soft Computing and Its Applications* **15** (1) (2023) 187–196.

[14] M. Berir. Analysis of the effect of white noise on the Halvorsen system of variable-order fractional derivatives using a novel numerical method. *International Journal of Advances in Soft Computing and Its Applications* **16** (3) (2024) 294–306.

[15] H. Qawaqneh. Functional analysis with fractional operators: properties and applications in metric spaces. *Advances in Fixed Point Theory* **14** (1) (2024) Article ID 62.

[16] I. H. Jebril, H. Bouhadjera, I. M. Batiha and B. Batiha. Common fixed point theorems in metric domains. *Advances in Fixed Point Theory* **15** (1) (2025) Article ID 4.

[17] A. Bataihah, M. Shatnawi, I. M. Batiha, I. H. Jebril and T. Abdeljawad. Some results on fixed points in B-metric spaces through an auxiliary function. *Nonlinear Functional Analysis and Applications* **30** (1) (2025) 251–263.

[18] I. M. Batiha, Z. Chebana, T. E. Oussaeif, S. Abu-Ghurra, A. Al-Nana, A. Bataihah and I. H. Jebril. Global existence for heat equation with nonlinear and damping piecewise Neumann boundary condition. *International Journal of Robotics and Control Systems* **5** (2) (2025) 846–861.

[19] S. Momani, I. M. Batiha, Z. Chebana, T. E. Oussaeif, A. Ouannas and S. Dehilis. Weak solution, blow-up and numerical study of a nonlinear reaction diffusion problem with an integral condition. *Progress in Fractional Differentiation and Applications* **11** (1) (2025) 45–61.

[20] I. M. Batiha, B. Laouadi, I. H. Jebril, L. Benaoua, T. E. Oussaeif and S. Alkhazaleh. Some new fixed point theorems of rational type contraction with an application to coupled fixed point theory. *Advances in Fixed Point Theory* **14** (4) (2024) Article ID 52.

[21] I. M. Batiha, I. H. Jebril, Z. Chebana, T. E. Oussaeif, S. Dehilis and S. Alkhazaleh. Finite-time blow-up and solvability of a weak solution for a superlinear reaction-diffusion problem with integral conditions of the second type. *Advances in Fixed Point Theory* **14** (4) (2024) Article ID 45.

[22] I. M. Batiha, A. Benguesmia, M. Alosaimi, T. E. Oussaeif, N. Anakira and M. Odeh. Superlinear problem with inverse coefficient for a time-fractional parabolic equation with integral over-determination condition. *Nonlinear Dynamics and Systems Theory* **24** (6) (2024) 561–574.

[23] A. Benbrahim, I. M. Batiha, I. H. Jebril, A. Bourobta, T. E. Oussaeif and S. Alkhazaleh. A priori predictions for a weak solution to time-fractional nonlinear reaction-diffusion equations incorporating an integral condition. *Nonlinear Dynamics and Systems Theory* **24** (5) (2024) 431–441.

[24] A. Benguesmia, I. M. Batiha, T. E. Oussaeif, A. Ouannas and W. G. Alshanti. Inverse problem of a semilinear parabolic equation with an integral overdetermination condition. *Nonlinear Dynamics and Systems Theory* **23** (3) (2023) 249–260.

[25] H. K. Pathak and Deepmala. Existence and uniqueness of solutions of functional equations arising in dynamic programming. *Applied Mathematics and Computation* **218** (13) (2012) 7221–7230.

[26] Z. Liu, Y. Xu, J. S. Ume and S. M. Kang. Solutions to two functional equations arising in dynamic programming. *Journal of Computational and Applied Mathematics* **192** (1) (2006) 251–269.

Nonlinear Dynamics and Systems Theory, **25** (6) (2025) 596–607

Solving a Class of Bilevel Programming Problems by DC Programming and DCA

W. Bouguern *, S. Addoune and H. Debbiche

Mathematical Analysis and Applications Laboratory, Department of Mathematics, University Mohamed El Bachir El Ibrahimi of Bordj Bou Arreridj, El Anasser 34030, Algeria

Received: January 8, 2025; Revised: November 4, 2025

Abstract: In this paper, we propose an optimization model to address a specific class of bilevel programming problems. We transform the bilevel problem into a single-level optimization problem using the optimal value function reformulation. Since the lower-level problem is non-convex, we rewrite the value function of the lower-level problem as a Difference of Convex Functions (DC). To achieve this, we employ a regularization approach in the value function of the lower-level problem, which enables us to formulate the problem as a DC program. The resulting problem is then solved using the DC algorithm (DCA). The efficiency of the proposed algorithm is demonstrated through the results obtained from our computational analysis.

Keywords: *bilevel programming; DC optimization; penalty function; regularization approach.*

Mathematics Subject Classification (2020): 90C26, 90C30, 49J52, 65-XX.

1 Introduction

Bilevel optimization is a key area of mathematical programming that is crucial for solving hierarchical decision-making problems. In nonlinear dynamical systems, it enhances control, responsiveness, and stability. For example, a nonlinear control model can represent the interaction between an upper-level controller that optimizes stability and a lower-level controller that executes decisions based on system dynamics. This framework is valuable in robotic control, smart grids, and energy management because it balances competing objectives under dynamic constraints [8]. Additionally, discrete event simulation (DES) and system dynamics (SD) have been used to analyze waiting times and queue lengths in healthcare systems such as outpatient departments (OPDs) [3]. While

* Corresponding author: mailto:wafa.bouguern@univ-bba.dz

these models do not explicitly employ bilevel programming, the implicit leader–follower interaction between hospital management and patient flow can naturally be formulated as a bilevel problem. Behavior patterns resemble the Nash equilibrium in decentralized decision-making.

A bilevel optimization problem involves two interdependent levels of decision-making: the leader at the upper level influences the objective function and the constraints for the follower problem. The follower then optimizes their decision-making based on the leader's choices. This dynamic generates a multifaceted issue that necessitates solutions considering the interaction between both levels of decision-making. Even when all functions in bilevel programming problems (BLPs) are linear, these problems are usually non-convex, which makes them difficult to solve. Nevertheless, researchers have developed various methodologies to address these challenges, including descent methods and smoothing techniques, among others. Furthermore, mathematical methods such as applying the KKT conditions to the lower-level problem or reformulating the lower-level value function (VFR) are used to convert BLPs into single-level problems [14], [12].

In this paper, we propose a numerical algorithm for a specific class of bilevel programming problems using DC programming and the DCA, originally introduced by Pham Dinh Tao in 1986 and further developed since 1994 [7]. This approach was applied to bilevel problems with a convex quadratic upper-level objective and a linear lower-level structure by Le Thi Hoai An and Tran Duc Quynh [13]. Similarly, in [2], the bilevel problem was reformulated using the KKT conditions and solved via DC programming. DC programming has recently gained broader attention in bilevel optimization [6], and continues to be extended to various problem classes, including absolute value equations [1].

The remainder of this paper is organized as follows. Section 2 provides a concise overview of DC programming and the DCA. Section 3 formulates the problem. Section 4 details the implementation of DC programming and the DCA to address the reformulated problem. Computational results are presented in Section 5, followed by conclusions and directions for future research in Section 6.

2 DC Programming and DCA

DC programming is a mathematical optimization domain that addresses problems in which the objective function f is represented as the difference of two convex functions. These functions are designated as the DC components of the function f, with $g - h$ signifying a DC decomposition of f.

Let the space $\mathbb{R}^n$ be equipped with the canonical inner product $\langle \cdot, \cdot \rangle$. The Euclidean norm is denoted by $\|\cdot\|$. A DC program takes the form

$$(P_{DC}) \qquad \min \{ f(x) = g(x) - h(x) : x \in \mathbb{R}^n \},$$

where $g, h : \mathbb{R}^n \to \bar{\mathbb{R}}$ are lower semicontinuous proper convex functions. The following necessary local optimality conditions:

$$\emptyset \neq \partial h(x^*) \subset \partial g(x^*) \ ^{\dagger} \quad \text{and} \quad \partial g(x^*) \cap \partial h(x^*) \neq \emptyset \ ^{\ddagger}$$

developed by Le Thi and Pham Dinh [7], have been widely used in DC programming, where

$$\partial h(x^*) = \{ p^* \in \mathbb{R}^n \mid h(x) \geq h(x^*) + \langle x - x^*, p^* \rangle, \forall x \in \mathbb{R}^n \}$$

† Such a point is called a stationary point.

‡ Such a point is called a critical point.

is the subdifferential of h at x^*.

The DCA is an efficient and adaptable optimization technique used to minimize differences of convex functions. The fundamental principle of the DCA is to iteratively approximate a non-convex optimization problem through a series of convex problems. Each iteration entails solving a convex subproblem derived from the original DC problem. The algorithm can be implemented as follows.

Algorithm 2.1 ***DCA Algorithm***
Initialization
Choose an initial point $x^0 \in \mathbb{R}^n$, the maximum number of iterations max.
Treatment

1. *For $k = 0, 1, \dots, max$*
   (a) *Calculate $p^k \in \partial h(x^k)$.*
   (b) *Calculate $x^{k+1} \in \arg\min \left\{ g(x) - h(x^k) - \langle x - x^k, p^k \rangle : x \in \mathbb{R}^n \right\}$.*
   (c) *If the convergence criterion is satisfied, then stop; otherwise set $k := k + 1$.*

Theorem 2.1 *[11] The DCA algorithm either converges after a finite number of iterations or produces an infinite sequence of points (x^k). If the sequences (x^k) and (p^k) are bounded, one of the functions g or h is strongly convex [1], and $\inf f > -\infty$, then every accumulation point of the sequence (x^k) is a critical point of the problem (P_{DC}).*

3 Problem Formulation

In this paper, we consider the following bilevel programming problem:

$$(BLP) \quad \begin{cases} \min\limits_{x,y} F(x,y) \\ \text{s.t.} \\ G_i(x,y) \leq 0, \ i = 1, \dots, m_1, \\ y \in \Psi(x), \end{cases}$$

where $\Psi(x)$ is the set of optimal solutions to the lower-level problem

$$(P_x) \quad \begin{cases} \min\limits_{y} f(x,y) = y^\top Q x + c^\top y \\ \text{s.t.} \\ l_i(y) \leq 0, \ i = 1, \dots, m_2, \end{cases}$$

where $F, f : \mathbb{R}^n \times \mathbb{R}^m \to \mathbb{R}$ are the objective functions of the leader and the follower, respectively, $c \in \mathbb{R}^m, Q \in \mathbb{R}^{m \times n}$. The functions F, G, l are assumed to be convex. Let

$$S = \{ y \in \mathbb{R}^m \mid l_i(y) \leq 0, \ i = 1, \dots, m_2 \}$$

denote the feasible set of the lower level problem (P_x),

$$\bar{S} = \{ (x,y) \in \mathbb{R}^n \times \mathbb{R}^m \mid G_i(x,y) \leq 0, \, l_j(y) \leq 0, \ i = 1, \dots, m_1, \ j = 1, \dots, m_2 \}$$

[1] The function f is strongly convex with modulus $\rho > 0$ if, for all $x, y \in \mathbb{R}^n$ and for all $\lambda \in [0,1]$, we have: $f\big(\lambda x + (1-\lambda) y\big) \leq \lambda f(x) + (1-\lambda) f(y) - \frac{\rho}{2} \lambda (1-\lambda) \|x - y\|^2$.

denote the constraint region of (BLP),

$$R(x) = \arg\min \left\{ y^\top Qx + c^\top y,\ y \in S \right\}$$

be the rational reaction set of the lower level for each x fixed, and

$$IR = \left\{ (x, y) \in \mathbb{R}^n \times \mathbb{R}^m \mid (x, y) \in \bar{S},\ y \in R(x) \right\}$$

denote the inducible region of (BLP).

The bilevel programming problem is known for its significant challenges stemming from its hierarchical structure. To tackle these complexities, researchers commonly reformulate the BLP into a single-level optimization problem. A primary approach for this transformation is the lower-level value function reformulation (LVFR), initially proposed in [12] for numerical applications and subsequently utilized to derive optimality conditions in [14]. This reformulation leads to the following equivalent problem:

$$(P) \quad \begin{cases} \min\limits_{x,y} F(x, y), \\ \text{s.t.} \\ G_i(x, y) \leq 0, \quad i = 1, \ldots, m_1, \\ l_i(y) \leq 0, \quad i = 1, \ldots, m_2, \\ y^\top Qx + c^\top y - V(x) \leq 0, \end{cases}$$

where the optimal value function of the lower-level problem (P_x) is given by

$$V(x) = \min_y \left\{ y^\top Qx + c^\top y \mid l_i(y) \leq 0,\ i = 1, \ldots, m_2 \right\}.$$

In this paper, we adopt an effective approach grounded in DC programming. Our methodology begins with regularizing the lower-level problem. Specifically, we replace (P_x) with the regularized problem (P_x^r), defined as

$$(P_x^r) \quad \begin{cases} \min\limits_{y} f(x, y) = y^\top Qx + c^\top y + \dfrac{r}{2}\|y\|^2, \\ \text{s.t.} \\ l_i(y) \leq 0, \quad i = 1, \ldots, m_2, \end{cases}$$

for $r > 0$. Let $\Psi_r(x)$ denote the set of optimal solutions to this problem. Regularization is commonly employed under certain assumptions to guarantee the uniqueness of solutions to the lower-level problem (see [4] and references therein).

In our work, we use this regularized formulation to express the lower-level value function as the difference of two convex functions. Building on this, the bilevel programming problem is reformulated into the following single-level problem:

$$(P_r) \quad \begin{cases} \min\limits_{x,y} F(x, y), \\ \text{s.t.} \\ G_i(x, y) \leq 0, \quad i = 1, \ldots, m_1, \\ l_i(y) \leq 0, \quad i = 1, \ldots, m_2, \\ y^\top Qx + c^\top y + \frac{r}{2}\|y\|^2 - V_r(x) \leq 0, \end{cases}$$

where the regularized value function is defined as

$$V_r(x) = \min_y \left\{ y^\top Qx + c^\top y + \frac{r}{2}\|y\|^2 \mid l_i(y) \leq 0,\ i = 1, \ldots, m_2 \right\}.$$

The problem (P_r) is a complex one due to its non-convex nature and the presence of the typically non-differentiable function $V_r(x)$.

The next section proposes an optimization model for solving problem (P_r).

4 The Proposed Optimization Model

In our work, we substituted the value function of the lower-level problem (P_x):

$$V(x) = \min_y \left\{ y^\top Qx + c^\top y \mid l_i(y) \leq 0,\ i = 1, \ldots, m_2 \right\}$$

with the value function of (P_x^r):

$$V_r(x) = \min_y \left\{ y^\top Qx + c^\top y + \frac{r}{2}\|y\|^2 \mid l_i(y) \leq 0,\ i = 1, \ldots, m_2 \right\}.$$

In this context, r denotes the regularization parameter. Incorporating the regularization term $\frac{r}{2}\|y\|^2$ into the objective function $y^\top Qx + c^\top y$ of the lower-level problem (P_x), we effectively control the size of y by penalizing larger values. Specifically, the term $\frac{r}{2}\|y\|^2$ serves as a penalty for large values of y, promoting a more stable and manageable solution. As the regularization parameter r decreases, the influence of the penalty term $\frac{r}{2}\|y\|^2$ diminishes. Thus, the solution to the regularized problem $\bar{y}_r$ will converge to the solution of the original issue $\bar{y}$ (without regularization).

In other words, as the regularization parameter r decreases, the objective value of the regularized problem, $V_r(x)$, approaches the objective value of the original problem, $V(x)$. If r is small, then the term $\frac{r}{2}\|\bar{y}_r\|^2$ will also be small. For all $\varepsilon > 0$, there exists $\delta > 0$ such that for all $0 < r < \delta$, we have

$$\bar{y}_r^\top Qx + c^\top \bar{y}_r + \frac{r}{2}\|\bar{y}_r\|^2 - \bar{y}^\top Qx - c^\top \bar{y} \leq \frac{\varepsilon}{2},$$

and

$$\frac{r}{2}\|\bar{y}_r\|^2 \leq \frac{\varepsilon}{2}.$$

Thus, we obtain the following inequality:

$$\left| \bar{y}^\top Qx + c^\top \bar{y} - \left(\bar{y}_r^\top Qx + c^\top \bar{y}_r \right) \right| \leq \varepsilon.$$

From this, we conclude that the regularized solution $\bar{y}_r$ approximates the original solution $\bar{y}$ within ε.

Now, we can express $V_r(x)$ as the difference of two convex functions, as demonstrated in the following proposition.

Proposition 4.1 *The function $V_r(x)$ is a DC (Difference of Convex) function. It can be expressed with a DC decomposition as*

$$V_r(x) = V_r^1(x) - V_r^2(x), \quad x \in \mathbb{R}^n,$$

where

$$V_r^1(x) = \frac{r}{2}\left[d\left(-\frac{Qx + c}{r}, S \right) \right]^2 \quad \text{and} \quad V_r^2(x) = \frac{1}{2r}\|Qx + c\|^2.$$

Here, $d\left(-\frac{Qx+c}{r}, S\right)$ denotes the Euclidean distance from the point $-\frac{Qx+c}{r}$ to the set S.

Proof.

$$
\begin{aligned}
V_r(x) &= \min_y \left\{ y^\top Qx + c^\top y + \frac{r}{2}\|y\|^2 \mid y \in S \right\} \\
&= \min_y \left\{ (Qx+c)^\top y + \frac{r}{2}\|y\|^2 \mid y \in S \right\} \\
&= \min_y \left\{ (Qx+c)^\top y + \frac{r}{2}\left[\left\| y + \frac{Qx+c}{r} \right\|^2 + \left\| \frac{Qx+c}{r} \right\|^2 - 2\left(\frac{Qx+c}{r}\right)^\top \left(y + \frac{Qx+c}{r} \right) \right] \mid y \in S \right\} \\
&= \min_y \left\{ (Qx+c)^\top y + \frac{r}{2}\left\| y + \frac{Qx+c}{r} \right\|^2 + \frac{1}{2r}\|Qx+c\|^2 - (Qx+c)^\top y - \frac{1}{r}\|Qx+c\|^2 \mid y \in S \right\} \\
&= \min_y \left\{ \frac{r}{2}\left\| y + \frac{Qx+c}{r} \right\|^2 - \frac{1}{2r}\|Qx+c\|^2 \mid y \in S \right\} \\
&= \min_y \left\{ \frac{r}{2}\left\| y + \frac{Qx+c}{r} \right\|^2 \mid y \in S \right\} - \frac{1}{2r}\|Qx+c\|^2 \\
&= \frac{r}{2}\left[d\left(-\frac{Qx+c}{r}, S \right) \right]^2 - \frac{1}{2r}\|Qx+c\|^2 \\
&= V_r^1(x) - V_r^2(x).
\end{aligned}
$$

Based on the preceding theories and results, we will examine the following problem:

$$
(P_r) \quad \begin{cases}
\min\limits_{x,y} F(x,y), \\
\text{s.t.} \\
G_i(x,y) \le 0, \quad i = 1, \ldots, m_1, \\
l_i(y) \le 0, \quad i = 1, \ldots, m_2, \\
y^\top Qx + c^\top y + \frac{r}{2}\|y\|^2 - V_r(x) \le 0.
\end{cases}
$$

As shown in Proposition 1, the function $V_r(x)$ can be rewritten as the difference of two convex functions. Additionally, since the inequality $y^\top Qx + c^\top y + \frac{r}{2}\|y\|^2 - V_r(x) \le 0$ is originally an equality constraint (see [14]), and given that $y^\top Qx + c^\top y + \frac{r}{2}\|y\|^2 - V_r(x) \ge 0$, by applying the exact penalty method, we obtain

$$
(P_{r,\mu}) \quad \begin{cases}
\min\limits_{x,y} F(x,y) + \mu\left(y^\top Qx + c^\top y + \dfrac{r}{2}\|y\|^2 - \left(V_r^1(x) - V_r^2(x)\right) \right) \\
\text{s.t.} \\
G_i(x,y) \le 0, \; i = 1, \ldots, m_1, \\
l_i(y) \le 0, \; i = 1, \ldots, m_2,
\end{cases}
$$

where μ is a positive penalty parameter.

We can also express the inner product $y^\top Qx$ as the difference of two convex functions as follows:

$$
y^\top Qx = \frac{1}{4}\|Qx+y\|^2 - \frac{1}{4}\|Qx-y\|^2.
$$

Thus, the last problem is equivalent to

$$
\begin{cases}
\min\limits_{x,y} \left(F(x,y) + \dfrac{\mu}{4}\|Qx+y\|^2 + \mu c^\top y + \dfrac{\mu r}{2}\|y\|^2 + \mu V_r^2(x) \right) - \left(\mu V_r^1(x) + \dfrac{\mu}{4}\|Qx-y\|^2 \right) \\
\text{s.t.} \\
G_i(x,y) \le 0, \; i = 1, \ldots, m_1, \\
l_i(y) \le 0, \; i = 1, \ldots, m_2.
\end{cases}
$$

The problem $(P_{r,\mu})$ is a DC program of the form

$$\min\left\{F_{\mu,v}(x,y) = g(x,y) - h(x,y) : (x,y) \in \bar{S}\right\},$$

where

$$g(x,y) = F(x,y) + \frac{\mu}{4}\|Qx+y\|^2 + \mu c^\top y + \frac{\mu r}{2}\|y\|^2 + \mu V_r^2(x),$$

and

$$h(x,y) = \mu V_r^1(x) + \frac{\mu}{4}\|Qx-y\|^2.$$

Note that the function $V_r^1(x)$ is differentiable (see, [9], Exercise 3.2), with

$$\nabla V_r^1(x) = \frac{r}{2}\nabla d^2\left(-\frac{Qx+c}{r}, S\right) = \frac{r}{2}\left[-\frac{2}{r}Q^\top\left[-\frac{Qx+c}{r} - \Pi\left(-\frac{Qx+c}{r}, S\right)\right]\right],$$

and $\Pi\left(-\frac{Qx+c}{r}, S\right)$ denotes the Euclidean projection from a point $-\frac{Qx+c}{r}$ to a nonempty closed convex set S in $\mathbb{R}^n$.
To calculate the projection $\Pi\left(-\frac{Qx+c}{r}, S\right)$, we aim to find the point in the set S that minimizes the distance to $-\frac{Qx+c}{r}$. Mathematically, this problem can be formulated as

$$\Pi\left(-\frac{Qx+c}{r}, S\right) = \arg\min_{y\in S}\left\|y + \frac{Qx+c}{r}\right\|^2, \tag{1}$$

where y is the point in S that minimizes this distance.

The subdifferential $\partial h(x,y)$ is computed as

$$\partial h(x,y) = \nabla h(x,y) = \begin{pmatrix} \mu\nabla V_r^1(x) + \frac{\mu}{2}Q^\top(Qx-y) \\ -\frac{\mu}{2}(Qx-y) \end{pmatrix}. \tag{2}$$

The DC Algorithm (DCA) applied to the DC program $(P_{r,\mu})$ involves, at each iteration k, computing the sequences (t^k, q^k) and (x^k, y^k) such that $(t^k, q^k) \in \partial h(x^k, y^k)$, and (x^{k+1}, y^{k+1}) is the optimal solution to the following program:

$$\min\left\{g(x,y) - \langle t^k, x\rangle - \langle q^k, y\rangle,\ (x,y) \in \bar{S}\right\}.$$

Alternatively,

$$\min\left\{g(x,y) - \left(\mu\nabla V_r^1(x^k) + \frac{\mu}{2}Q^\top(Qx^k - y^k)\right)^\top x + \left(\frac{\mu}{2}(Qx^k - y^k)\right)^\top y,\ (x,y) \in \bar{S}\right\}. \tag{3}$$

Instead of using a fixed regularization parameter r, we often change r during iteration. This adaptive approach allows the algorithm to dynamically refine the regularization during execution, potentially leading to better performance and convergence. The scheme of the algorithm is as follows.

Algorithm 4.1 ***BL-DCA Algorithm***
Initialization: *Let $\varepsilon > 0$, choose an initial point $(x^0, y^0) \in \bar{S}$, select parameters $\mu_0 > 0$, $r_0 > 0$ and $\alpha > 0$, set $0 < \beta < 1$, the maximum number of iterations max.*
Treatment:

1. *For $k = 0, 1, \ldots, max$*

(a) Compute $\Pi\left(-\frac{Qx^k+c}{r}, S\right)$ *using* (1).

(b) Determine $(t^k, q^k) \in \partial h(x^k, y^k)$ *by applying* (2).

(c) Solve the convex problem (3) *to find* (x^{k+1}, y^{k+1}).

(d) If $\left\|(x^{k+1}, y^{k+1}) - (x^k, y^k)\right\| \leq \varepsilon$, *then stop.* (x^{k+1}, y^{k+1}) *is the optimal solution of* (P).

(e) Update the penalty parameter and the regularization parameter:

$$\mu^{k+1} = \mu^k + \alpha, \quad r^{k+1} = \beta r^k.$$

(f) Set $k := k+1$.

Remark 4.1 We can address another class of bilevel programming problems using the same technique, where the lower-level problem is a linear optimization problem defined as follows for every fixed x:

$$(P'_x) \quad \begin{cases} \min\limits_{y} \ f(x,y) = d^\top y \\ \text{s.t.} \\ Ax + By \geq b, \\ y \geq 0. \end{cases}$$

We can express (P'_x) in the form of (P_x). The dual problem of (P'_x) is given by

$$(PD_x) \quad \begin{cases} \min\limits_{\lambda} \ f(x,y) = \lambda^\top Ax - \lambda^\top b \\ \text{s.t.} \\ B^\top \lambda \leq d, \\ \lambda \geq 0, \end{cases}$$

where λ represents the dual variables. Under certain hypotheses, we can apply the strong duality theorem to establish the equality of the optimal values of the two problems. By substituting the optimal value function $V_p(x)$ of the problem (P'_x) with the optimal value function $V_d(x)$ of the problem (PD_x), we derive a problem analogous to the one analyzed earlier. When the objective function of the upper-level problem is linear, our method encompasses an important class of problems known as **"Linear bilevel programming problems"**.

5 Computational Tests

We implemented the BL-DCA method using Julia 1.10.1. We selected problems with linear constraints to employ CPLEX, a solver renowned for its speed and efficacy in addressing various optimization problems, including linear and quadratic programming. The algorithm was assessed on several problems from the Bilevel Optimization Library (BOLIB) [15], which provides an extensive array of test problems with established solutions. Each example in this collection includes comprehensive descriptions of input functions, constraints, and established solutions, facilitating the effective implementation and evaluation of the BL-DCA algorithm.

For our experiments, we set $\varepsilon = 10^{-2}$, with execution time reported in seconds. The values used for (μ_0, α), (r_0, β), and the initial point (x^0, y^0) are provided in Table 1. We denote the optimal solutions obtained by the BL-DCA algorithm as (x^*, y^*), and the number of iterations as Iter. The global optimal solution, taken from the corresponding reference, is denoted as Optimal Solution.

5.1 Test problems

$$P_1: \begin{cases} \min\limits_{x,y}\ x_1 + y_1^2 + y_2^2 \\ \text{s.t.} \\ -1 \le x_1 \le 1 \\ -1 - x_2 \le 0 \\ 1 + x_2 \le 0 \\ y \in \arg\min\limits_{y} \begin{cases} x_1 y_1 + x_2 y_2 \\ \text{s.t.} \\ -2y_1 + y_2 \le 0 \\ y_1 \le 2 \\ 0 \le y_2 \le 2 \end{cases} \end{cases}
\qquad
P_2: \begin{cases} \min\limits_{x,y}\ 2x_1 + x_2 - 2y_1 + y_2 \\ \text{s.t.} \\ -1 \le x_1 \le 1 \\ -1 \le x_2 \le -0.75 \\ y \in \arg\min\limits_{y} \begin{cases} x_1 y_1 + x_2 y_2 \\ \text{s.t.} \\ -2y_1 + y_2 \le 0 \\ y_1 \le 2 \\ 0 \le y_2 \le 2 \end{cases} \end{cases}$$

$$P_3: \begin{cases} \min\limits_{x,y}\ (x_1 - 0.5)^2 + (x_2 - 0.5)^2 - 3y_1 - 3y_2 \\ \text{s.t.} \\ y \in \arg\min\limits_{y} \begin{cases} x_1 y_1 + x_2 y_2 \\ \text{s.t.} \\ y_1 + y_2 \le 2 \\ -y_1 + y_2 \le 0 \\ y_1, y_2 \ge 0 \end{cases} \end{cases}
\qquad
P_4: \begin{cases} \min\limits_{x,y}\ -x - y \\ \text{s.t.} \\ -0.5 \le x \le 0.5 \\ y \in \arg\min\limits_{y} \begin{cases} xy \\ \text{s.t.} \\ -1 \le y \le 1 \end{cases} \end{cases}$$

$$P_5: \begin{cases} \min\limits_{x,y}\ (x_1 - 0.5)^2 + (x_2 - 0.5)^2 + x_3^2 - 3y_1 - 3y_2 - 6y_3 \\ \text{s.t.} \\ y \in \arg\min\limits_{y} \begin{cases} x_1 y_1 + x_2 y_2 + x_3 y_3 \\ \text{s.t.} \\ y_1 + y_2 + y_3 \le 2 \\ -y_1 + y_2 \le 0 \\ y_1, y_2, y_3 \ge 0 \end{cases} \end{cases}$$

$$P_6: \begin{cases} \min\limits_{x,y}\ (y_1 - x_1 + 20)^2 + (y_2 - x_2 + 20)^2 \\ \text{s.t.} \\ y \in \arg\min\limits_{y} \begin{cases} 5x_1 y_1 - 3x_1 y_2 + 5x_2 y_2 + y_1 + y_2 \\ \text{s.t.} \\ 0 \le y_1 \le 6 \\ 0 \le y_2 \le 6 \end{cases} \end{cases}$$

$$P_7: \quad \begin{cases} \min\limits_{x,y} \ -x_1 + 10y_1 - y_2 \\ \text{s.t.} \\ x \geq 0 \\ y \in \arg\min\limits_{y} \begin{cases} -y_1 - y_2 \\ \text{s.t.} \\ x + y_1 \leq 1 \\ x + y_2 \leq 1 \\ y_1 + y_2 \leq 1 \\ y \geq 0 \end{cases} \end{cases}$$

$$P_8: \quad \begin{cases} \min\limits_{(x,y)\geq 0} \ -4x_1 + 8x_2 + x_3 - x_4 + 9y_1 - 9y_2 \\ \text{s.t.} \\ -9x_1 + 3x_2 - 8x_3 + 3x_4 + 3y_1 \leq -1 \\ 4x_1 - 10x_2 + 3x_3 + 5x_4 + 8y_1 + 8y_2 \leq 25 \\ 4x_1 - 2x_2 - 2x_3 + 10x_4 - 5y_1 + 8y_2 \leq 21 \\ 9x_1 - 9x_2 + 4x_3 - 3x_4 - y_1 - 9y_2 \leq -1 \\ -2x_1 - 2x_2 + 8x_3 - 5x_4 + 5y_1 + 8y_2 \leq 20 \\ 7x_1 + 2x_2 - 5x_3 + 4x_4 - 5y_1 \leq 11 \\ y \in \arg\min\limits_{y\geq 0} \begin{cases} -9y_1 + 9y_2 \\ \text{s.t.} \\ -6x_1 + x_2 + x_3 - 3x_4 - 9y_1 - 7y_2 \leq -15 \\ 4x_2 + 5x_3 + 10x_4 \leq 26 \\ -9x_1 + 9x_2 - 9x_3 + 5x_4 - 5y_1 - 4y_2 \leq -5 \\ 5x_1 + 3x_2 + x_3 + 9x_4 + y_1 + 5y_2 \leq 32 \end{cases} \end{cases}$$

5.2 Results Analysis

Problems P_1–P_5 and P_7 were taken from the BOLIB. The solutions obtained using the BL-DCA algorithm are either close to or identical to the optimal solutions, and the algorithm demonstrates convergence within a reasonable number of iterations and computational time; most problems show that, with appropriate values for μ and r, the algorithm can achieve optimal solutions in a small number of iterations. Specifically, Problem P_1 converges to the optimal solution in four iterations when suitable settings for r are used, and the time required is relatively small. Problems P_7 and P_8 highlight the algorithm's effectiveness in solving linear bilevel programming problems. Additionally, Problem P_6, which we proposed, was solved manually to verify the optimal solution; the manually computed solution was identical to the one obtained by applying the BL-DCA algorithm. These results suggest that the choice of initial values and the update rules for μ and r significantly influence the algorithm's performance, including the number of iterations and the computational time. In summary, the BL-DCA algorithm has demonstrated high efficiency in experiments, particularly when its parameters are appropriately tuned. It performs exceptionally well in terms of both solution quality and computation time.

Pr.	(μ_0, α)	(r_0, β)	(x^0, y^0)	(x^*, y^*)	Time	Iter	Optimal Solution
P_1 [15]	$(1, 2)$	$(1, 0.6)$	$(0, -1, 0, 0)$	$(-0.01, -1, 1, 1.99)$	0.26	10	$(0, -1, 1, 2)$
	$(10, 4)$	$(0.1, 0.2)$	$(0, -1, 0, 0)$	$(0.06, -1, 1, 1.99)$	0.13	4	
	$(1, 2)$	$(0.5, 0.6)$	$(-1, -1, 0, 0)$	$(0.09, -1, 1, 1.99)$	0.96	7	
P_2 [15]	$(0.1, 2)$	$(0.1, 0.1)$	$(-1, -1, 0, 0)$	$(-0.99, -0.98, 1.99, 1.99)$	0.12	4	$(-1, -1, 2, 2)$
	$(100, 5)$	$(0.01, 0.1)$	$(-1, -1, 0, 0)$	$(-0.99, -0.98, 1.99, 1.99)$	0.10	3	
	$(0.01, 5)$	$(0.1, 0.1)$	$(1, -0.75, 0, 0)$	$(-0.99, -0.98, 1.99, 1.99)$	0.14	4	
P_3 [15]	$(1, 2)$	$(0.1, 0.6)$	$(0, 0, 0, 0)$	$(-0.02, -0.02, 1, 0.99)$	0.15	4	$(0, 0, 1, 1)$
	$(10, 2)$	$(0.01, 0.1)$	$(0, 0, 0, 0)$	$(-0.001, -0.001, 1, 0.99)$	0.12	3	
	$(1, 10)$	$(0.1, 0.01)$	$(0, 0, 0, 0)$	$(0.03, 0.03, 1, 0.99)$	0.06	2	
P_4 [15]	$(0.1, 2)$	$(0.5, 0.6)$	$(-0.5, 0)$	$(-0.07, 0.99)$	0.23	8	$(0, 1)$
	$(1, 2)$	$(0.01, 0.06)$	$(0, 0)$	$(-0.07, 0.99)$	0.24	8	
	$(10, 2)$	$(0.01, 0.06)$	$(0, 0)$	$(0.0.99)$	0.24	9	
P_5 [15]	$(10^{-3}, 0.002)$	$(3, 0.1)$	$(0, 0, 0, 0, 0, 0)$	$(0.49, 0.49, 0, 0, 0, 1.99)$	0.06	2	$(0.5, 0.5, 0, 0, 0, 2)$
	$(0.1, 0.01)$	$(3, 0.1)$	$(0, 0, 0, 0, 0, 0)$	$(0.49, 0.49, 0.05, 0, 0, 1.99)$	0.11	4	
	$(1, 2)$	$(0.1, 0.1)$	$(0.5, 0.5, 0, 0, 0, 0)$	$(0.49, 0.49, 0.07, 0, 0, 1.99)$	0.04	2	
P_6	$(0.01, 0.01)$	$(5, 0.5)$	$(0, 0, 0, 0)$	$(19.97, 20.01, 0, 0)$	0.24	8	$(20, 20, 0, 0)$
	$(0.001, 0.01)$	$(5, 0.1)$	$(0, 0, 0, 0)$	$(19.97, 20, 0, 0)$	0.14	4	
	$(10^{-4}, 0.01)$	$(5, 0.01)$	$(2, 2, 6, 6)$	$(19.99, 19.99, 0, 0)$	0.10	3	
P_7 [15]	$(0.1, 0.001)$	$(4, 0.01)$	$(0, 0, 0)$	$(0, 0, 1)$	0.13	4	$(0, 0, 1)$
	$(100, 100)$	$(4, 0.01)$	$(0.5, 0.5, 0)$	$(0, 0, 0.99)$	0.12	3	
	$(1000, 10)$	$(0.01, 0.01)$	$(0.5, 0.5, 0)$	$(0, 0, 0.99)$	0.04	2	
P_8 [10]	$(10^{-5}, 10^{-5})$	$(0.1, 0.6)$	$(0, 0, 0.125,$ $0, 0, 2.1607)$	$(1.49, 0, 0.799$ $0, 0, 2.075)$	0.05	2	$(1.50, 0, 0.8$ $0, 0, 2.075)$

Table 1: Numerical Results for the BL-DCA Algorithm.

6 Conclusions and Future Work

In this paper, we use DC programming approaches to introduce a novel method for addressing a class of bilevel programming problems. The key innovation lies in regularizing the lower-level value function, enabling the problem to be effectively reformulated as a DC program. This transformation offers a new perspective on handling non-convex bilevel problems where traditional methods fail. Although DC programming provides only local solutions, it proves to be highly effective for non-convex problems. In future work, we plan to develop additional methods within the DC programming framework to ensure global solutions and extend the algorithm to address other classes of bilevel programming problems.

References

[1] N. Anane, Z. Kebaili and M. Achache. A DC algorithm for solving non-uniquely solvable absolute value equations. *Nonlinear Dynamics and Systems Theory* **23** (2) (2023) 119–129.

[2] A. Anzi and M. S. Radjef. A DC Algorithm for Solving Quadratic-linear Bilevel Optimization Problems. In: *Modelling, Computation and Optimization in Information Systems and Management Sciences.* Proceedings of the 3rd International Conference on Modelling, Computation and Optimization in Information Systems and Management Sciences-MCO 2015-Part I. Springer International Publishing, 2015, 119–129.

[3] A. Boukoftane, M. A. Kalwar, N. Oukid, K. Zennir, M. S. Memon and M. A. Khan. Application of discrete event simulation and system dynamics modeling in optimizing the performance of outpatient department. *Nonlinear Dynamics and Systems Theory* **24** (4) (2024) 354–365.

[4] S. Dempe. A bundle algorithm applied to bilevel programming problems with non-unique lower level solutions. *Computational Optimization and Applications* **15** (2000) 145–166.

[5] S. Dempe and S. Franke. Solution of bi-level optimization problems using the KKT approach. *Optimization* **68** (2019) 1471–1489.

[6] L. L. Gao, J. J. Ye, H. Yin, et al. Moreau envelope based difference-of-weakly-convex reformulation and algorithm for bilevel programs. *arXiv preprint* arXiv:2306.16761 (2023).

[7] H. A. Le Thi and P. D. Tao. DC programming and DCA: thirty years of developments. *Mathematical Programming* **169** (1) (2018) 5–68.

[8] Z. F. Li, K. W. Ng, and X. T. Deng. Continuous-time optimal portfolio selection using mean-CaR models. *Nonlinear Dynamics and Systems Theory* **7** (2007) 35–49.

[9] B. S. Mordukhovich and N. M. Nam. *An Easy Path to Convex Analysis and Applications.* Morgan & Claypool Publishers, 2014.

[10] K. Moshirvaziri, M. A. Amouzegar and S. E. Jacobsen. Test problem construction for linear bilevel programming problems. *Journal of Global Optimization* **8** (1996) 235–243.

[11] Y. S. Niu. On the convergence analysis of DCA. *arXiv preprint* arXiv:2211.10942 (2022).

[12] J. V. Outrata. On the numerical solution of a class of Stackelberg problems. *Zeitschrift für Operations Research* **34** (1990) 255–277.

[13] T. D. Quynh, P. D. Tao, et al. A DC programming approach for a class of bilevel programming problems and its application in portfolio selection. *Numerical Algebra, Control and Optimization* **2** (1) (2012) 167–185.

[14] J. J. Ye and D. L. Zhu. Optimality conditions for bi-level programming problems. *Optimization* **33** (1995) 9–27.

[15] S. Zhou, A. B. Zemkoho and A. Tin. BOLIB 2019: Bilevel Optimization LIBrary of test problems version 2, 2019.

Nonlinear Dynamics and Systems Theory, **25** (6) (2025) 608–620

Adaptive Controller with Fixed-Time Convergence for Combination Synchronization of Multiple Master and Slave Chaotic Systems

Chaima Boulezaz [1] and Rabiaa Ouahabi [2*]

[1] *Applied Mathematics & Modeling Laboratory, University of Constantine 1, Brothers Mentouri, 25000 Constantine, Algeria.*
[2] *Mathematical Modeling and Simulation Laboratory, Department of Mathematics, University of Constantine 1, Brothers Mentouri, Algeria.*

Received: December 24, 2024; Revised: November 20, 2025

Abstract: This paper mainly studies the fixed-time combination synchronization between different multiple chaotic systems using adaptive control. Asymptotic combination synchronization has previously been considered, but the fixed-time combination synchronisation of multiple chaotic systems with unknown parameters is the first of its kind. The fixed time control and adaptive control algorithms are successfully included to realize the combination synchronization between different multiple chaotic systems. The advantages of the proposed scheme include the possibility of realizing synchronization between almost all different chaotic systems in a short fixed time. According to the Lyapunov theory and fixed time laws, the unknown parameters are estimated and the settling time is calculated. Numerical simulation results are presented to prove the effectiveness of the proposed scheme.

Keywords: *chaotic systems; Lyapunov stability; fixed time stability; synchronization; adaptive control.*

Mathematics Subject Classification (2020): 93D40, 93D15, 34H05, 37C75.

* Corresponding author: mailto:rabiaa.ouahabi@umc.edu.dz

1 Introduction

Chaotic synchronization is one of the most important branches of chaos theory due to its real applications in numerous fields including secure communications [1], optical communication [2], biological systems [3], finance [4], neural networks [5], cryptography [6, 7], and lasers [8].

Various control techniques have been proposed to achieve chaos synchronization, namely active control [9, 10], sliding mode [11], event-triggered strategy [12], backstepping [13], adaptive control [14, 15].

In recent years, more attention has been paid to the study of combination synchronization. This method was initially proposed by Luo [16], when two master systems were synchronized with one slave system. Subsequently, Ayub et al. [17] proposed dual combination-combination synchronization (DCCS) between four master and four slave systems.

The DCCS scheme is a promising technique to improve both privacy and security in communication networks, to encode and decode information at the hardware level.

In the literature, there is also a number of results on combination synchronization, see [18, 19].

On the other hand, note that all the above papers [18,19] concern only the asymptotic chaos synchronization, in which the master and slave systems synchronize with the infinite settling time.

Later, some papers studied combination synchronization in finite-time, see [20], but this method has some limitations, in particular, the settling time of synchronisation depends on the initial conditions.

This is a shortcoming because the application of this method in reality is impractical, especially if the initial conditions are not known in advance, in addition, the design of the synchronization scheme applied in these studies relates to the synchronization between two identical chaotic systems with known parameters. This is also a deficiency since the parameters of chaotic systems may be unknown, moreover, generalized synchronization is worth studying more than identical synchronization.

So, achieving chaos combination synchronization in determined time independent of any initial value in the practical engineering application is a desirable objective.

Researchers have recently been interested in studying synchronization in fixed time, see [21, 22], and so far, there are few results in the literature on this subject.

Compared to the current results, there are no published papers in which the adaptive fixed-time combination synchronization of multiple master and slave chaotic systems has been studied. This has prompted us to undertake this work to address some of the aforementioned deficiencies.

Inspired by the discussion above, this paper discussed the combination synchronization of different multiple chaotic systems with unknown parameters in a fixed time.

The main contribution of this paper is to show how a basic technique can be used to design an appropriate controller to accomplish fixed time combination synchronization and it is summarized as follows.

- Based on the fixed time stability theory and adaptive method, an effective control is designed to solve the fixed time combination synchronization of different multiple chaotic systems.

- A new theorem is proposed to demonstrate that the presented algorithm is an appropriate choice to achieve the combination synchronization of chaotic systems with unknown parameters.

- The settling time of the fixed time combination synchronization is bounded for any initial condition states.

The features of the proposed scheme that made it innovative and very important are:

- The scheme can be applied to almost all chaotic and even hyperchaotic dynamic systems.
- The possibility of applying it in case all master and slave systems are different and customizing it in case they are identical.
- The combination synchronization is achievable in a short fixed time.

The remainder of this paper is organizes as follows.

Some necessary definitions and lemmas are presented in Section 2. Section 3 contains the proposed scheme that is designed to obtain the desired fixed time combination synchronization. Some numerical simulations are presented in Section 4. The conclusion of the work is given in the last section.

2 Definitions and Lemmas

This section presents some of the definitions and lemmas related to this work.

Consider the nonlinear autonomous system

$$\begin{cases} \frac{dX(t)}{dt} = F(X(t)), \\ X(0) = X_0, \end{cases} \tag{1}$$

where $X \in \mathbb{R}^n$. Here, the results are presented under the assumption that the origin is an equilibrium point of the system (1).

Definition 2.1 The origin of (1) is said to be **fixed-time stable** if it is globally finite-time stable and the settling-time function $T^*(X_0)$ is bounded, i.e., $\exists T^*_{Max} > 0 :$ $T^*(X_0) < T^*_{Max}, \forall\ X_0 \in \mathbb{R}^n$.

Lemma 2.1 *[23] If there exists a continuous radically unbounded function* $V :$ $\mathbb{R}^n \longrightarrow \mathbb{R}^+ \cup \{0\}$ *such that*

- $V(x) = 0 \Leftrightarrow x = 0$,
- *any solution* $X(t)$ *of (1) satisfies the inequality*

$$\begin{array}{l} \dot{V}(X(t)) + \beta_1 V^{\alpha_1}(X(t)) + \beta_2 V^{\alpha_2}(X(t)) \ \leq 0 \\ \text{for } \beta_1,\ \beta_2,\ \alpha_1,\ \alpha_2 > 0,\ \alpha_1 < 1, \quad \alpha_2 > 1, \end{array}$$

then the origin of (1) is fixed-time stable and the settling-time function is estimated by

$$T^*(X_0) \leq \frac{1}{\beta_1\,(1-\alpha_1)} + \frac{1}{\beta_2\,(\alpha_2-1)}, \forall X_0 \in \mathbb{R}^n.$$

Lemma 2.2 *[24] For any V_i, $(i = \overline{1,n})$, $0 < a < 1$, $b > 1$,*

$$\begin{cases} \sum\limits_{i=1}^{n} (V_i)^a \geq \left[\sum\limits_{i=1}^{n} (V_i)\right]^a, \\ \sum\limits_{i=1}^{n} (V_i)^b \geq n^{1-b} \left[\sum\limits_{i=1}^{n} (V_i)\right]^b. \end{cases}$$

3 Formulation of Fixed Time Combination Synchronization Scheme

In this section, we propose a new control law to achieve the adaptive fixed time combination synchronization of multiple master and slave systems. Under the proposed control laws, errors converge to zero in a bounded time. Consider the first two master chaotic systems given as

$$\begin{cases} \dot{x} = f_1(x) + A(x)\eta, \\ \dot{y} = f_2(y) + B(y)\xi, \end{cases} \tag{2}$$

where $x = (x_1, x_2, ..., x_n)^T$, $y = (y_1, y_2, ..., y_n)^T$ are the state vectors, $f_1, f_2 : \mathbb{R}^n \longrightarrow \mathbb{R}^n$ are two nonlinear functions, $A(x) \in \mathbb{R}^{n\times r}$, $B(y) \in \mathbb{R}^{n\times s}$ are matrix functions, $\eta \in \mathbb{R}^r$, $\xi \in \mathbb{R}^s$ are unknown parameter vectors.

The second two master chaotic systems are described as follows:

$$\begin{cases} \dot{\bar{x}} = \bar{f}_1(\bar{x}) + \bar{A}(\bar{x})\bar{\eta}, \\ \dot{\bar{y}} = \bar{f}_2(\bar{y}) + \bar{B}(\bar{y})\bar{\xi}, \end{cases} \tag{3}$$

where $\bar{x} = (\bar{x}_1, \bar{x}_2, ..., \bar{x}_n)^T$, $\bar{y} = (\bar{y}_1, \bar{y}_2, ..., \bar{y}_n)^T$ are the state vectors, $\bar{f}_1, \bar{f}_2 : \mathbb{R}^n \longrightarrow \mathbb{R}^n$ are two nonlinear functions, $\bar{A}(\bar{x}) \in \mathbb{R}^{n\times\bar{r}}$, $\bar{B}(\bar{y}) \in \mathbb{R}^{n\times\bar{s}}$ are matrix functions, $\bar{\eta} \in \mathbb{R}^{\bar{r}}$, $\bar{\xi} \in \mathbb{R}^{\bar{s}}$ are unknown parameter vectors.

The combination of the state vectors of two primary (2) and two secondary (3) master systems is given, respectively, by

$$X = \begin{pmatrix} x \\ y \end{pmatrix} = (x_1, ..., x_n, y_1, y_2, ..., y_n)^T, \bar{X} = \begin{pmatrix} \bar{x} \\ \bar{y} \end{pmatrix} = (\bar{x}_1, ..., \bar{x}_n, \bar{y}_1, \bar{y}_2, ..., \bar{y}_n)^T.$$

The combination of nonlinear functions of two primary and two secondary master systems is represented, respectively, by

$$f(X) = \begin{pmatrix} f_1(x) \\ f_2(y) \end{pmatrix} = [f_{11}(x), f_{12}(x), ..., f_{1n}(x), f_{21}(y), f_{22}(y), ..., f_{2n}(y)]^T, \tag{4}$$

$$\bar{f}(\bar{X}) = \begin{pmatrix} \bar{f}_1(\bar{x}) \\ \bar{f}_2(\bar{y}) \end{pmatrix} = \left[\bar{f}_{11}(\bar{x}), \bar{f}_{12}(\bar{x}), ..., \bar{f}_{1n}(\bar{x}), \bar{f}_{21}(\bar{y}), \bar{f}_{22}(\bar{y}), ..., \bar{f}_{2n}(\bar{y})\right]^T. \tag{5}$$

Consider the first two chaotic slave systems given below:

$$\begin{cases} \dot{z} = g_1(z) + C(z)\rho + u_1, \\ \dot{w} = g_2(w) + D(w)\theta + u_2, \end{cases} \tag{6}$$

where $z = (z_1, z_2, ..., z_n)^T$, $w = (w_1, w_2, ..., w_n)^T$ are the state vectors, $g_1, g_2 : \mathbb{R}^n \longrightarrow \mathbb{R}^n$ are two nonlinear functions, $C(z) \in \mathbb{R}^{n\times q}$, $D(w) \in \mathbb{R}^{n\times l}$ are matrix functions,

$\rho \in \mathbb{R}^q$, $\theta \in \mathbb{R}^l$ are unknown parameter vectors, $u_1 = (u_{11},\ u_{12}, ...,\ u_{1n})$, and $u_2 = (u_{21},\ u_{22}, ...,\ u_{2n})$ represent the controllers which are to be designed.

Suppose the second two slave chaotic systems are given as follows:

$$\begin{cases} \dot{\bar{z}} = \bar{g}_1(\bar{z}) + \bar{C}(\bar{z})\,\bar{\rho} + \bar{u}_1, \\ \dot{\bar{w}} = \bar{g}_2(\bar{w}) + \bar{D}(\bar{w})\,\bar{\theta} + \bar{u}_2, \end{cases} \tag{7}$$

where $\bar{z} = (\bar{z}_1, \bar{z}_2, ..., \bar{z}_n)^T$, $\bar{w} = (\bar{w}_1, \bar{w}_2, ..., \bar{w}_n)^T$ are the state vectors, $\bar{g}_1, \bar{g}_2 : \mathbb{R}^n \longrightarrow \mathbb{R}^n$ are two nonlinear functions, $\bar{C}(\bar{z}) \in \mathbb{R}^{n\times\bar{q}}$, $\bar{D}(\bar{w}) \in \mathbb{R}^{n\times\bar{l}}$ are matrix functions, $\bar{\rho} \in \mathbb{R}^{\bar{q}}$, $\bar{\theta} \in \mathbb{R}^{\bar{l}}$ are unknown parameter vectors, $\bar{u}_1, \bar{u}_2 \in \mathbb{R}^n$ represent the controllers of the second slave systems, where $\bar{u}_1 = (\bar{u}_{11},\ \bar{u}_{12}, ...,\ \bar{u}_{1n})$, $\bar{u}_2 = (\bar{u}_{21},\ \bar{u}_{22}, ...,\ \bar{u}_{2n})$.

The combination of the state vectors of two primary (6) and two secondary (7) slave systems is given, respectively, by

$Y = \binom{z}{w} = (z_1,\ z_2, ...,\ z_n,\ w_1, ...,\ w_n)^T$, $\bar{Y} = \binom{\bar{z}}{\bar{w}} = (\bar{z}_1,\ \bar{z}_2, ...,\ \bar{z}_n,\ \bar{w}_1, ...,\ \bar{w}_n)^T$.

The combination of nonlinear functions of two primary and two secondary slave systems is represented, respectively, by

$$g(Y) = \begin{pmatrix} g_1(z) \\ g_2(w) \end{pmatrix} = [g_{11}(z),\ g_{12}(z), ...,\ g_{1n}(z),\ g_{21}(w),\ g_{22}(w), ...,\ g_{2n}(w)]^T, \tag{8}$$

$$\bar{g}(\bar{Y}) = \begin{pmatrix} \bar{g}_1(\bar{z}) \\ \bar{g}_2(\bar{w}) \end{pmatrix} = [\bar{g}_{11}(\bar{z}),\ \bar{g}_{12}(\bar{z}), ...,\ \bar{g}_{1n}(\bar{z}),\ \bar{g}_{21}(\bar{w}),\ \bar{g}_{22}(\bar{w}), ...,\ \bar{g}_{2n}(\bar{w})]^T. \tag{9}$$

Remark 3.1 The matrix functions are combined as shown below:

$\psi(X) = \begin{pmatrix} A(x) & 0 \\ 0 & B(y) \end{pmatrix}$, $\bar{\psi}(\bar{X}) = \begin{pmatrix} \bar{A}(\bar{x}) & 0 \\ 0 & \bar{B}(\bar{y}) \end{pmatrix}$, $\phi(Y) = \begin{pmatrix} C(z) & 0 \\ 0 & D(w) \end{pmatrix}$, $\bar{\phi}(\bar{Y}) = \begin{pmatrix} \bar{C}(\bar{z}) & 0 \\ 0 & \bar{D}(\bar{w}) \end{pmatrix}$.

The combination synchronization error between the systems (2), (3) and the systems (6), (7) is defined by

$$e = Y + \bar{Y} - (X + \bar{X}),$$

where $e = \binom{e_1}{e_2} = \binom{Y-X}{\bar{Y}-\bar{X}}$, $e_1 = (e_{11}, e_{12}, ..., e_{1n})^T$, and $e_2 = (e_{21}, e_{22}, ..., e_{2n})^T$.

Then we obtain the error dynamical system

$$\dot{e} = \dot{Y} + \dot{\bar{Y}} - \left(\dot{X} + \dot{\bar{X}}\right). \tag{10}$$

Theorem 3.1 *Let T^* be given by*

$$T^* = \frac{1}{2^{\frac{\mu+1}{2}}\left(\frac{1-\mu}{2}\right)k} + \frac{1}{2^{\frac{\lambda+1}{2}}(Q)^{\frac{1-\lambda}{2}}\left(\frac{\lambda-1}{2}\right)k}, \tag{11}$$

where $Q = 2n + m + \bar{m} + p + \bar{p}$.

Adaptive combination synchronization between systems (2), (3) and systems (6), (7) in fixed time (11) can be obtained if the following conditions are met.

1. Control laws are designed as

$$\begin{aligned} u(t) + \bar{u}(t) &= -\left[g(Y) + \bar{g}(\bar{Y}) + \phi(Y)\tilde{\gamma} + \bar{\phi}(\bar{Y})\tilde{\bar{\gamma}} \right] \\ &+ \left(f(X) + \bar{f}(\bar{X}) + \psi(X)\tilde{\delta} + \bar{\psi}(\bar{X})\tilde{\bar{\delta}} \right) - k\left(|e|^{\mu} + |e|^{\lambda} \right) sgn(e). \end{aligned}$$

2. Parameter update laws are given by

$$\begin{cases} \dot{\tilde{\delta}} = -[\psi(X)]^T e + k\left(\left|\delta - \tilde{\delta}\right|^{\mu} + \left|\delta - \tilde{\delta}\right|^{\lambda} \right) sgn\left(\delta - \tilde{\delta}\right), \\ \dot{\tilde{\bar{\delta}}} = -\left[\bar{\psi}(\bar{X})\right]^T e + k\left(\left|\bar{\delta} - \tilde{\bar{\delta}}\right|^{\mu} + \left|\delta - \tilde{\bar{\delta}}\right|^{\lambda} \right) sgn\left(\bar{\delta} - \tilde{\bar{\delta}}\right), \\ \dot{\tilde{\gamma}} = [\phi(Y)]^T e + k\left(|\gamma - \tilde{\gamma}|^{\mu} + |\gamma - \tilde{\gamma}|^{\lambda} \right) sgn(\gamma - \tilde{\gamma}), \\ \dot{\tilde{\bar{\gamma}}} = \left[\bar{\phi}(\bar{Y})\right]^T e + k\left(\left|\bar{\gamma} - \tilde{\bar{\gamma}}\right|^{\mu} + \left|\bar{\gamma} - \tilde{\bar{\gamma}}\right|^{\lambda} \right) sgn\left(\bar{\gamma} - \tilde{\bar{\gamma}}\right), \end{cases} \tag{12}$$

where $k > 0$, $0 < \mu < 1$, $\lambda > 1$.

Proof. Substituting (12) into (10) yields the error dynamics

$$\begin{aligned} \dot{e} &= \phi(Y)(\gamma - \tilde{\gamma}) + \bar{\phi}(\bar{Y})\left(\bar{\gamma} - \tilde{\bar{\gamma}}\right) - \left(\psi(X)\left(\delta - \tilde{\delta}\right) + \bar{\psi}(\bar{X})\left(\bar{\delta} - \tilde{\bar{\delta}}\right) \right) \\ &-k\left(|e|^{\mu} + |e|^{\lambda} \right) sgn(e). \end{aligned} \tag{13}$$

Take the Lyapunov function candidate as

$$V = \frac{1}{2}\left[\begin{array}{c} e^T e + \left(\delta - \tilde{\delta}\right)^T \left(\delta - \tilde{\delta}\right) + \left(\bar{\delta} - \tilde{\bar{\delta}}\right)^T \left(\bar{\delta} - \tilde{\bar{\delta}}\right) + (\gamma - \tilde{\gamma})^T (\gamma - \tilde{\gamma}) + \\ + \left(\bar{\gamma} - \tilde{\bar{\gamma}}\right)^T \left(\bar{\gamma} - \tilde{\bar{\gamma}}\right) \end{array} \right]. \tag{14}$$

Compute the derivative of Lyapunov function

$$\dot{V} = \frac{1}{2}\left[\begin{array}{c} \dot{e}^T e + \left(\delta - \tilde{\delta}\right)^T \left(-\dot{\tilde{\delta}}\right) + \left(\bar{\delta} - \tilde{\bar{\delta}}\right)^T \left(-\dot{\tilde{\bar{\delta}}}\right) + (\gamma - \tilde{\gamma})^T \left(-\dot{\tilde{\gamma}}\right) \\ + \left(\bar{\gamma} - \tilde{\bar{\gamma}}\right)^T \left(-\dot{\tilde{\bar{\gamma}}}\right) \end{array} \right].$$

Substituting expressions (12) and (13), we get

$$
\begin{aligned}
\dot{V} &= \left[\begin{array}{c} \phi(Y)(\gamma-\tilde{\gamma})+\bar{\phi}(\bar{Y})\left(\bar{\gamma}-\tilde{\bar{\gamma}}\right)-\left(\psi(X)\left(\delta-\tilde{\delta}\right)+\bar{\psi}(\bar{X})\left(\bar{\delta}-\tilde{\bar{\delta}}\right)\right) \\ -k\left(|e|^{\mu}+|e|^{\lambda}\right) sgn(e) \end{array}\right]^{T} e \\
&\quad+\left(\delta-\tilde{\delta}\right)^{T}\left[[\psi(X)]^{T} e-k\left(\left|\delta-\tilde{\delta}\right|^{\mu}+\left|\delta-\tilde{\delta}\right|^{\lambda}\right) sgn\left(\delta-\tilde{\delta}\right)\right] \\
&\quad+\left(\bar{\delta}-\tilde{\bar{\delta}}\right)^{T}\left[\left[\bar{\psi}(\bar{X})\right]^{T} e-k\left(\left|\bar{\delta}-\tilde{\bar{\delta}}\right|^{\mu}+\left|\delta-\tilde{\bar{\delta}}\right|^{\lambda}\right) sgn\left(\bar{\delta}-\tilde{\bar{\delta}}\right)\right] \\
&\quad+(\gamma-\tilde{\gamma})^{T}\left[-[\phi(Y)]^{T} e-k\left(|\gamma-\tilde{\gamma}|^{\mu}+|\gamma-\tilde{\gamma}|^{\lambda}\right) sgn(\gamma-\tilde{\gamma})\right] \\
&\quad+\left(\bar{\gamma}-\tilde{\bar{\gamma}}\right)^{T}\left[-\left[\bar{\phi}(\bar{Y})\right]^{T} e-k\left(\left|\bar{\gamma}-\tilde{\bar{\gamma}}\right|^{\mu}+\left|\bar{\gamma}-\tilde{\bar{\gamma}}\right|^{\lambda}\right) sgn\left(\bar{\gamma}-\tilde{\bar{\gamma}}\right)\right] \\
&= (\gamma-\tilde{\gamma})^{T}[\phi(Y)]^{T} e+\left(\bar{\gamma}-\tilde{\bar{\gamma}}\right)^{T}\left[\bar{\phi}(\bar{Y})\right]^{T} e-\left(\delta-\tilde{\delta}\right)^{T}[\psi(X)]^{T} e \\
&\quad-\left(\bar{\delta}-\tilde{\bar{\delta}}\right)\left[\bar{\psi}(\bar{X})\right]^{T} e-k(sgn(e))^{T}\left(|e|^{\mu}+|e|^{\lambda}\right)^{T} e \\
&\quad+\left(\delta-\tilde{\delta}\right)^{T}[\psi(X)]^{T} e-k\left(\delta-\tilde{\delta}\right)^{T}\left(\left|\delta-\tilde{\delta}\right|^{\mu}+\left|\delta-\tilde{\delta}\right|^{\lambda}\right) sgn\left(\delta-\tilde{\delta}\right) \\
&\quad+\left(\bar{\delta}-\tilde{\bar{\delta}}\right)^{T}\left[\bar{\psi}(\bar{X})\right]^{T} e-k\left(\bar{\delta}-\tilde{\bar{\delta}}\right)^{T}\left(\left|\bar{\delta}-\tilde{\bar{\delta}}\right|^{\mu}+\left|\delta-\tilde{\bar{\delta}}\right|^{\lambda}\right) sgn\left(\bar{\delta}-\tilde{\bar{\delta}}\right)- \\
&\quad-(\gamma-\tilde{\gamma})^{T}[\phi(Y)]^{T} e-k(\gamma-\tilde{\gamma})^{T}\left(|\gamma-\tilde{\gamma}|^{\mu}+|\gamma-\tilde{\gamma}|^{\lambda}\right) sgn(\gamma-\tilde{\gamma})- \\
&\quad-\left(\bar{\gamma}-\tilde{\bar{\gamma}}\right)^{T}\left[\bar{\phi}(\bar{Y})\right]^{T} e-k\left(\bar{\gamma}-\tilde{\bar{\gamma}}\right)^{T}\left(\left|\bar{\gamma}-\tilde{\bar{\gamma}}\right|^{\mu}+\left|\bar{\gamma}-\tilde{\bar{\gamma}}\right|^{\lambda}\right) sgn\left(\bar{\gamma}-\tilde{\bar{\gamma}}\right)
\end{aligned}
$$

$$
\begin{aligned}
\dot{V} &= -k(sgn(e))^{T}\left(|e|^{\mu}+|e|^{\lambda}\right)^{T} e-k\left(\delta-\tilde{\delta}\right)^{T}\left(\left|\delta-\tilde{\delta}\right|^{\mu}+\left|\delta-\tilde{\delta}\right|^{\lambda}\right) sgn\left(\delta-\tilde{\delta}\right) \\
&\quad-k\left(\bar{\delta}-\tilde{\bar{\delta}}\right)^{T}\left(\left|\bar{\delta}-\tilde{\bar{\delta}}\right|^{\mu}+\left|\delta-\tilde{\bar{\delta}}\right|^{\lambda}\right) sgn\left(\bar{\delta}-\tilde{\bar{\delta}}\right) \\
&\quad-k(\gamma-\tilde{\gamma})^{T}\left(|\gamma-\tilde{\gamma}|^{\mu}+|\gamma-\tilde{\gamma}|^{\lambda}\right) sgn(\gamma-\tilde{\gamma}) \\
&\quad-k\left(\bar{\gamma}-\tilde{\bar{\gamma}}\right)^{T}\left(\left|\bar{\gamma}-\tilde{\bar{\gamma}}\right|^{\mu}+\left|\bar{\gamma}-\tilde{\bar{\gamma}}\right|^{\lambda}\right) sgn\left(\bar{\gamma}-\tilde{\bar{\gamma}}\right)
\end{aligned}
$$

$$
\begin{aligned}
\dot{V} &= -k\sum_{i=1}^{2n}\left(|e_i|^{\mu+1}+|e_i|^{\lambda+1}\right)-k\sum_{i=1}^{m}\left(\left|\delta_i-\tilde{\delta}_i\right|^{\mu+1}+\left|\delta_i-\tilde{\delta}_i\right|^{\lambda+1}\right) \\
&\quad-k\sum_{i=1}^{\bar{m}}\left(\left|\bar{\delta}_i-\tilde{\bar{\delta}}_i\right|^{\mu+1}+\left|\delta_i-\tilde{\bar{\delta}}_i\right|^{\lambda+1}\right)-k\sum_{i=1}^{p}\left(|\gamma_i-\tilde{\gamma}_i|^{\mu+1}+|\gamma_i-\tilde{\gamma}_i|^{\lambda+1}\right) \\
&\quad-k\sum_{i=1}^{\bar{p}}\left(\left|\bar{\gamma}_i-\tilde{\bar{\gamma}}_i\right|^{\mu+1}+\left|\bar{\gamma}_i-\tilde{\bar{\gamma}}_i\right|^{\lambda+1}\right),
\end{aligned}
$$

then

$$\dot{V} = -k\left[\begin{array}{c}\sum_{i=1}^{2n}\left(\left(e_i^2\right)^{\frac{\mu+1}{2}}\right)+\sum_{i=1}^{m}\left(\left(\delta_i-\tilde{\delta}_i\right)^2\right)^{\frac{\mu+1}{2}}+\sum_{i=1}^{\bar{m}}\left(\left(\bar{\delta}_i-\tilde{\bar{\delta}}_i\right)^2\right)^{\frac{\mu+1}{2}}\\ +\sum_{i=1}^{p}\left((\gamma_i-\tilde{\gamma}_i)^2\right)^{\frac{\mu+1}{2}}+\sum_{i=1}^{\bar{p}}\left(\left(\bar{\gamma}_i-\tilde{\bar{\gamma}}_i\right)^2\right)^{\frac{\mu+1}{2}}\end{array}\right] -k\left[\begin{array}{c}\sum_{i=1}^{2n}\left(\left(e_i^2\right)^{\frac{\lambda+1}{2}}\right)+\sum_{i=1}^{m}\left(\left(\delta_i-\tilde{\delta}_i\right)^2\right)^{\frac{\lambda+1}{2}}+\sum_{i=1}^{\bar{m}}\left(\left(\bar{\delta}_i-\tilde{\bar{\delta}}_i\right)^2\right)^{\frac{\lambda+1}{2}}\\ +\sum_{i=1}^{p}\left((\gamma_i-\tilde{\gamma}_i)^2\right)^{\frac{\lambda+1}{2}}+\sum_{i=1}^{\bar{p}}\left(\left(\bar{\gamma}_i-\tilde{\bar{\gamma}}_i\right)^2\right)^{\frac{\lambda+1}{2}}\end{array}\right].$$

According to the equation (14),

$$V=\frac{1}{2}\left[\sum_{i=1}^{2n}(e_i)^2+\sum_{i=1}^{m}\left(\delta_i-\tilde{\delta}_i\right)^2+\sum_{i=1}^{\bar{m}}\left(\bar{\delta}_i-\tilde{\bar{\delta}}_i\right)^2+\sum_{i=1}^{p}(\gamma_i-\tilde{\gamma}_i)^2+\sum_{i=1}^{\bar{p}}\left(\bar{\gamma}_i-\tilde{\bar{\gamma}}_i\right)^2\right].$$

According to Lemma (2.2),

$$\dot{V}\le -2^{\frac{\mu+1}{2}}k\ \left(\sum_{i=1}^{Q}V_i\right)^{\frac{\mu+1}{2}} - 2^{\frac{\lambda+1}{2}}k\ (Q)^{\frac{1-\lambda}{2}}\ \left(\sum_{i=1}^{Q}V_i\right)^{\frac{\lambda+1}{2}}.$$

This means

$$\dot{V}\le -2^{\frac{\mu+1}{2}}k\ V^{\frac{\mu+1}{2}}-2^{\frac{\lambda+1}{2}}k\ (Q)^{\frac{1-\lambda}{2}}\ V^{\frac{\lambda+1}{2}}.$$

According to Lemma (2.1), we can conclude that the origin e_0 of system (10) is fixed time stable under the proposed controller (12), this means that the adaptive combination synchronization is achieved between the systems (2), (3) and the systems (6), (7) in fixed time convergence, and the settling-time function $T^*(e_0)$ is bounded by (11), and also, $e(t) = 0$ for $t \ge T^*_{Max}$. This completes the proof.

4 Numerical Simulations

In this section, four different master systems and four different response systems are used to verify the effectiveness of the proposed scheme.

First two master systems [25], [26] are given, respectively, by

$$\begin{cases}\dot{x}_1=-\eta_1x_1+\eta_2x_2x_3,\\ \dot{x}_2=\eta_3x_2-\eta_4x_1x_3,\\ \dot{x}_3=-\eta_5x_3+\eta_6x_1x_2,\end{cases}\tag{15}$$

$$\begin{cases}\dot{y}_1=\xi_1(y_2-y_1),\\ \dot{y}_2=-y_1y_3+\xi_2y_2,\\ \dot{y}_3=y_1y_2-\xi_3y_3,\end{cases}\tag{16}$$

where η_i, $(i=\overline{1,6})$ and ξ_i, $(i=\overline{1,3})$ are unknown parameters, according to [25] and [26], the systems (15) and (16) are chaotic when the parameters take the values ($\eta_1 = 4$, $\eta_2 = 3$, $\eta_3 = 1$, $\eta_4 = 7$, $\eta_5 = 1$, $\eta_6 = 2$) and ($\xi_1 = 36$, $\xi_2 = 28$, $\xi_3 = 3$).

The second two master systems defined in [27] are given as follows:

$$\begin{cases} \dot{\bar{x}}_1 = \bar{x}_2\bar{x}_3, \\ \dot{\bar{x}}_2 = \bar{x}_1 - \bar{x}_2, \\ \dot{\bar{x}}_3 = \bar{\eta}_1 \left|\bar{x}_1\right| - \bar{\eta}_2 x_1^2, \end{cases} \tag{17}$$

$$\begin{cases} \dot{\bar{y}}_1 = \bar{\xi}_1(\bar{y}_2 - \bar{y}_1), \\ \dot{\bar{y}}_2 = -\bar{y}_1\bar{y}_3 + \bar{\xi}_2\bar{y}_2, \\ \dot{\bar{y}}_3 = \exp(\bar{y}_1\bar{y}_2) - \bar{\xi}_3\bar{y}_3, \end{cases} \tag{18}$$

where $\bar{\eta}_i$, $(i = 1{,}2)$ and $\bar{\xi}_i$, $(i = \overline{1,3})$ are unknown parameters. The systems (17) and (18) are chaotic when the parameters are given by $(\bar{\eta}_1 = 5,\ \bar{\eta}_2 = 2)$ and $(\bar{\xi}_1 = 33,\ \bar{\xi}_2 = 19.5,\ \bar{\xi}_3 = 8)$.

The two first slave systems [28], [29] are given as follows:

$$\begin{cases} \dot{z}_1 = \rho_1(z_2 - z_1) + u_{11}, \\ \dot{z}_2 = \rho_2 z_1 - \rho_3 z_1 z_2 + u_{12}, \\ \dot{z}_3 = -\rho_4 z_3 + \rho_5 z_1^2 + u_{13}, \end{cases} \tag{19}$$

$$\begin{cases} \dot{w}_1 = \theta_1(w_2 - w_1) + u_{21}, \\ \dot{w}_2 = w_1 w_3 + \theta_2 w_2 + u_{22}, \\ \dot{w}_3 = -w_1^2 - \theta_3 w_3 + u_{23}, \end{cases} \tag{20}$$

where ρ_i, $(i = \overline{1,5})$ and θ_i, $(i = \overline{1,3})$ are unknown parameters, according to [28] and [29], the systems (19) and (20) are chaotic when the parameters take the values $(\rho_1 = 10,\ \rho_2 = 40,\ \rho_3 = 1,\ \rho_4 = 2.5,\ \rho_5 = 4)$ and $(\theta_1 = 30,\ \theta_2 = 15,\ \theta_3 = 11)$.

Second slave systems [30], [31] are defined as follows:

$$\begin{cases} \dot{\bar{z}}_1 = \bar{z}_2 + \bar{u}_{11}, \\ \dot{\bar{z}}_2 = \bar{z}_3 + \bar{\rho}_1\bar{z}_2 + \bar{u}_{12}, \\ \dot{\bar{z}}_3 = \bar{\rho}_2\bar{z}_1 + \bar{\rho}_3\bar{z}_2 + \bar{\rho}_4\bar{z}_3 + \bar{\rho}_5\bar{z}_1^2 + \bar{u}_{13}, \ , \end{cases} \tag{21}$$

$$\begin{cases} \dot{\bar{w}}_1 = \bar{\theta}_1(\bar{w}_2 - \bar{w}_1 + \bar{w}_2\bar{w}_3) + \bar{u}_{21}, \\ \dot{\bar{w}}_2 = -\bar{w}_1\bar{w}_3 + \bar{\theta}_2\bar{w}_2 + \bar{u}_{22}, \\ \dot{\bar{w}}_3 = \bar{w}_1\bar{w}_2 - \bar{\theta}_3\bar{w}_3 + \bar{u}_{23}, \end{cases} \tag{22}$$

where $\bar{\rho}_i$, $(i = \overline{1,5})$ and $\bar{\theta}_i$, $(i = \overline{1,3})$ are unknown parameters, according to [30] and [31], the systems (21) and (22) are chaotic when the parameters are $(\bar{\rho}_1 = -0.5,\ \bar{\rho}_2 = -6,\ \bar{\rho}_3 = -2.85,\ \bar{\rho}_4 = -0.5,\ \bar{\rho}_5 = 3)$ and $(\bar{\theta}_1 = 35,\ \bar{\theta}_2 = 14,\ \bar{\theta}_3 = 5)$.

In the numerical simulation, we choose arbitrarily the initial state vectors as

$$\begin{aligned} X(0) &= (-1,\ -10,\ -4,\ -20,\ 10,\ -1)^T,\ \bar{X}(0) = (1,\ 1,\ 2,\ 1,\ 1,\ 10)^T, \\ Y(0) &= (10,\ 3,\ 1,\ 20,\ -20,\ 8)^T,\ \bar{Y}(0) = (-10,\ 10,\ -5,\ 3,\ 15,\ -25)^T. \end{aligned}$$

The initial values of unknown parameters are arbitrarily taken as

$$\begin{aligned} \delta &= \begin{pmatrix} \eta_i \left(i = \overline{1,6}\right) \\ \xi_i \left(i = \overline{1,3}\right) \end{pmatrix} = (10,\ -8,\ 3,\ 1,\ 7,\ -4,\ 1,\ 5,\ 10)^T, \\ \bar{\delta} &= \begin{pmatrix} \bar{\eta}_i \left(i = \overline{1,2}\right) \\ \bar{\xi}_i \left(i = \overline{1,3}\right) \end{pmatrix} = (-5,\ 8,\ -12,\ 3,\ 10)^T, \end{aligned}$$

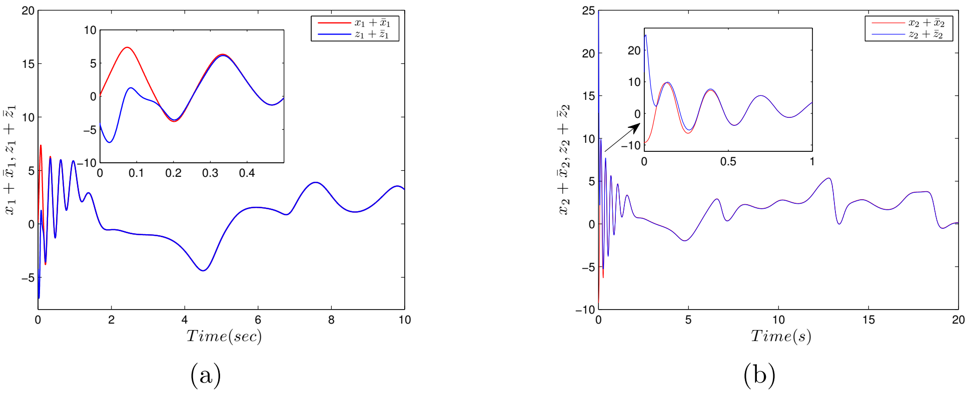

Figure 1: Synchronization for the state trajectories between **(a)**: $z_1 + \bar{z}_1$ and $x_1 + \bar{x}_1$, **(b)**: $z_2 + \bar{z}_2$ and $x_2 + \bar{x}_2$.

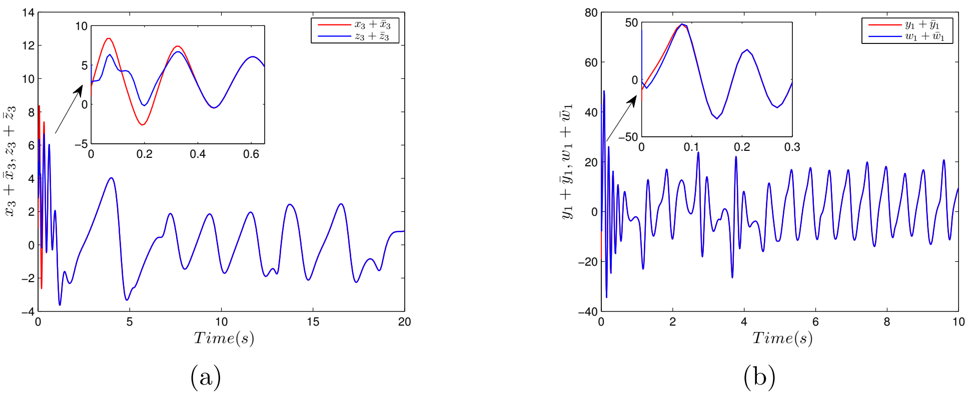

Figure 2: Synchronization for the state trajectories between **(a)**: $z_3 + \bar{z}_3$ and $x_3 + \bar{x}_3$, **(b)**: $w_1 + \bar{w}_1$ and $y_1 + \bar{y}_1$.

$$\begin{aligned}
\gamma &= \begin{pmatrix} \rho_i \left(i = \overline{1,5}\right) \\ \theta_i \left(i = \overline{1,3}\right) \end{pmatrix} = (5, \ -10, \ 45, \ 30, \ -8, \ -20, \ 40, \ 1)^T, \\
\bar{\gamma} &= \begin{pmatrix} \bar{\rho}_i \left(i = \overline{1,5}\right) \\ \bar{\theta}_i \left(i = \overline{1,3}\right) \end{pmatrix} = (-10, \ 1, \ 12, \ -20, \ 2, \ 16, \ 4, \ -6)^T.
\end{aligned}$$

The control gain is given by $k = 6$. Figures 1, 2 and 3 depict the combination synchronization between four master systems (2), (3) and four slave systems (6), (7).

5 Conclusion

The results obtained indicate that in this paper, we have sufficiently proved the combination synchronization of multiple chaotic systems with unknown parameters in a fixed time using an appropriate control algorithm, this algorithm is based on integrating an adaptive control strategy and a fixed time control. According to the Lyapunov theory

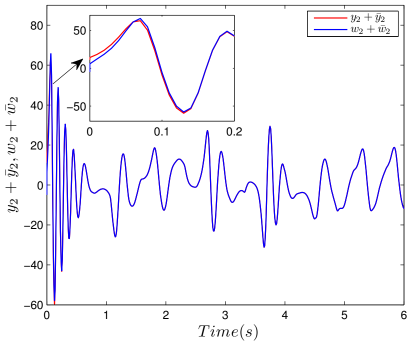

(a)

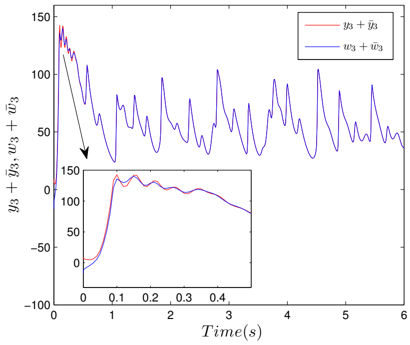

(b)

Figure 3: Synchronization for the state trajectories between
(a): $w_2 + \bar{w}_2$ and $y_2 + \bar{y}_2$, **(b)**: $w_3 + \bar{w}_3$ and $y_3 + \bar{y}_3$.

and fixed time laws, the unknown parameters were estimated and the settling time was also determined.

The proposed scheme was applied to eight different chaotic systems with unknown parameters. Numerical simulation results were presented to demonstrate the effectiveness of theoretical analysis of the proposed scheme. The proposed scheme is an important extension of several existing schemes, which gives this work substantial merits.

References

[1] K. Murali and M. Lakshmanan. Secure communication using a compound signal from generalized synchronizable chaotic systems, *Physics Letters A* **241** (6) (1998) 303–310.

[2] T. Yiwen, L. Qiliang, D. Wenlong, H. Miao and Z. Ran. Optical chaotic communication using correlation demodulation between two synchronized chaos lasers. **498** (2021) 127232.

[3] O. Lars Folke and D. Hans. Chaos in biological systems. *Quarterly Reviews of Biophysics* **18** (2) (1985) 165–225.

[4] G. Dominique. Chaos in economics and finance. *Annual Reviews in Control* **33** (1) (2009) 89–93.

[5] T. Weipeng, T. Qingyong, Z. Youmei, Z. Jianping and W. Zhen. Chaos synchronization of stochastic reaction-diffusion time-delay neural networks via non-fragile output-feedback control. *Applied Mathematics and Computation* **354** (2019) 115–127.

[6] T. Je Sen, A. Moatsum and S. You Cheng. Implementation and practical problems of chaos-based cryptography revisited. *Journal of Information Security and Applications* **50** (2020) 102421.

[7] A. Peyman, S. Saeed and R. Amir Masoud. Deterministic chaos game: a new fractal based pseudo-random number generator and its cryptographic application. *Journal of Information Security and Applications* **52** (2020) 102472.

[8] X. Shuiying, H. Yanan, W. Haoning, W. Aijun and H. Yue. Zero-lag chaos synchronization properties in a hierarchical tree-type network consisting of mutually coupled semiconductor lasers, *Nonlinear Dynamics* **99** (4) (2020) 2893–2906.

[9] S. Vaidyanathan and K. Rajagopal. Chaos synchronization between fractional-order lesser date moth chaotic system and integer-order chaotic system via active control. *Nonlinear Dynamics and Systems Theory* **22** (2022) 407–413.

[10] Y. Ghettout, L. Meddour, T. Hamaizia and R. Ouahabi. Dynamic analysis of a new hyperchaotic system with infinite equilibria and its synchronization. *Nonlinear Dynamics and Systems Theory* **24** (2024) 147–158.

[11] M. Saleh. Chaos synchronization of uncertain chaotic systems using composite nonlinear feedback based integral sliding mode control. *ISA Transactions* **77** (2018) 100–111.

[12] H. Wangli, L. Tinghui, T. Yang, D. Wenli, T. Yu-Chu and Q. Feng. Secure communication based on quantized synchronization of chaotic neural networks under an event-triggered strategy. *IEEE Transactions on Neural Networks and Learning Systems* **31** (9) (2019) 3334–3345.

[13] M. Jesus, V. Christos, S. Fernando, J. Sajad, K. Jacques and R. Karthikeyan. Stabilization and synchronization of a complex hidden attractor chaotic system by backstepping technique. *Entropy* **23** (7) (2021) 921.

[14] O. Rabiaa and H. Nasr-Eddine. Design of new scheme adaptive generalized hybrid projective synchronization for two different chaotic systems with uncertain parameters. *Discrete & Continuous Dynamical Systems-B* **26** (5) (2021) 2361.

[15] R. Rameshbabu, K. Kavitha, P. Gomathi and K. Kalaichelvi. A new hidden attractor hyperchaotic system and its circuit implementation, adaptive synchronization and FPGA implementation, *Nonlinear Dynamics and Systems Theory* **2** (2023) 214–226.

[16] R. Luo, Y. Wang and S. Deng. Combination synchronization of three classic chaotic systems using active backstepping design. *Chaos: An Interdisciplinary Journal of Nonlinear Science* **21** (4) (2011) 043114.

[17] K. Ayub, K. Dinesh and P. Nitish. Dual combination combination multi switching synchronization of eight chaotic systems. *Chinese Journal of Physics* **55** (4) (2017) 1209–1218.

[18] A. Al Themairi, A. Tarek, F. Ahmed and others. Tracking control method for double compound-combination synchronization of fractional chaotic systems and its application in secure communication, *Mathematical Problems in Engineering* **2022** (2022).

[19] M. Gamal, A. Asma, A. Tarek and F. Ahmed. Compound-combination synchronization for fractional hyperchaotic models with different orders. *Symmetry* **15** (2023) 279.

[20] V. Behrouz, M. Saleh, H. Seyedeh Somayeh and F. Afef. Fast reaching finite time synchronization approach for chaotic systems with application in medical image encryption. *IEEE Access* **9** (2021) 25911–25925.

[21] A. Yingdong and W. Huanqing. Fixed-time anti-synchronization of unified chaotic systems via adaptive backstepping approach. *IEEE Transactions on Circuits and Systems II: Express Briefs* **70** (2022) 626–630.

[22] T. Huaigu, W. Zhen, Z. Hui, C. Zelin and Z. Peijun. Dynamical analysis and fixed-time synchronization of a chaotic system with hidden attractor and a line equilibrium. *The European Physical Journal Special Topics* (2022) 2455–2466.

[23] P. Andrey. Nonlinear feedback design for fixed-time stabilization of linear control systems. *IEEE Transactions on Automatic Control* **57** (8) (2011) 2106–2110.

[24] H. Godfrey Harold, L. John Edensor, P. George, P. György et al. Inequalities. *Cambridge University Press* (1952).

[25] P. Gholamin and S. A. H. Refahi. A new three-dimensional chaotic system: dynamical properties and simulation. *Chinese Journal of Physics* **55** (4) (2017) 1300–1309.

[26] L. Jinhu and C. Guanrong. A new chaotic attractor coined. *International Journal of Bifurcation and Chaos* **12** (3) (2002) 659–661.

[27] S. Aceng, V. Sundarapandian, Z. Sen, Z. Yicheng, M. Mohamad Afendee and M. Mustafa. A new double-wing chaotic system with coexisting attractors and line equilibrium: bifurcation analysis and electronic circuit simulation. *IEEE Access* **7** (4) (2019) 115454–115462.

[28] L. Chongxin, L. Tao, L. Ling and L. Kai. A new chaotic attractor. *Chaos, Solitons & Fractals* **22** (5) (2004) 1031-1038.

[29] K. Dongwon and C. Pyung Hun. A new butterfly-shaped chaotic attractor. *Results in physics* **3** (2013) 14–19.

[30] D. Kuibiao, L. Jing and Y. Simin. Dynamics analysis and synchronization of a new chaotic attractor. *Optik* **125** (13) (2014) 3071–3075.

[31] W. Guangyi, Z. Xun, Z. Yan and L. Yuxia. A new modified hyperchaotic Lü system. *Physica A: Statistical Mechanics and its Applications* **371** (2) (2006) 260–272.

Nonlinear Dynamics and Systems Theory, **25** (6) (2025) 621–629

Analysis and Prediction of Stunting Rate in East Java Province Using Support Vector Regression and Decision Tree Method

T. Herlambang [1], F. Fauzi [2], B. Suharto [3*], I. Kurniastuti [1], Z. Othman [4], R. W. Abdullah [5], and K. Oktafianto [6]

[1] *Department of Information System, Universitas Nahdlatul Ulama Surabaya, Indonesia.*
[2] *Undergradute Program of Information System, Faculty of Economy Business and Digital Technology, Universitas Nahdlatul Ulama Surabaya.*
[3] *Department of Tourism and Hospitality, Faculty of Vocational, Airlangga University, Surabaya.*
[4] *Department of Diploma Studies, Fakulti Teknologi Maklumat dan Komunikasi, Universiti Teknikal Melaka Malaysia, Malaysia.*
[5] *Center of Advanced Computing Technology(C-ACT), Fakulti Teknologi Maklumat dan Komunikasi, Universiti Teknikal Melaka Malaysia, Malaysia.*
[6] *Department of Mathematics, University of PGRI Ronggolawe, Indonesia.*

Received: October 22, 2024; Revised: November 16, 2025

Abstract: Currently, in the health sector, Indonesia is facing several problems that the government is focusing on, one of which is stunting. The problem of stunting is a focus for the government since it ranks second after the problem of maternal mortality during childbirth. Stunting is a term used in the health sector describing a condition of growth failure in children under five due to chronic malnutrition in the first 1000 days of life. The causes of stunting can be identified from low nutritional intake and health status of pregnant women at risk of giving birth to babies with low body weight and below-standard baby length. With the current advances in the field of information technology, the stunting rate can be estimated using a machine learning method. There are numerous machine learning methods for prediction, such as Support Vector Regression (SVR), Decision Tree, K-Nearest Neighbour (K-NN) and many more. In this study, we aim to compare two prediction methods, namely Support Vector Regression (SVR) and Decision Tree, and determine how both methods succeed in predicting well. The Support Vector Regression (SVR) method achieved the best error value of 0.137 and the Decision Tree method had the best error value of 0.164.

Keywords: *stunting; prediction; machine learning; Support Vector Regression; decision tree.*

Mathematics Subject Classification (2020): 62J05, 70-10, 90Bxx.

* Corresponding author: mailto:bambang.suharto@vokasi.unair.ac.id

1 Introduction

Stunting is the focus of health concerns for the Indonesian government and the East Java provincial government. Stunting is a condition of malnutrition associated with insufficient nutrients in the past so it is considered a chronic nutritional problem [1]. Children experiencing stunting are more likely to grow into unhealthy and poor adults. Stunting of children is also associated with increased vulnerability to disease, both infectious and non-communicable diseases (NCDs), as well as increased risk of overweight and obesity [2].

The stunting problem in East Java initially occurred in areas with a low economic level, a low level of education, and a culture of early marriage, typically in Madura and the eastern part of East Java [3]. East Java provincial Nutritional Status Monitoring (DPSG) data shows that the prevalence of stunting among children under five in East Java is 27.1%, consisting of 17.6% short and 9.5% very short. The prevalence of stunting among children under five in one of the Madura Island districts, namely Bangkalan, is the highest in East Java, at 53.2%, with a prevalence of very short toddlers of 27.4% [4].

To address this issue, a method is required to predict the stunting rate in East Java province with the help of relevant advances in information technology. Prediction, in its definition, is the activity of estimating what will happen in the future using past data [5]. Through accurate and computerized prediction methods, decision making on policies to be taken to deal with this stunting problem becomes more measurable. In this research, the authors use the Support Vector Regression (SVR) and Decision Tree methods to predict the rate of stunting in East Java.

The Support Vector Regression (SVR) method has been widely used in various prediction studies. The Support Vector Regression (SVR) method is a derivative of the Support Vector Machine (SVM) method which has gained recognition for its ability to handle high-dimensional data and work well on relatively small datasets but with a large number of features [6]. Meanwhile, Decision Tree is a learning method that constructs a prediction model in the form of a tree structure. The tree consists of nodes representing decisions based on attribute values, and branches representing the results of those decisions [7]. In the previous research, both methods were used to predict the risk of stunting in families [8].

In this study, the Support Vector Regression (SVR) and Decision Tree methods were used to compare the performance of each method in predicting the rate of stunting in East Java. This approach is expected to provide a clear view of the stunting rate, making it easier for the parties involved to make decisions.

2 Research Methods

The dataset used in this study comes from the official website of the Ministry of Home Affairs (`https://aksi.bangda.kemendagri.go.id/emonev/`) which consists of 156 rows and 6 columns with a time span ranging from January 02, 2021 to December 18, 2024. The data in this study were analyzed using the Python programming language with a dataset as in Table 1 below.

After the data are obtained and explored, the next step is to carry out the stages of the research methodology one by one as shown in Figure 1 below.

1. **Problem Identification**: This research raises a case study on the prediction of stunting prevalence rates in East Java province.

Year	Regency	Number of Toddlers	Short Stunting	Very Short Stunting	Preva-lence(%)
02/01/2021	Pacitan	3068	2337	653	9.7
15/01/2021	Ponorogo	44307	482	1784	14.9
18/01/2021	Trenggalek	36144	2932	574	9.7
21/01/2021	Tulungagung	63329	167	431	3.3
31/01/2021	Blitar	76118	4258	1395	7.4
02/02/2021	Kediri	79244	8445	2327	13.6
15/02/2021	Malang	88532	651	1351	8.9
...	...	...	...	...	...
18/12/2024	Kota Batu	10945	106	269	12.1

Table 1: Dataset.

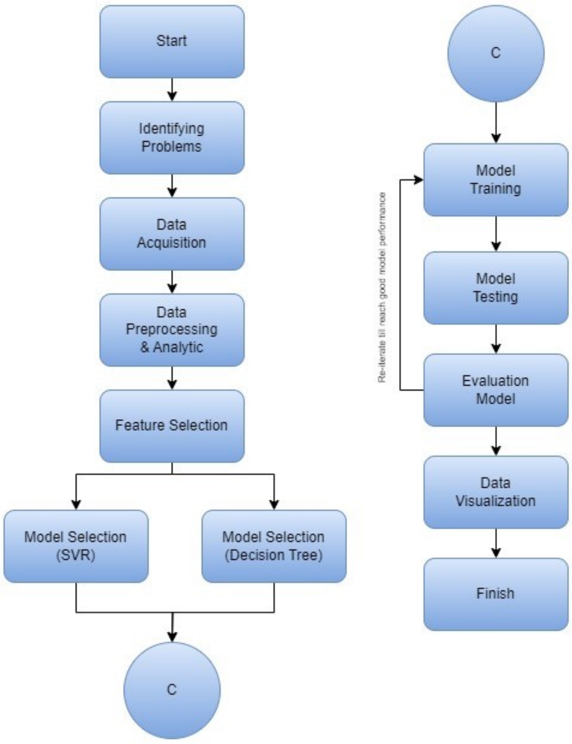

Figure 1: Research Methods.

2. **Data Acquisition**: The data used in this study is secondary data sourced from the official website of the Ministry of Home Affairs (`https://aksi.bangda.kemendagri.go.id/emonev/`) which consists of 156 rows and 6 columns with a time span ranging from January 02, 2021 to December 18, 2024.

3. **Data Preprocessing & Analytics**: The data preprocessing and analytics are basically used to see the initial condition of the dataset obtained from the source. At this stage, the dataset is identified from the data type to missing values that may occur in the dataset.

4. **Feature Selection**: This study uses the Pearson Product correlation analysis technique to find a linear relationship between two variables having a normal distribution [9]. Below is the function of the Pearson Product

$$r_{xy} = \frac{N\Sigma XY - (\Sigma X)(\Sigma Y)}{\sqrt{[N\Sigma X^2 - (\Sigma X)^2][N\Sigma Y^2 - (\Sigma Y)^2]}}. \tag{1}$$

Notes:

- r_{xy}: Relationship coefficient
- N: Number of samples used
- ΣX: The total score of the question
- ΣY: Sum of total scores

5. **Model Selection**: Support Vector Regression (SVR) is a development algorithm of the Support Vector Machine (SVM) algorithm introduced by Cortes and Vapnik [10]. Like SVM, SVR also uses the best hyperplane in the form of a regression function by making the error as small as possible. The function of SVR can generally be written as follows:

$$f(x) = w\varphi(x) + b \tag{2}$$

with

- $f(x)$: Regression function
- w: Vector
- b: bias

and the decision boundary equation

$$W_x + b = +\varepsilon,$$

$$W_x + b = -\varepsilon$$

so that the hyperplane fulfills the equation

$$-\varepsilon < y - (W_x + b) < +\varepsilon$$

with the minimization function

$$\min \frac{1}{2}\|w\|^2 + C\sum_{i=1}^{n} |\xi_i|$$

and the constraint function

$$|y_i - w_i x_i| \leq \varepsilon + |\xi_i|.$$

Then, the Decision Tree algorithm begins by calculating the entropy value to measure the level of uncertainty or impurity in the dataset [11]. The equation for finding the entropy value is as follows:

$$\text{Entropy}(S) = \sum_{i=1}^{m} -p(w_i|S) \cdot \log_2(p(w_i|S)). \tag{3}$$

Description:

- S: The case set being analyzed.
- m: Total number of different classes within the data set S.
- $p(w_i|S)$: Probability of occurrence of class w_i in the data set S.

The next step is to calculate the gain value, which is a measure of how much information is obtained from separating data based on certain attributes. The gain calculation function is as follows:

$$\text{Gain}(S, J) = \text{Entropy}(S) - \sum_{i=j}^{n} p(v_i|S) \cdot \text{Entropy}(S_i). \tag{4}$$

Notes:

- S: The case set being analyzed
- J: Features/attributes considered in data splitting
- n: Number of classes in the node
- $p(v_i|S)$: Proportion of v values appearing in the class in the node
- S_i: The entropy of the composition of v values for the j-th class in the i-th data node.

6. **Model Training**: At this stage, the predicted values of the Support Vector Regression (SVR) and Decision Tree algorithms are trained based on the distribution of training data and testing data to obtain error values and accuracy values.

7. **Model Testing**: Model testing of learning outcomes against prepared testing data.

8. **Model Evaluation**: At the evaluation stage, the model trained and tested is calculated for accuracy based on the resulting error value. This research uses the Root Mean Square Error (RMSE) method to calculate the error value generated by the model. The function of the Root Mean Square Error (RMSE) is as follows:

$$\text{RMSE} = \sqrt{\frac{\sum_{i=1}^{n} (y_i - \widehat{y_i})^2}{n}} \tag{5}$$

with

- n: Quantity of data
- y_i: Actual value at the i-th data
- $\widehat{y_i}$: Predicted value at the i-th data

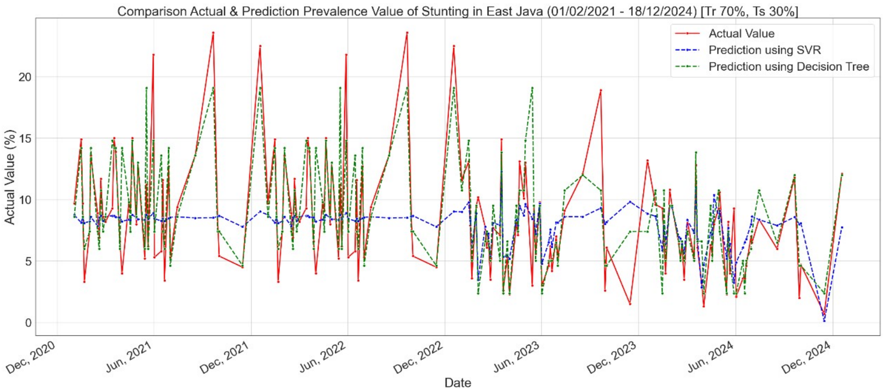

Figure 2: First Simulation Plot SVR Decision Tree (70% training data, 30% testing data).

3 Result and Discussion

The results of the testing simulation carried out with the proportion of training data and testing data are shown in Figure 2 to Figure 5.

The first simulation shown by Figure 2, produced SVR algorithm parameter values, that is, Cost = 1, Epsilon = 0.001, and Gamma = 0.1 on the Radial Basis Function kernel with a ratio of 70% training data and 30% testing data, with the SVR algorithm forecasting results not yet close to the actual value or less than optimal and the Decision Tree algorithm results close to the actual value. The results show that the first simulation produced an RMSE value of 0.1647. Meanwhile, the Decision Tree algorithm with the parameters of a max depth = 100 and min samples split = 10, produced an RMSE value of 0.2004.

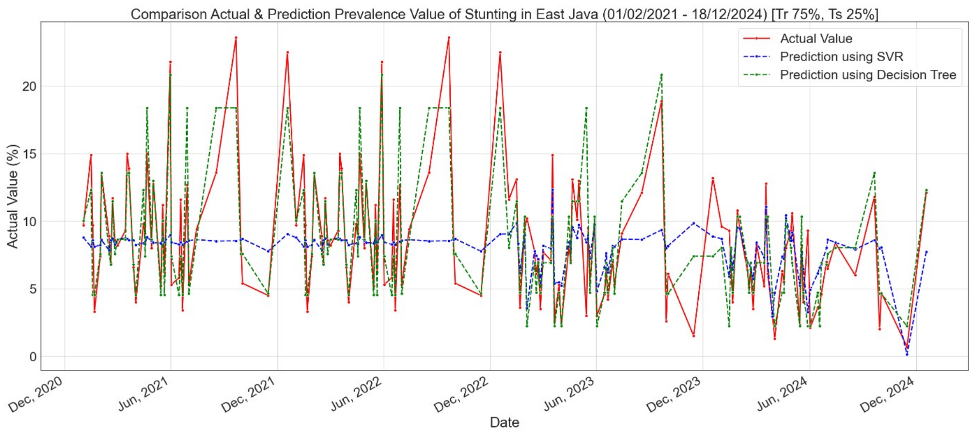

Figure 3: Second Simulation Plot SVR Decision Tree (75% training data, 25% testing data).

The results of the second simulation presented on Figure 3, show the parameter values of the SVR algorithm, namely Cost = 1 Epsilon = 0.001 Gamma = 0.1 on the

Radial Basis Function kernel with a ratio of 75% training data and 25% testing data with forecasting results close to the actual value or maximum enough. The first simulation resulted in an RMSE value of 0.1448. Meanwhile, the Decision Tree algorithm with the parameters such as max depth = 100 and min samples split = 10, produced an RMSE value of 0.1751.

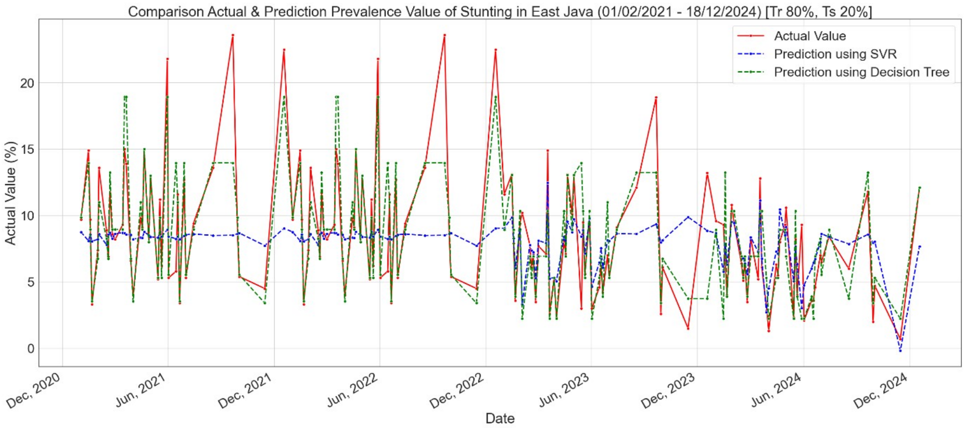

Figure 4: Third Simulation Plot SVR Decision Tree (80% training data, 20% testing data).

In the third simulation shown in Figure 4, the parameter values of the SVR algorithm are Cost = 1 Epsilon = 0.001 Gamma = 0.1 on the Radial Basis Function kernel with a ratio of 80% training data and 20% testing data with forecasting results close to the actual value or maximum enough. These first simulation results have an RMSE value of 0.1450. Meanwhile, using the Decision Tree algorithm with the parameters of max depth = 100 and min samples split = 10, the RMSE value is 0.1642.

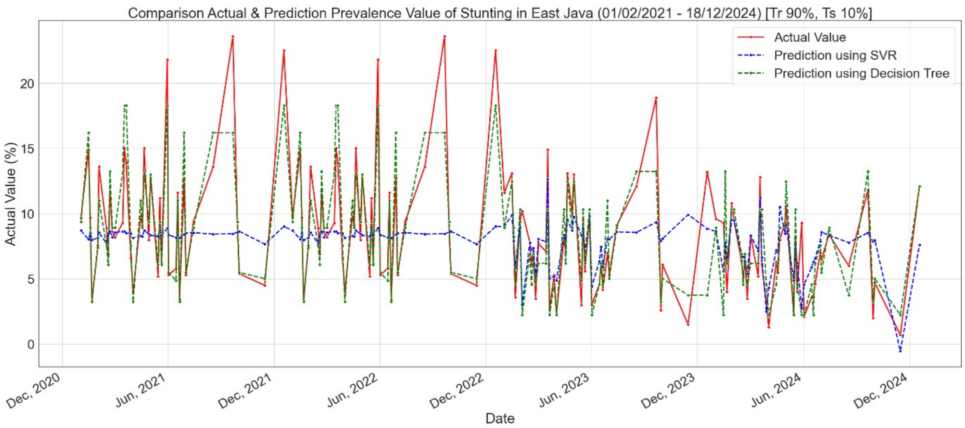

Figure 5: Fourth Simulation Plot SVR Decision Tree (90% training data, 10% testing data).

In the fourth simulation presented in Figure 5, the parameter values of the SVR algorithm are Cost = 1 Epsilon = 0.001 Gamma = 0.1 on the Radial Basis Function kernel with a ratio of 90% training data and 10% testing data with forecasting results close to the actual value or maximum enough. The results of this first simulation have an RMSE value of 0.1377. When using the Decision Tree algorithm with the parameters of max depth = 100 and min samples split = 10, the RMSE value is 0.2030.

The recapitulation of the simulation results of the Support Vector Regression (SVR) and Decision Tree algorithms can be seen in the table below.

Percentage Comparison of Training Data and Testing Data	**RMSE value by Support Vector Regression (SVR)**	**RMSE value by Decision Tree**
70% : 30%	0.1647	0.2004
75% : 25%	0.1448	0.1751
80% : 20%	0.1450	**0.1642**
90% : 10%	**0.1377**	0.2030

Table 2: Comparison of RMSE values.

In the table above, it can be seen that the maximum results produced by the Support Vector Regression (SVR) algorithm occurred in the fourth simulation with an RMSE value of 0.1377, while the best results of the Decision Tree algorithm occurred in the third simulation with an RMSE value of 0.1642.

4 Conclusion

Based on the simulation results, it can be concluded that the SVR algorithm produces the best simulation results in the fourth simulation with an RMSE value of 0.1377 and the Decision Tree algorithm produces the best simulation results in the third simulation with an RMSE value of 0.1642. The results prove that the Support Vector Regression and Decision Tree methods are able to provide good prediction results and fulfil the objective of this study and could be optimized in the next study.

Acknowledgment

The authors would like to thank LPPM-Universitas Nahdlatul Ulama Surabaya (UNUSA) for their support in providing the facility for this research. Additionally, gratitude is extended to the Centre of Research and Innovation Management of Universiti Teknikal Malaysia Melaka (UTeM) for sponsoring the publication fees under the Tabung Penerbitan CRIM UTeM.

References

[1] A. N. P. Wulandari, A. T. Devanti, A. F. Salsabila, R. A. Ardito, A. Amanullah, and E. Rahmawati. Preventing Stunting Through the GPS (Stunting Prevention Movement) Program in Murukan Village, Jombang Regency, East Java. *Gembira Journal: Community Service* **2** (2) (2024) 540–545.

[2] I. C. Dewi, and N. R. N. Auliyyah. Stunting Education as a Means to Minimize High Stunting Rates in Gambiran Village, Kalisat District. *JIWAKERTA: Scientific Journal of Practical Work Insights* **1** (2) (2020) 25–29.

[3] M. A. Syahputra, and A. C. Sitohang. The Effect of Poverty and Stunting on the Human Development Index (HDI) in East Java From 2019 to 2023. *GEMAH RIPAH: Business Journal* **4** (1) (2024) 74–79.

[4] T. Septiyanto, F. A. Mufarroha, D. R. Anamisa, and A. Jauhari. Predicting the Number of Stunting Cases in Madura Using Machine Learning. *JoMMiT: Multimedia and IT Journal* **7** (2) (2023) 70–76.

[5] D. A. Ningsih, R. Buaton, and A. Sihombing. Predicting Child Stunting Rates in Langkat District Using Multiple Linear Regression: (Case Study: PPKB-PPA Office of Langkat District). *Saturnus: Journal of Technology and Information Systems* **2** (4) (2024) 131–145.

[6] I. S. I. Putri, R. S. Pradini, and M. Anshori. Decision Tree Regression for Predicting the Prevalence of Stunting in East Nusa Tenggara Province. *Journal of Information Technology and Computers* **10** (2) (2024) 413–427.

[7] V. Asy'ari, M. Y. Anshori, T. Herlambang, I. W. Farid, D. F. Karya, and M. Adinugroho. Forecasting average room rate using k-nearest neighbor at Hotel S. In: *International Conference on Advanced Mechatronics, Intelligent Manufacture and Industrial Automation (ICAMIMIA)*), IEEE, Nov. 2023, 496–500.

[8] D. Novita, T. Herlambang, V. Asy'ari, A. Alimudin, and H. Arof. Comparison of K-Nearest Neighbor and Neural Network For Prediction International Visitor in East Java. *BAREKENG: Journal of Mathematics and Applied Sciences* **18** (3) (2024) 2057–2070.

[9] M. Y. Anshori, V. Asy'Ari, T. Herlambang, and I. W. Farid. Forecasting Occupancy Rate Using Neural Network at Hotel R. *International Conference on Advanced Mechatronics, Intelligent Manufacture and Industrial Automation (ICAMIMIA)*. (2023) 347–351.

[10] F. A. Susanto, M. Y. Anshori, D. Rahmalia, K. Oktafianto, D. Adzkiya, P. Katias and T. Herlambang. Estimation of Closed Hotels and Restaurants in Jakarta as Impact of Corona Virus Disease (Covid-19) Spread Using Backpropagation Neural Network. *Nonlinear Dynamics and Systems Theory* **22** (4) (2022) 457–467.

[11] M. Y. Anshori, T. Shawyun, D. V. Madrigal, D. Rahmalia, F. A. Susanto, T. Herlambang and D. Adzkiya. Estimation of Closed Hotels and Restaurants in Jakarta as Impact of Corona Virus Disease Spread Using Adaptive Neuro Fuzzy Inference System. *International Journal of Artificial Intelligence (IJAI)* **11** (2) (2022) 462–472.

Nonlinear Dynamics and Systems Theory, **25** (6) (2025) 630–642

Solving Two–Dimensional Lane–Emden System Equations by MDTM

M. Laib and N. Teyar *

Department of Mathematics, Faculty of Exact Sciences, Brothers Mentouri University, Constantine, Algeria.

Received: February 23, 2025; Revised: November 4, 2025

Abstract: In this paper, we introduce and solve the nonlinear forms of two-dimensional Lane–Emden system equations. Using the properties of a Modified Differential Transform Method, we obtain exact analytical solutions for these equations without resorting to linearization, discretization, or perturbation, while requiring minimal computation.

Keywords: *two–dimensional Lane–Emden system equations; reduced differential transform method; modified differential transform method; initial value problems.*

Mathematics Subject Classification (2020): 35C10, 65L05, 35J15, 35J47, 70F15, 35J75.

1 Introduction of Lane-Emden System Equations

The linear and nonlinear two–dimensional Lane–Emden type equations were first introduced by Wazwaz, Rach and Duan in [1], as follows:

$$u_{xx} + \frac{\propto}{x} u_x + u_{yy} + \frac{\beta}{y} u_y + g(x,y) f(u) = 0, \tag{1}$$

$$x > 0, \qquad y > 0, \qquad \propto > 0, \qquad \beta > 0,$$

$$u(x,0) = h(x), \quad u_y(x,0) = 0, \quad u(0,y) = h(y), \quad u_x(0,y) = 0, \tag{2}$$

where $g(x,y) f(u)$ is a linear or nonlinear term.

In [2], N. Teyar introduced the linear and nonlinear two–dimensional Lane–Emden system equations

* Corresponding author: mailto:teyarnadir@gmail.com

$$\begin{cases} u_{xx} + \frac{\propto}{x} u_x + u_{yy} + \frac{\beta}{y} u_y + f(x, y, v) = 0, \\ \\ v_{xx} + \frac{\gamma}{x} v_x + v_{yy} + \frac{\theta}{y} v_y + g(x, y, u) = 0, \end{cases} \tag{3}$$

$x > 0, \quad y > 0, \quad \propto > 0, \quad \beta > 0, \quad \gamma > 0, \quad \theta > 0,$

$$\begin{cases} u(x, 0) = h(x), & u_y(x, 0) = 0, \\ v(x, 0) = k(x), & v_y(x, 0) = 0, \\ u(0, y) = h(y), & u_x(0, y) = 0, \\ v(0, y) = k(y), & v_x(0, y) = 0. \end{cases} \tag{4}$$

This type of systems can model configurations such as double stars in gravitational interaction or gaseous structures in hydrostatic equilibrium under the influence of several components. Because of the spherical symmetry of the solutions of the Lane–Emden equation, the second line of conditions (4) is not mentioned in general. These equations generalize the Lane-Emden equation to a coupled two-field system in two dimensions, which could describe: 1- Anisotropic self-gravitating fluids (e.g., accretion disks, gas clouds); 2- Two interacting astrophysical components (e.g., a coupled gas-star system); 3- Modified gravity effects (e.g., alternative gravity models for stellar structures).

In this paper, we apply modified differential transform methods for solving this kind of elliptic system problems, with singularities in both x and y, for obtaining exact solutions, by using a new product and quotient properties of the MDTM proved in [2], which implies a minimum of computation. We will obtain exact analytic solutions for these system equation. Liliane Maia, Gabrielle Nornberg and Filomena Pacella in [3], introduce a dynamical system approach for the second-order Lane–Emden type problems by defining some new variables that allow us to transform the radial fully nonlinear Lane-Emden equations into a quadratic dynamical system. For the one-dimension Lane-Emden equation, the original formal conservation of specific entropy along streamlines was given by a PDE in function of t (time) and r (radius).

2 Definition and Properties of Modified Differential Transform Method (MDTM)

We introduce the basic definitions of the modified differential transform method as follows.

Definition 2.1 The modified differential transform of $u(x, y)$ with respect to the variable y at y_0 is defined as

$$U(x, h) = \frac{1}{h!} \left(\frac{\partial^h}{\partial x^h} u(x, y) \right)_{y=y_0}, \qquad k \in \mathbb{N}, \tag{5}$$

where $u(x, y)$ is the original function and $\mathrm{U}(x, h)$ is the transformed function.

Definition 2.2 *The modified inverse differential transform $U(x, h)$ of $u(x, y)$ is defined as*

$$\mathrm{u(x, y)} = \sum_{\mathrm{h}=0}^{\infty} \mathrm{U(x, h)(y - y_0)^h}. \tag{6}$$

Original functions	Transformed functions
$w(x,y)=\alpha u(x,y)\pm\beta v(x,y)$	$W(x,h)=\alpha U(x,h)+\beta V(x,h)$
$w(x,y)=x^m y^n$	$W(x,h)=x^m\delta(h-n)$
$w(x,y)=x^m y^n u(x,y)$	$W(x,h)=x^m U(x,h-n)$
$w(x,y)=u(x,y)\,v(x,y)$	$W(x,h)=\sum_{s=0}^{k}U(x,s)\,V(x,h-s)$
$w(x,y)=[u(x,y)]^3$	$W(x,h)=\sum_{r=0}^{h}\sum_{s=0}^{r}U(x,h-r)\,U(x,s)\,U(x,r-s)$
$w(x,y)=\frac{\partial u(x,y)}{\partial x}$	$W(x,h)=\frac{\partial U(x,h)}{\partial x}$
$w(x,y)=\frac{\partial^2 u(x,y)}{\partial x^2}$	$W(x,h)=\frac{\partial^2 U(x,h)}{\partial x^2}$
$w(x,y)=\frac{\partial u(x,y)}{\partial y}$	$W(x,h)=(h+1)\,U(x,h+1)$
$w(x,y)=\frac{\partial^2 u(x,y)}{\partial y^2}$	$W(x,h)=(h+1)\,(h+2)\,U(x,h+2)$
$w(x,y)=e^{au(x,y)}$	$W(x,h)=\begin{cases} e^{aU(x,0)},\ h=0 \\ a\sum_{s=0}^{h-1}\frac{s+1}{h}U(x,s+1)\,W(x,h-s-1),\ h\geq 1\end{cases}$

Table 1: Fundamental properties of the MDTM.

Then combining equations (5) *and*(6)*, we write*

$$u(x,y)=\sum_{h=0}^{\infty}\frac{1}{h!}\left(\frac{\partial^h}{\partial x^h}u(x,y)\right)_{y=y_0}(y-y_0)^h. \tag{7}$$

When (x,y_0) *is taken as* $(x,0)$*, then* (7) *can be expressed as*

$$u(x,y)=\sum_{h=0}^{\infty}U(x,h)y^h.$$

Some important properties of the MDTM used in this paper, are listed in Table 1.

3 Theorems and Corollaries

Theorem 3.1 *[2] If* $w(x,y)=\frac{u(x,y)}{v(x,y)}$ *and* $V(x,0)\neq 0$*, then the modified differential transform version is*

$$W(x,h)=\begin{cases}\frac{U(x,0)}{V(x,0)}, & \text{if } h=0,\\ \\ \frac{U(x,h)-\sum_{i=0}^{h-1}W(x,i)V(x,h-i)}{V(x,0)}, & \text{if } h\geq 1.\end{cases}$$

Corollary 3.1 *[2] If* $w(x,y)=\frac{x^m y^n}{v(x,y)}$ *and* $V(x,0)\neq 0$*, then the modified differential transform version is*

$$W(x,h)=\begin{cases}\frac{x^m\delta(n)}{V(x,0)} & \text{if } h=0,\\ \\ \frac{x^m\delta(h-n)-\sum_{i=0}^{h-1}W(x,i)V(x,h-i)}{V(x,0)} & \text{if } h\geq 1.\end{cases}$$

Corollary 3.2 *[2] If* $w(x,y)=\frac{1}{v(x,y)}$ *and* $V(x,0)\neq 0$*, then the modified differential transform version is*

$$W(x,h)=\begin{cases}\frac{1}{V(x,0)} & \text{if } h=0,\\ \\ \frac{-\sum_{i=0}^{h-1}W(x,i)V(x,h-i)}{V(x,0)} & \text{if } h\geq 1.\end{cases}$$

Theorem 3.2 *[2] If* $w(x,y) = \frac{u(x,y)}{x^m y^n}$ *and* $(x,y) \neq (0,0)$*, then the modified differential transform version of* $w(x,y)$ *is*

$$W(x,h) = \frac{U(x,h+n)}{x^m}.$$

Corollary 3.3 *[2] If* $w(x,y) = \frac{u(x,y)}{x}, x \neq 0$*, then the modified differential transform version is*

$$W(x,h) = \frac{U(x,h)}{x}.$$

Corollary 3.4 *[2] If* $w(x,y) = \frac{u(x,y)}{y}, y \neq 0$*, then the modified differential transform version is*

$$W(x,h) = U(x,h+1).$$

4 Main Result and Description of Method

The classical Lane-Emden equation describes the structure of a self-gravitating, spherically symmetric polytropic gas cloud:

$$\frac{1}{r^2}\frac{d}{dr}\left(r^2\frac{d\theta}{dr}\right) + \theta^n = 0,$$

where $\theta(r)$ represents a dimensionless density profile, and n is the polytropic index. We will solve the following system of two equations:

$$\begin{cases} u_{xx} + \frac{\propto}{x}u_x + u_{yy} + \frac{\beta}{y}u_y + f\left(x,y,v\right) = 0, \\ v_{xx} + \frac{\gamma}{x}v_x + v_{yy} + \frac{\theta}{y}v_y + g\left(x,y,u\right) = 0, \end{cases} \tag{8}$$

$$x > 0, \qquad y > 0, \qquad \propto > 0, \qquad \beta > 0, \qquad \gamma > 0, \qquad \theta > 0,$$

$$u\left(x,0\right) = h\left(x\right), \qquad u_y\left(x,0\right) = 0, \qquad v\left(x,0\right) = k\left(x\right), \qquad v_y\left(x,0\right) = 0. \tag{9}$$

In Table 2, we compare the physical meaning of some variables in the classical Lane-Emden equation and the variables in our system of equations.

The following theorem constitutes the main result of this paper.

Theorem 4.1 *The Lane-Emden system of equations given by* (8)*, subject to the initial conditions* (9)*, can be effectively solved using the Modified Differential Transform Method (MDTM), yielding exact symmetric solutions.*

Proof: From Table 1 and Corollaries 3.3, 3.4, the modified differential transform version of (8) is

$$\begin{cases} \frac{\partial^2 U(x,h)}{\partial x^2} + \frac{\propto}{x}\frac{\partial U(x,h)}{\partial x} + \left(h+\beta+1\right)\left(h+2\right)U\left(x,h+2\right) + F\left(x,h\right) = 0, \\ \frac{\partial^2 V(x,h)}{\partial x^2} + \frac{\gamma}{x}\frac{\partial V(x,h)}{\partial x} + \left(h+\theta+1\right)\left(h+2\right)V\left(x,h+2\right) + G\left(x,h\right) = 0, \end{cases}$$

Feature	**Classical Lane-Emden**	**Our System**
Dimension	$1D$ (radial r)	$2D$ (x, y)
Symmetry	Spherical	Possibly cylindrical or more general
Nonlinear source term	θ^n	$f(x,y,v), g(x,y,u)$ (self-interacting fields or relativistic corrections)
Number of equations	Single equation	Coupled system
Physical meaning	Polytropic stars	Two-component fluid, modified gravity, or plasma model

Table 2: Comparison of Classical Lane-Emden system and our System.

where $F(x,h)$ and $G(x,h)$ are, respectively, the modified differential transform version of $f(x,y,v)$ and $g(x,y,v)$. Also, the modified MDTM versions of initial conditions (9) are

$$U(x,0) = H(x), \qquad U(x,1) = 0, \qquad V(x,0) = K(x), \qquad V(x,1) = 0.$$

Then

$$\begin{cases} U(x,h+2) = \frac{-1}{(h+\beta+1\ )(h+2)}\left[\frac{\partial^2 U(x,h)}{\partial x^2} + \frac{\propto}{x}\frac{\partial U(x,h)}{\partial x} + F(x,h)\right] \\ V(x,h+2) = \frac{-1}{(h+\theta+1\ )(h+2)}\left[\frac{\partial^2 V(x,h)}{\partial x^2} + \frac{\gamma}{x}\frac{\partial V(x,h)}{\partial x} + G(x,h)\right]. \end{cases}$$

For $h = 0$: $$\begin{cases} U(x,2) = \frac{-1}{2(\beta+1\ )}\left[\frac{\partial^2 U(x,0)}{\partial x^2} + \frac{\propto}{x}\frac{\partial U(x,0)}{\partial x} + F(x,0)\right] \\ V(x,2) = \frac{-1}{2(\theta+1\ )}\left[\frac{\partial^2 V(x,0)}{\partial x^2} + \frac{\gamma}{x}\frac{\partial V(x,0)}{\partial x} + G(x,0)\right]. \end{cases}$$

For $h = 1$:

$$\begin{cases} U(x,3) = \frac{-1}{3(\beta+2\ )}\left[\frac{\partial^2 U(x,1)}{\partial x^2} + \frac{\propto}{x}\frac{\partial U(x,1)}{\partial x} + F(x,1)\right] \\ V(x,3) = \frac{-1}{3(\theta+2\ )}\left[\frac{\partial^2 V(x,1)}{\partial x^2} + \frac{\gamma}{x}\frac{\partial V(x,1)}{\partial x} + G(x,1)\right]. \end{cases}$$

For $h = 2$:

$$\begin{cases} U(x,4) = \frac{-1}{4(\beta+3\ )}\left[\frac{\partial^2 U(x,2)}{\partial x^2} + \frac{\propto}{x}\frac{\partial U(x,2)}{\partial x} + F(x,2)\right] \\ V(x,4) = \frac{-1}{4(\theta+3\ )}\left[\frac{\partial^2 V(x,2)}{\partial x^2} + \frac{\gamma}{x}\frac{\partial V(x,2)}{\partial x} + G(x,2)\right]. \end{cases}$$

For $h = 3$:

$$\begin{cases} U(x,5) = \frac{-1}{5(\beta+4\ )}\left[\frac{\partial^2 U(x,3)}{\partial x^2} + \frac{\propto}{x}\frac{\partial U(x,3)}{\partial x} + F(x,3)\right] \\ V(x,5) = \frac{-1}{5(\theta+4\ )}\left[\frac{\partial^2 V(x,3)}{\partial x^2} + \frac{\gamma}{x}\frac{\partial V(x,3)}{\partial x} + G(x,3)\right]. \end{cases}$$

.
.
.
.
.

After computing the first terms $U(x,h)$, we obtain the series solution

$$u(x,y)=\sum_{h=0}^{\infty}U(x,h)y^h.$$

5 Applications

Example 1.

$$\begin{cases} u_{xx}+\frac{2}{x}u_x+u_{yy}+\frac{3}{y}u_y+6e^{-2v}=0, \\ v_{xx}+\frac{3}{x}v_x+v_{yy}+\frac{4}{y}v_y-14u=0, \end{cases} \tag{10}$$

$$u(x,0)=\frac{1}{x^2}, \qquad u_y(x,0)=0, \qquad v(x,0)=2lnx, \qquad v_y(x,0)=0, \tag{11}$$

with exact solutions

$$u(x,y)=\frac{1}{x^2+y^2}, \quad v(x,y)=\ln(x^2+y^2).$$

The terms $\dfrac{2}{x}u_x$ and $\dfrac{3}{y}u_y$ suggest a formulation in cylindrical or spherical coordinates, commonly used for modeling a stellar structure or gravitational equilibrium in astrophysical settings.

The term $6e^{-2v}$ suggests a nonlinear source term, which could represent an energy density or a self-interaction potential, as in plasma physics or cosmology.

The coupling between u and v in the equations suggests an interaction between two physical fields, possibly related to density-pressure relations in a self-gravitating system. From Table 1 and Corollaries 3.3, 3.4, the modified differential transform version of (10) is

$$\begin{cases} \frac{\partial^2 U(x,h)}{\partial x^2}+\frac{2}{x}\frac{\partial U(x,h)}{\partial x}+(h+4)(h+2)U(x,h+2)+6F(x,h)=0, \\ \frac{\partial^2 V(x,h)}{\partial x^2}+\frac{3}{x}\frac{\partial V(x,h)}{\partial x}+(h+5)(h+2)V(x,h+2)-14U(x,h)=0, \end{cases}$$

where $F(x,h)$ is the modified differential transform version of e^{-2v} (Table 1), such as

$$F(x,h)=\begin{cases} e^{-2V(x,0)}=\frac{1}{x^4}, & h=0, \\ -2\sum_{s=0}^{h-1}\frac{s+1}{h}V(x,s+1)F(x,h-s-1), & h\geq 1. \end{cases}$$

Also, the modified MDTM versions of initial conditions (11) are

$$U(x,0)=\frac{1}{x^2}, \qquad U(x,1)=0, \qquad V(x,0)=2lnx, \qquad V(x,1)=0.$$

Then

$$\begin{cases} U(x,h+2)=\frac{-1}{(h+4)(h+2)}\left[\frac{\partial^2 U(x,h)}{\partial x^2}+\frac{2}{x}\frac{\partial U(x,h)}{\partial x}+6F(x,h)\right], \\ V(x,h+2)=\frac{-1}{(h+5)(h+2)}\left[\frac{\partial^2 V(x,h)}{\partial x^2}+\frac{3}{x}\frac{\partial V(x,h)}{\partial x}-14U(x,h)\right]. \end{cases}$$

For $h=0$: $$\begin{cases} U(x,2) = \frac{-1}{8}\left[\frac{\partial^2 U(x,0)}{\partial x^2} + \frac{2}{x}\frac{\partial U(x,0)}{\partial x} + 6F(x,0)\right], \\ \quad = \frac{-1}{8}\left[\frac{6}{x^4} + \frac{2}{x}.\frac{-2}{x^3} + \frac{6}{x^4}\right] = \frac{-1}{x^4}, \\ V(x,2) = \frac{-1}{10}\left[\frac{\partial^2 V(x,0)}{\partial x^2} + \frac{3}{x}\frac{\partial V(x,0)}{\partial x} - 14U(x,0)\right], \\ \quad = \frac{-1}{10}\left[\frac{-2}{x^2} + \frac{3}{x}.\frac{2}{x} - \frac{14}{x^2}\right] = \frac{10}{10x^2} = \frac{1}{x^2}. \end{cases}$$

For $h=1$: $(F(x,1) = -2V(x,1)\,F(x,0) = 0)$

$$\begin{cases} U(x,3) = \frac{-1}{15}\left[\frac{\partial^2 U(x,1)}{\partial x^2} + \frac{2}{x}\frac{\partial U(x,1)}{\partial x} - V(x,1)\,F(x,0)\right] = 0, \\ V(x,3) = \frac{-1}{18}\left[\frac{\partial^2 V(x,1)}{\partial x^2} + \frac{3}{x}\frac{\partial V(x,1)}{\partial x} - 14U(x,1)\right] = 0. \end{cases}$$

For $h=2$:

$$\begin{cases} U(x,4) = \frac{-1}{24}\left[\frac{\partial^2 U(x,2)}{\partial x^2} + \frac{2}{x}\frac{\partial U(x,2)}{\partial x} + 6F(x,2)\right], \\ \quad = \frac{-1}{24}\left[\frac{-20}{x^6} + \frac{2}{x}.\frac{4}{x^5} - \frac{12}{x^6}\right] = \frac{1}{x^6}, \\ V(x,4) = \frac{-1}{28}\left[\frac{\partial^2 V(x,2)}{\partial x^2} + \frac{3}{x}\frac{\partial V(x,2)}{\partial x} - 14U(x,2)\right], \\ \quad = \frac{-1}{28}\left[\frac{6}{x^4} + \frac{3}{x}.\frac{-2}{x^3} + \frac{14}{x^4}\right] = \frac{-14}{28x^4} = \frac{-1}{2x^4}. \end{cases}$$

For $h=3$:

$$\begin{cases} U(x,5) = \frac{-1}{35}\left[\frac{\partial^2 U(x,3)}{\partial x^2} + \frac{2}{x}\frac{\partial U(x,3)}{\partial x} + 6F(x,3)\right] = 0, \\ V(x,5) = \frac{-1}{40}\left[\frac{\partial^2 V(x,3)}{\partial x^2} + \frac{3}{x}\frac{\partial V(x,3)}{\partial x} - 14U(x,3)\right] = 0. \end{cases}$$

For $h=4$:

$$\begin{cases} U(x,6) = \frac{-1}{48}\left[\frac{\partial^2 U(x,4)}{\partial x^2} + \frac{2}{x}\frac{\partial U(x,4)}{\partial x} + 6F(x,4)\right] = \frac{1}{x^8}, \\ V(x,6) = \frac{-1}{54}\left[\frac{\partial^2 V(x,4)}{\partial x^2} + \frac{3}{x}\frac{\partial V(x,4)}{\partial x} - 14U(x,4)\right] = \frac{1}{3x^6}. \end{cases}$$

Then by substituting the quantities $U(x,h)$, $V(x,h)$ in (7), we get the series solutions

$$u(x,y) = \frac{1}{x^2}\left(1 - \left(\frac{y}{x}\right)^2 + \left(\frac{y}{x}\right)^4 - \left(\frac{y}{x}\right)^6 \cdots\right)$$

$$v(x,y) = 2lnx + \left(\frac{y}{x}\right)^2 - \frac{1}{2}\left(\frac{y}{x}\right)^4 + \frac{1}{3}\left(\frac{y}{x}\right)^6 \cdots$$

And the exact solutions are

$$u(x,y) = \frac{1}{x^2+y^2}, \quad v(x,y) = \ln\left(x^2+y^2\right)$$

on the region $x \geq y$.

By applying the symmetric conditions of (11)
$u(0,y) = \frac{1}{y^2}, u_x(0,y) = 0, v(0,y) = 2lny, v_x(0,y) = 0,$
we obtain the series solutions

$u\left(x,y\right)=\frac{1}{y^2}\left(1-\left(\frac{x}{y}\right)^2+\left(\frac{x}{y}\right)^4-\left(\frac{x}{y}\right)^6\cdots\right)$
$v\left(x,y\right)=2lny+\left(\frac{x}{y}\right)^2-\frac{1}{2}\left(\frac{x}{y}\right)^4+\frac{1}{3}\left(\frac{x}{y}\right)^6\cdots$
which converge to the same exact solutions on the region $x \leq y$.

Example 2.

$$\begin{cases} u_{xx}+\frac{1}{x}u_x+u_{yy}+\frac{1}{y}u_y-24v^{-1}=0, \\ v_{xx}+\frac{2}{x}v_x+v_{yy}+\frac{3}{y}v_y+6u^{-1}=0, \end{cases} \tag{12}$$

$$u\left(x,0\right)=x^4, \qquad u_y\left(x,0\right)=0, \qquad v\left(x,0\right)=\frac{1}{x^2}, \qquad v_y\left(x,0\right)=0 \tag{13}$$

with exact solutions

$$u\left(x,y\right)=\left(x^2+y^2\right)^2, \quad v\left(x,y\right)=\frac{1}{x^2+y^2}.$$

This system could model two interdependent physical quantities evolving under nonlinear interactions and spatial symmetries possibly within a self-gravitating system, plasma configuration, or cosmological model. The presence of the terms $+6u^{-1}$, $-24v^{-1}$ in the equations indicates a nonlinear coupling between two functions u and v. Physically, this might correspond to the interactions between two fields such as pressure and density, or temperature and concentration in self-regulating systems like stars or gases under gravity.

From Table 1 and Corollaries 3.3, 3.4, the modified differential transform version of (12) is

$$\begin{cases} \frac{\partial^2 U(x,h)}{\partial x^2}+\frac{1}{x}\frac{\partial U(x,h)}{\partial x}+\left(h+2\right)^2 U\left(x,h+2\right)-24F\left(x,h\right)=0, \\ \frac{\partial^2 V(x,h)}{\partial x^2}+\frac{2}{x}\frac{\partial V(x,h)}{\partial x}+\left(h+4\right)\left(h+2\right)V\left(x,h+2\right)+6G\left(x,h\right)=0. \end{cases},$$

where $F\left(x,h\right)$ and $G\left(x,h\right)$ are the modified differential transform versions of v^{-1}, u^{-1}, respectively, such as (from Corollary 3.2)

$$F\left(x,h\right)=\begin{cases} \frac{1}{V(x,0)}=x^2, & h=0, \\ \frac{-\sum_{i=0}^{h-1}F(x,i)V(x,h-i)}{V(x,0)}, & h\geq 1. \end{cases}$$

$$G\left(x,h\right)=\begin{cases} \frac{1}{U(x,0)}=\frac{1}{x^4}, & h=0, \\ \frac{-\sum_{i=0}^{h-1}G(x,i)U(x,h-i)}{U(x,0)}, & h\geq 1. \end{cases}$$

Also, the MDTM versions of initial conditions (13) are

$$U\left(x,0\right)=x^4, \qquad U\left(x,1\right)=0, \qquad V\left(x,0\right)=\frac{1}{x^2}, \qquad V\left(x,1\right)=0.$$

Then

$$\begin{cases} U\left(x,h+2\right)=\frac{-1}{(h+2)^2}\left[\frac{\partial^2 U(x,h)}{\partial x^2}+\frac{1}{x}\frac{\partial U(x,h)}{\partial x}-24F\left(x,h\right)\right], \\ V\left(x,h+2\right)=\frac{-1}{(h+4\ )(h+2)}\left[\frac{\partial^2 V(x,h)}{\partial x^2}+\frac{2}{x}\frac{\partial V(x,h)}{\partial x}+6G\left(x,h\right)\right]. \end{cases}$$

For $h=0$: $$\begin{cases} U(x,2) = \frac{-1}{4}\left[\frac{\partial^2 U(x,0)}{\partial x^2} + \frac{1}{x}\frac{\partial U(x,0)}{\partial x} - 24F(x,0)\right], \\ \quad = \frac{-1}{4}\left[12x^2 + \frac{1}{x}.4x^3 - 24x^2\right] = 2x^2, \\ V(x,2) = \frac{-1}{8}\left[\frac{\partial^2 V(x,0)}{\partial x^2} + \frac{2}{x}\frac{\partial V(x,0)}{\partial x} + 6G(x,0)\right], \\ \quad = \frac{-1}{8}\left[\frac{6}{x^4} + \frac{2}{x}.\frac{-2}{x^3} + 6\frac{1}{x^4}\right] = \frac{-8}{8x^4} = \frac{-1}{x^4}. \end{cases}$$

For $h=1$: $(F(x,1)=0, \quad G(x,1)=0)$

$$\begin{cases} U(x,3) = \frac{-1}{9}\left[\frac{\partial^2 U(x,1)}{\partial x^2} + \frac{1}{x}\frac{\partial U(x,1)}{\partial x} - 24F(x,1)\right] = 0, \\ V(x,3) = \frac{-1}{15}\left[\frac{\partial^2 V(x,1)}{\partial x^2} + \frac{2}{x}\frac{\partial V(x,1)}{\partial x} + 6G(x,1)\right] = 0. \end{cases}$$

For $h=2$:

$$\begin{cases} U(x,4) = \frac{-1}{16}\left[\frac{\partial^2 U(x,2)}{\partial x^2} + \frac{1}{x}\frac{\partial U(x,2)}{\partial x} - 24F(x,2)\right], \\ \quad = \frac{-1}{16}\left[4 + \frac{1}{x}.4x - 24\right] = 1, \\ V(x,4) = \frac{-1}{24}\left[\frac{\partial^2 V(x,2)}{\partial x^2} + \frac{2}{x}\frac{\partial V(x,2)}{\partial x} + 6G(x,2)\right], \\ \quad = \frac{-1}{24}\left[\frac{-20}{x^6} + \frac{2}{x}.\frac{4}{x^5} - \frac{12}{x^6}\right] = \frac{24}{24x^6} = \frac{1}{x^6}. \end{cases}$$

For $h=3$:

$$\begin{cases} U(x,5) = \frac{-1}{25}\left[\frac{\partial^2 U(x,3)}{\partial x^2} + \frac{1}{x}\frac{\partial U(x,3)}{\partial x} - 24F(x,3)\right] = 0, \\ V(x,5) = \frac{-1}{35}\left[\frac{\partial^2 V(x,3)}{\partial x^2} + \frac{2}{x}\frac{\partial V(x,3)}{\partial x} + 6G(x,3)\right] = 0. \end{cases}$$

For $h=4$:

$$\begin{cases} U(x,6) = \frac{-1}{36}\left[\frac{\partial^2 U(x,4)}{\partial x^2} + \frac{1}{x}\frac{\partial U(x,4)}{\partial x} - 24F(x,4)\right] = 0, \\ V(x,6) = \frac{-1}{48}\left[\frac{\partial^2 V(x,4)}{\partial x^2} + \frac{2}{x}\frac{\partial V(x,4)}{\partial x} + 6G(x,4)\right] = \frac{-1}{x^8}. \end{cases}$$

Then by substituting the quantities $U(x,h)$ in (7), we get the exact solution

$$u(x,y) = x^4 + 2x^2y^2 + y^4 = (x^2+y^2)^2$$

and the series solution

$$v(x,y) = \frac{1}{x^2}\left(1 - \left(\frac{y}{x}\right)^2 + \left(\frac{y}{x}\right)^4 - \left(\frac{y}{x}\right)^6 \cdots\right).$$

The exact solution is

$$v(x,y) = \frac{1}{x^2+y^2}$$

on the region $x \geq y$.

By appling the symmetric conditions of (13)

$u(0,y) = y^4, \qquad u_x(0,y) = 0, \qquad v(0,y) = \frac{1}{y^2}, \qquad v_x(0,y) = 0,$

we obtain the series solutions

$v(x,y) = \frac{1}{y^2}\left(1 - \left(\frac{x}{y}\right)^2 + \left(\frac{x}{y}\right)^4 - \left(\frac{x}{y}\right)^6 \cdots\right)$
which converge to the same exact solutions on the region $x \le y$.

Example 3.

$$\begin{cases} u_{xx} + \frac{3}{x}u_x + u_{yy} + \frac{4}{y}u_y - \frac{14}{\sqrt{v}} = 0, \\ v_{xx} + \frac{1}{x}v_x + v_{yy} + \frac{1}{y}v_y - 24e^u = 0, \end{cases} \tag{14}$$

$$u(x,0) = 2lnx, \quad u_y(x,0) = 0, \quad v(x,0) = x^4, \quad v_y(x,0) = 0 \tag{15}$$

with exact solutions

$$u(x,y) = \ln(x^2+y^2), \quad v(x,y) = (x^2+y^2)^2.$$

From Table 1 and Corollaries 3.3, 3.4, the modified differential transform version of (14) is

$$\begin{cases} \frac{\partial^2 U(x,h)}{\partial x^2} + \frac{3}{x}\frac{\partial U(x,h)}{\partial x} + (h+5)(h+2)U(x,h+2) - 14F(x,h) = 0, \\ \frac{\partial^2 V(x,h)}{\partial x^2} + \frac{1}{x}\frac{\partial V(x,h)}{\partial x} + (h+2)^2 V(x,h+2) - 24G(x,h) = 0, \end{cases}$$

where $F(x,h)$, $G(x,h)$ are the modified differential transform versions of

$$\frac{1}{\sqrt{v}} \text{ and } e^u, \text{ respectively, such as}$$

$$G(x,h) = \begin{cases} e^{U(x,0)} = x^2, & h = 0, \\ \sum_{s=0}^{h-1} \frac{s+1}{h} U(x,s+1)\, G(x,h-s-1), & h \ge 1. \end{cases}$$

Also, the MDTM versions of initial conditions (15) are

$$U(x,0) = 2lnx, \quad U(x,1) = 0, \quad V(x,0) = x^4, \quad V(x,1) = 0.$$

Then

$$\begin{cases} U(x,h+2) = \frac{-1}{(h+5)(h+2)}\left[\frac{\partial^2 U(x,h)}{\partial x^2} + \frac{3}{x}\frac{\partial U(x,h)}{\partial x} - 14F(x,h)\right], \\ V(x,h+2) = \frac{-1}{(h+2)^2}\left[\frac{\partial^2 V(x,h)}{\partial x^2} + \frac{1}{x}\frac{\partial V(x,h)}{\partial x} - 24G(x,h)\right]. \end{cases}$$

For $h = 0$, we have

$$F(x,0) = \frac{1}{0!}\left(\frac{\partial^0}{\partial y^0}\left(\frac{1}{\sqrt{v(x,y)}}\right)\right)_{y=0} = \frac{1}{\sqrt{V(x,0)}} = \frac{1}{x^2}.$$

So,
$$\begin{cases} U(x,2) = \frac{-1}{10}\left[\frac{\partial^2 U(x,0)}{\partial x^2} + \frac{3}{x}\frac{\partial U(x,0)}{\partial x} - 14F(x,0)\right], \\ \qquad = \frac{-1}{10}\left[\frac{-2}{x^2} + \frac{3}{x}.\frac{2}{x} - \frac{14}{x^2}\right] = \frac{1}{x^2}, \\ V(x,2) = \frac{-1}{4}\left[\frac{\partial^2 V(x,0)}{\partial x^2} + \frac{1}{x}\frac{\partial V(x,0)}{\partial x} - 24G(x,0)\right], \\ \quad = \frac{-1}{4}\left[12x^2 + \frac{1}{x}.4x^3 - 24x^2\right] = \frac{8x^2}{4} = 2x^2. \end{cases}$$

For $h=1$, we have

$$\begin{aligned} F(x,1) &= \frac{1}{1!}\left(\frac{\partial}{\partial y}\left(\frac{1}{\sqrt{v(x,y)}}\right)\right)_{y=0} = \frac{-1}{2}\left(\frac{\partial v(x,y)}{\partial y}.\frac{1}{v(x,y)\sqrt{v(x,y)}}\right)_{y=0} \\ &= \frac{-1}{2}.V(x,1).\frac{1}{V(x,0)\sqrt{V(x,0)}} = 0 , \end{aligned}$$

$$G(x,1) = U(x,1)\,G(x,0) = 0.$$

So,

$$\begin{cases} U(x,3) = \frac{-1}{18}\left[\frac{\partial^2 U(x,1)}{\partial x^2} + \frac{3}{x}\frac{\partial U(x,1)}{\partial x} - 14F(x,1)\right] = 0, \\ V(x,3) = \frac{-1}{9}\left[\frac{\partial^2 V(x,1)}{\partial x^2} + \frac{1}{x}\frac{\partial V(x,1)}{\partial x} - 24G(x,1)\right] = 0. \end{cases}$$

For $h=2$, we have

$$\begin{aligned} F(x,2) &= \frac{1}{2!}\left(\frac{\partial^2}{\partial y^2}\left(\frac{1}{\sqrt{v(x,y)}}\right)\right)_{y=0} = \frac{-1}{4}\left(\frac{\partial}{\partial y}\left(\frac{\partial v(x,y)}{\partial y}.(v(x,y))^{-\frac{3}{2}}\right)\right)_{y=0} \\ &= \frac{-1}{4}\left(\frac{\partial^2 v(x,y)}{\partial y^2}.(v(x,y))^{-\frac{3}{2}} - \frac{3}{2}.\ (v(x,y))^{-\frac{5}{2}}.\frac{\partial v(x,y)}{\partial y}\right)_{y=0} \end{aligned}$$

$$\begin{aligned} &= \frac{-1}{2}.V(x,2)\,(V(x,0))^{-\frac{3}{2}} + \frac{3}{8}.(V(x,0))^{-\frac{5}{2}}.V(x,1) \\ &= \frac{-1}{2}.V(x,2)\,(V(x,0))^{-\frac{3}{2}} = \frac{-1}{2}.\frac{2x^2}{x^6} \\ &= -\frac{1}{x^4}\ . \end{aligned}$$

$$G(x,2) = \sum_{s=0}^{1}\frac{s+1}{2}U(x,s+1)\,G(x,1-s) = \frac{1}{2}U(x,1)\,G(x,1) + U(x,2)\,G(x,0)$$

$$= \frac{1}{x^2}.x^2 = 1.$$

So,

$$\begin{cases} U(x,4) = \frac{-1}{28}\left[\frac{\partial^2 U(x,2)}{\partial x^2} + \frac{3}{x}\frac{\partial U(x,2)}{\partial x} - 14F(x,2)\right], \\ \qquad = \frac{-1}{28}\left[\frac{6}{x^4} + \frac{3}{x}.\frac{-2}{x^3} + \frac{14}{x^4}\right], \\ \qquad = \frac{-1}{2x^4}, \\ V(x,4) = \frac{-1}{16}\left[\frac{\partial^2 V(x,2)}{\partial x^2} + \frac{1}{x}\frac{\partial V(x,2)}{\partial x} - 24G(x,2)\right], \\ \qquad = \frac{-1}{16}\left[4 + \frac{1}{x}.4x - 24\right] = 1. \end{cases}$$

For $h=3$:

$$\begin{cases} U(x,5) = \frac{-1}{25}\left[\frac{\partial^2 U(x,3)}{\partial x^2} + \frac{3}{x}\frac{\partial U(x,3)}{\partial x} - 14F(x,3)\right] = 0, \\ V(x,5) = \frac{-1}{35}\left[\frac{\partial^2 V(x,3)}{\partial x^2} + \frac{1}{x}\frac{\partial V(x,3)}{\partial x} - 24G(x,3)\right] = 0. \end{cases}$$

For $h = 4$:

$$\begin{cases} U(x,6) = \frac{-1}{36}\left[\frac{\partial^2 U(x,4)}{\partial x^2} + \frac{3}{x}\frac{\partial U(x,4)}{\partial x} - 14F(x,4)\right] = \frac{1}{3x^6}, \\ V(x,6) = \frac{-1}{48}\left[\frac{\partial^2 V(x,4)}{\partial x^2} + \frac{1}{x}\frac{\partial V(x,4)}{\partial x} - 24G(x,4)\right] = 0. \end{cases}$$

Then by substituting the quantities $U(x,h)$ in (7), we get the exact solution

$$v(x,y) = x^4 + 2x^2y^2 + y^4 = \left(x^2 + y^2\right)^2$$

and the series solution

$$u(x,y) = 2lnx + \left(\frac{y}{x}\right)^2 - \frac{1}{2}\left(\frac{y}{x}\right)^4 + \frac{1}{3}\left(\frac{y}{x}\right)^6 \cdots$$

the exact solution is

$$u(x,y) = \ln(x^2 + y^2)$$

on the region $x \geq y$.

By applying the symmetric conditions of (15)

$u(0,y) = 2lny, \quad u_x(0,y) = 0, \quad v(0,y) = y^4, \quad v_x(0,y) = 0,$

we obtain the series solutions

$u(x,y) = 2lny + \left(\frac{x}{y}\right)^2 - \frac{1}{2}\left(\frac{x}{y}\right)^4 + \frac{1}{3}\left(\frac{x}{y}\right)^6 \cdots$

which converge to the same exact solutions on the region $x \leq y$.

6 Conclusion

In this study, we are the first to introduce the two-dimensional Lane–Emden system equations and to derive exact analytical solutions without resorting to linearization, discretization, or perturbation techniques. By successfully applying the Modified Differential Transformation Method (MDTM) to these nonlinear forms, we obtain highly accurate solutions with significantly reduced computational effort. This approach leverages novel product and quotient properties specific to various differential transform methods, which we previously established in another paper.

References

[1] A.M. Wazwaz, R.Rach and J.S. Duan. Solving the two-dimensional Lane–Emden type equations by the Adomian decomposition method. *J. Appl. Math. Stat.* **3** (2016) 15–26.

[2] N. Teyar. Properties of MDTM and RDTM for Nonlinear Two-Dimensional Lane-Emden Equations. *Nonlinear Dynamics and Systems Theory* **24** (3) (2024) 309–320.

[3] L. Maia, G. Nornberge and F. Pacella. *A Dynamical System Approach for Lane–Emden Type Problems.* Rio de Janeiro: IMPA, 2021, Brazil.

[4] R. Abazari and M. Abazari. Numerical study of Burgers–Huxley equations via reduced differential transform method. *Comp. Appl. Math.* **32** (1) (2013) 1–17.

[5] X. Bao and Y. Chan. An application of nonlinear integro-differential equations by differential transform method with Adomian polynomials. *International Journal of Dynamical Systems and Differential Equations* **12** (6) (2022) 467–476.

[6] M. J. Jang, C. L. Chen and Y. C. Liu. Two-dimensional differential transform for partial differential equations. *Appl.Math. Comput.* **121** (2001) 261–270.

[7] O. Figen Kangalgil and F. Ayaz. Solitary wave solutions for the KdV and mKdV equations by differential transform method. *Chaos Solitons Fractals* **41** (2009) 464–472.

[8] B. İbiş and M. Bayram. Approximate solutions for some nonlinear evolutions equations by using the reduced differential transform method. *Int. J. Appl. Math. Res.* **1** (3) (2012) 288–302.

[9] A.S.V.R. Kanth and K.Aruna. Comparison of two Dimensional DTM and PDTM for solving Time-Dependent Emden-Fowler Type Equations. *Int. J. Nonlinear Sci.* **2012** (13) 228–239.

[10] Y. Keskin and G. Oturanc. Reduced differential transform method for generalized KdV equations. *Math. Comput. Appl.* **15** (3) (2010) 382–393

[11] A. M. Al-Rozbayani and A. F. Qasim. Modified α-Parameterized Differential Transform Method for Solving Nonlinear Generalized Gardner Equation. *Journal of Applied Mathematics* (2023) Article ID 3339655.

[12] A. Saravanan and N. Magesh. A comparison between the reduced differential transform method and the Adomian decomposition method for the Newell–Whitehead–Segel equation. *J. Egyptian Math. Soc.* **21** (3) (2013) 259–265.

Nonlinear Dynamics and Systems Theory, **25** (6) (2025) 643–655

Two-Parameter Quasi-Boundary Regularization for Backward Cauchy Problems

Nawel Moudjeb[1], Khaled Bessila[2], Ali Abdessemed[2] and Okba Zehrour[1*]

[1] *Dynamic Systems and Control Laboratory, Oum El Bouaghi University, Oum El Bouaghi, Algeria.*
[2] *Applied Mathematics and Modeling Laboratory, Constantine 1 University, Constantine, Algeria.*

Received: April 10, 2025 ; Revised: December 1, 2025

Abstract: We propose a two-parameter quasi-boundary regularization method for solving the ill-posed backward Cauchy problem. The Lambert W function is employed for the first time to derive enhanced stability bounds and refined convergence rates. Our approach perturbs the final data via two distinct parameters, providing better control of approximation errors. We prove the regularised problem's well-posedness and derive novel Hölder-Lambert stability estimates. Numerical experiments confirm that our method improves the accuracy of estimated errors, especially under high noise levels.

Keywords: *ill-posed problems; regularization; quasi-boundary value method; backward parabolic problem; stability analysis; Hölder–Lambert stability.*

Mathematics Subject Classification (2020): 35R20, 35R25, 35K90, 93C20, 93D20.

1 Introduction

Let H be a Hilbert space with the inner product $(.,.)$ and the norm $\|.\|$, and A be a self-adjoint operator on H. Assume that A admits an orthonormal eigenbasis $(\varphi_i)_{i\geq 1}$ in H, associated to the eigenvalues $(\lambda_i)_{i\geq 1}$ such that

$$0 < \lambda_1 < \lambda_2 < ...\text{et} \lim_{i\longrightarrow +\infty} \lambda_i = +\infty.$$

* Corresponding author: mailto:okbazehrour@yahoo.fr

The problem is to find a function $u : [0,T] \to H$, the solution of the final-value problem (FVP):

$$u'(t) + Au(t) = 0, \ 0 \le t \le T, \tag{1}$$

with a final condition

$$u(T) = f \tag{2}$$

for some predefined final value $f \in H$.

The FVP (1),(2) is an ill-posed problem. Even in the case of a unique solution that exists on $[0,T]$, the latter does not depend continuously on the final value of f. This type of problem has been considered by several authors using different regularisation methods, one of which is the quasi-reversibility method introduced by Lattes and Lions [1] and developed by Payne [2], Miller [3] and Showalter [4]. We replaced the operator A with a perturbation operator in this method. The other method of regularisation is the quasi-boundary value method introduced by Showalter [5] and developed in [6–10]. This method perturbs the final condition with one regularisation parameter. Moreover, in [6], the final condition (2) is replaced by

$$u(T) + \alpha u(0) = f,$$

and in [7], by

$$u(T) - \alpha u'(0) = f.$$

In other studies [11–13], the perturbation is applied directly to the final data instead of the condition, with either one or two regularization parameters. The origin of this method goes back to [11], by giving a specific value to f.

In this work, we propose a new version of the quasi-boundary regularization method based on a two-parameter perturbation, α and τ, of the final data f. The parameter α accounts for measurement errors, while τ reflects the regularity of the solution. Furthermore, we introduce, for the first time in this context, the Lambert W function as a central analytical tool such that equation (2) is replaced by

$$u(T) = f_{\alpha,\tau}, \tag{3}$$

where $\tau \ge 0$, $\alpha \in (0,1)$ and

$$f_{\alpha,\tau} = \sum_{i=1}^{\infty} \frac{b_i e^{-\lambda_i(T+\tau)}}{e^{-\lambda_i(T+\tau)} + \alpha\lambda_i^2}\varphi_i. \tag{4}$$

The backward Cauchy problem studied in this work naturally arises in nonlinear dynamical systems, especially in optimal control, inverse heat conduction, and system identification scenarios. Such problems typically involve reconstructing past states from final-time measurements, often subject to high noise levels. The ill-posedness of these problems directly impacts stability, accuracy, and predictive capability in nonlinear dynamical settings. Our proposed two-parameter quasi-boundary regularization method addresses these fundamental challenges by enhancing stability and convergence properties, making it particularly suitable for the reliable prediction and control of complex nonlinear systems.

We analyze the modified problem rigorously, proving the existence and uniqueness of the regularized solution. We then generate stability estimates that outperform the classical Holder results, introducing a new Holder-Lambert convergence rate. Furthermore, we provide error bounds for both exact and noisy data, and validate our theoretical results by comparing the numerical results in [13] with the remarkable accuracy and efficiency of our method, especially for small values of the noise level.

In Section 2, we introduce the Lambert W function, formulate the modified problem and present our theoretical results, including stability and convergence theorems. In Section 3, we provide numerical experiments that illustrate the effectiveness of the proposed method.

2 The Lambert W Function and the Approximate Problem

For historical notes and the upcoming Lambert W special function in the mathematical literature, we would like to refer the reader to the papers [14–17] and references there. To stay in the real case, it is the function usually denoted by $W(x)$ and defined as the inverse of the function (xe^x), it is generally used for solving transcendental algebraic equations. The function (xe^x) being one-to-one an $x \geq 1$, the principal Lambert function $W(x)$ is its reciprocal. We may find different analytic and differential properties of $W(x)$. In our context, we need its asymptotic expansion established in [15, 16], and given by

$$W(x) = \log(x) - \log(\log(x)) + \sum_{n\geq 1} \frac{(-1)^n}{(\log x)^n} a_n(x) \ ; x \gg A, \tag{5}$$

where $a_n(x) = \sum_{m=1}^{n} (-1)^m s(n, n-m+1) \frac{(\log(\log(x)))^m}{m!}$, $s(n, k)$ are Stirling numbers of the first kind. Therefore, our results are much sharper and more exact through the use of (5) than any others known in the literature on the regularization of ill-posed problems, particularly backward in time heat problems.

We turn now to the study of the approximate problem $QBVP$ (1),(3). We first show that $QBVP$ (1),(3) is a well-posed problem. If $(\varphi_i)_{i\geq 1}$ is an orthonormal basis in H, then for all $f \in H$, we have

$$f = \sum_{i=1}^{\infty} b_i \varphi_i, \ b_i = (f, \varphi_i) \ , \forall i \geq 1. \tag{6}$$

If the problem FVP (1),(2) (respectively, $QBVP$ (1),(3)) admits a solution u (respectively, $u_{\alpha,\tau}$), then

$$u(t) = \sum_{i=1}^{\infty} b_i e^{\lambda_i (T-t)} \varphi_i \quad , \forall t \in [0, T], \tag{7}$$

and

$$u_{\alpha,\tau}(t) = \sum_{i=1}^{\infty} \frac{b_i e^{-\lambda_i (t+\tau)}}{e^{-\lambda_i (T+\tau)} + \alpha \lambda_i^2} \varphi_i \quad , \forall t \in [0, T]. \tag{8}$$

To start, for the upcoming results, we need the following lemma, which introduces the Lambert W special function.

Lemma 2.1 *For all $t \in [0,T]$, $\tau \geqslant 0$ and $\alpha \in (0,1)$, we have*

$$\frac{e^{-\lambda(t+\tau)}}{e^{-\lambda(T+\tau)}+\alpha\lambda^2} \leqslant \frac{1}{\left(\alpha W\left(\frac{(T+\tau)^2}{2\alpha}\right)\right)^{\frac{T-t}{T+\tau}}} \left(\frac{(T+\tau)^2}{2+W\left(\frac{(T+\tau)^2}{2\alpha}\right)}\right)^{\frac{T-t}{T+\tau}}. \tag{9}$$

Proof. Let $t \in [0,T]$, $\tau \geqslant 0$ and $\alpha \in (0,1)$. If we consider the function

$$h(\lambda) = \frac{1}{e^{-\lambda(T+\tau)}+\alpha\lambda^2},\ \lambda \in \mathbb{R}_+^*,$$

then $h(\lambda)$ attains its maximum at

$$\lambda_0 = \frac{1}{T+\tau} W\left(\frac{(T+\tau)^2}{2\alpha}\right), \tag{10}$$

hence

$$\frac{1}{e^{-\lambda(T+\tau)}+\alpha\lambda^2} \leqslant \frac{1}{\alpha W\left(\frac{(T+\tau)^2}{2\alpha}\right)} \frac{(T+\tau)^2}{\left(2+W\left(\frac{(T+\tau)^2}{2\alpha}\right)\right)}. \tag{11}$$

Consequently, the lemma follows from the equality

$$\frac{e^{-\lambda(t+\tau)}}{e^{-\lambda(T+\tau)}+\alpha\lambda^2} = \frac{e^{-\lambda(t+\tau)}}{\left(e^{-\lambda(T+\tau)}+\alpha\lambda^2\right)^{\frac{T-t}{T+\tau}}\left(e^{-\lambda(T+\tau)}+\alpha\lambda^2\right)^{\frac{t+\tau}{T+\tau}}}$$

and the estimate (11) above.

Theorem 2.1 *For all $f \in H$, the regularized problem QBVP (1),(3) has a unique solution $u_{\alpha,\tau}$. Moreover, the following estimate holds:*

$$\|u_{\alpha,\tau}(t)\| \leq \frac{1}{\left(\alpha W\left(\frac{(T+\tau)^2}{2\alpha}\right)\right)^{\frac{T-t}{T+\tau}}} \left(\frac{(T+\tau)^2}{2+W\left(\frac{(T+\tau)^2}{2\alpha}\right)}\right)^{\frac{T-t}{T+\tau}} \|f\|,\ t \in [0,T], \tag{12}$$

where $\tau \geqslant 0$, $\alpha \in (0,1)$ and W is the Lambert function.

Proof. For $t \in [0,T]$, let us take

$$u_{\alpha,\tau(n)}(t) = \sum_{i=1}^{n} \frac{b_i e^{-\lambda_i(t+\tau)}}{e^{-\lambda_i(T+\tau)}+\alpha\lambda_i^2}\varphi_i.$$

Since $\left(u_{\alpha,\tau(n)}\right)_{n\geqslant 1}$ represents the sequence of partial sums of the series (8), it suffices to show that $u_{\alpha,\tau(n)} \in C^1([0,T],H)$ and $\left\|\lim\limits_{n\longrightarrow+\infty} u_{\alpha,\tau(n)}(0)\right\| < +\infty$.
Set

$$v_{\alpha,\tau}(t) = -\sum_{i=1}^{+\infty} \frac{\lambda_i b_i e^{-\lambda_i(t+\tau)}}{e^{-\lambda_i(T+\tau)}+\alpha\lambda_i^2}\varphi_i.$$

So,

$$u'_{\alpha,\tau(n)}(t) - v_{\alpha,\tau}(t) = \sum_{i=n+1}^{+\infty} \frac{\lambda_i b_i e^{-\lambda_i (t+\tau)}}{e^{-\lambda_i (T+\tau)} + \alpha\lambda_i^2} \varphi_i.$$

Using the hypothesis $\lambda_i^2 \longrightarrow +\infty$ and the inequality

$$\frac{\lambda_i^2 b_i^2 e^{-2\lambda_i (t+\tau)}}{(e^{-\lambda_i (T+\tau)} + \alpha\lambda_i^2)^2} \leq \frac{b_i^2}{\alpha^2} \ , \ \forall i \geq 1, \tag{13}$$

we get

$$\lim_{n\longrightarrow +\infty} \sup_{t\in[0,T]} \left\| u'_{\alpha,\tau(n)}(t) - v_{\alpha,\tau}(t) \right\| = 0.$$

Then the sequence $(u'_{\alpha,\tau(n)})_{n\geqslant 1}$ converges uniformly in t. Moreover, the use of the Weierstrass criterion insures that $u_{\alpha,\tau} \in C^1([0,T], H)$ and

$$u'_{\alpha,\tau}(t) = -\sum_{i=1}^{\infty} \frac{\lambda_i b_i e^{-\lambda_i (t+\tau)}}{e^{-\lambda_i (T+\tau)} + \alpha\lambda_i^2} \varphi_i ; \forall t \in [0,T], \tau \geqslant 0. \tag{14}$$

Using (13), we have $u_{\alpha,\tau}(t) \in D(A)$ and

$$Au_{\alpha,\tau}(t) = \sum_{i=1}^{+\infty} \frac{\lambda_i b_i e^{-\lambda_i (t+\tau)}}{e^{-\lambda_i (T+\tau)} + \alpha\lambda_i^2} \varphi_i, \ \forall t \in [0,T], \ \tau \geqslant 0. \tag{15}$$

So, by virtue of (8), (14) and (15), we find that $u_{\alpha,\tau}$ is a classical solution of $QBVP$ (1),(3).
Let $t \in [0,T]$. From (8), we have

$$\|u_{\alpha,\tau}(t)\|^2 \leq \sum_{i=1}^{+\infty} b_i^2 \left(\frac{e^{-\lambda_i (t+\tau)}}{e^{-\lambda_i (T+\tau)} + \alpha\lambda_i^2} \right)^2 , \tag{16}$$

and using Lemma 2.1, the estimate (12) is then deduced from (15).

Remark 2.1 We note in Theorem 2.1 above, we have a new stability order given by

$$\omega(\alpha,\tau,T) = \frac{1}{\left(\alpha W^2\left(\frac{(T+\tau)^2}{2\alpha}\right)\right)^{\frac{T-t}{T+\tau}}}, \ \alpha > 0, \ \tau \geqslant 0,$$

where W^2 is the square of $W(x)$. This order does not exist in the literature concerning inverse problems backward in time. Our order of stability involves the Lambert W function, and improves significantly the existing Hölder order $\alpha^{\frac{t-\tau}{T+\tau}}$ known up to date. According to the asymptotic expansion of W given in (5), we largely have

$$\frac{1}{\alpha W^2\left(\frac{(T+\tau)^2}{2\alpha}\right)} \ll \frac{1}{\alpha}, \alpha > 0,$$

for α small enough; $W\left(\frac{(T+\tau)^2}{2\alpha}\right)$ is approximatively

$$\log\left(\frac{(T+\tau)^2}{2\alpha}\right)-\log\left(\log\left(\frac{(T+\tau)^2}{2\alpha}\right)\right)+O\left(\left(\frac{\log\left(\log\left(\frac{(T+\tau)^2}{2\alpha}\right)\right)}{\log\left(\frac{(T+\tau)^2}{2\alpha}\right)}\right)^2\right),$$

the term $\frac{1}{W^2\left(\frac{(T+\tau)^2}{2\alpha}\right)}$ restrains $\frac{1}{\alpha}$ from going to infinity rapidly; and consequently, stability is much more controlled, particularly when using numerical schemes for applications. Moreover, this mixed Hölder-Lambert type of stability is much more sharp and exact than the Hölder type, stability is much more weighted by the presence of the term $W^2\left(\frac{(T+\tau)^2}{2\alpha}\right)$, particularly for applications and numerical computations. Finally, the choice of a second parameter τ in our approach gives rather good uniform results and regularity around the origin instant $t_0=0$. This improves many results where the stability is of order $\alpha^{-\frac{t}{T}}$, which is meaningless whenever t is in the neighborhood of the origin.

Theorem 2.2 *For every $f\in H$ and $\tau\geq 0$, $\|u_{\alpha,\tau}(T)-f\|\longrightarrow 0$ as $\alpha\to 0$. That is, $u_{\alpha,\tau}(T)$ converges to f in H.*

Proof. Let $f\in H$, $\tau\geq 0$, and $\varepsilon>0$. Choose some N for which $\sum_{i=N+1}^{+\infty} b_i^2<\frac{\varepsilon}{2}$.
From (4) and (8), we have

$$\|u_{\alpha,\tau}(T)-f\|^2\leq \alpha^2\sum_{i=1}^{N}\lambda_i^4 b_i^2 e^{2\lambda_i(T+\tau)}+\frac{\varepsilon}{2}. \tag{17}$$

If we take $\alpha^2<\varepsilon\left(2\sum_{i=1}^{N}\lambda_i^4 b_i^2 e^{2\lambda_i(T+\tau)}\right)^{-1}$, then we get

$$\lim_{\alpha\to 0}\|u_{\alpha,\tau}(T)-f\|=0,$$

as required.

Theorem 2.3 *For all $f\in H$ and $\tau\geq 0$, the FVP (1),(2) has a solution u given by (7) if and only if the sequence $(u_{\alpha,\tau}(0))$ converges in H. Furthermore, the sequence $(u_{\alpha,\tau})$ converges to u as α tends to zero, uniformly in t.*

Proof. Let $f\in H$ and $\tau\geq 0$. Assume that $\lim_{\alpha\to 0}u_{\alpha,\tau}(0)=u_0$ exists. Since $u_0\in H$, we have

$$u_0=\sum_{i=1}^{+\infty}u_{0i}\varphi_i.$$

The solution of the initial problem

$$\begin{cases} v'(t)+Av(t)=0 \quad, \ 0\leq t\leq T,\\ v(0)=u_0,\end{cases}$$

is given by

$$v(t)=\sum_{i=1}^{+\infty}u_{0i}e^{-\lambda_i t}\varphi_i. \tag{18}$$

Let $t \in [0,T]$. From (8), we get

$$\|u_{\alpha,\tau}(t) - v(t)\| \leq \|u_{\alpha,\tau}(0) - u_0\|.$$

This means that $u_{\alpha,\tau}$ converges uniformly to v in H.
Moreover, $\lim_{\alpha\to 0} u_{\alpha,\tau}(T) = v(T)$. Using Theorem 2.2, we have $v(T) = f$ and v is a solution of the FVP (1),(2). Assuming that u is the solution to FVP (1),(2), given by (7), we prove that $(u_{\alpha,\tau}(0))$ converges in H. From (7) and (8), we have

$$\|u_{\alpha,\tau}(t) - u(t)\|^2 = \sum_{i=1}^{+\infty} \left(\frac{b_i e^{-\lambda_i \tau}}{e^{-\lambda_i(T+\tau)} + \alpha\lambda_i^2} - b_i e^{\lambda_i T} \right)^2 e^{-2\lambda_i t}$$

so that

$$\|u_{\alpha,\tau}(t) - u(t)\| \leq \|u_{\alpha,\tau}(0) - u(0)\|. \tag{19}$$

Since u is the solution of FVP (1)-(2), $u(0) \in H$ and $\sum_{i=1}^{+\infty} b_i^2 e^{2\lambda_i T} < +\infty$.
Let $\varepsilon > 0$ and choose some N for which $\sum_{i=N+1}^{+\infty} b_i^2 e^{2\lambda_i T} < \frac{\varepsilon}{2}$. From (7),(8), we have

$$\|u_{\alpha,\tau}(0) - u(0)\|^2 \leq \alpha^2 \sum_{i=1}^{N} e^{4\lambda_i T} \lambda_i^4 e^{2\lambda_i \tau} b_i^2 + \frac{\varepsilon}{2}. \tag{20}$$

So, when taking α such that $\alpha^2 < \varepsilon(2\sum_{i=1}^{N} e^{4\lambda_i T}\lambda_i^4 e^{2\lambda_i\tau} b_i^2)^{-1}$, the sequence $(u_{\alpha,\tau}(0))$ converges to $u(0)$ as α tends to zero. Furthermore, from (19),(20), $u_{\alpha,\tau}$ converges to u, which ends the proof.

The following theorem expresses the error estimate in the case of exact data.

Theorem 2.4 *Let $f \in H$, $\tau \geq 0$ and $\alpha \in (0,1)$. Suppose that FVP (1),(2) has a unique solution u such that the series $C_{T,\tau} = \sum_{i=1}^{+\infty} b_i^2 \lambda_i^4 e^{2\lambda_i(T+\tau)}$ is convergent. Then the following estimate holds for all $t \in [0,T]$:*

$$\|u(t) - u_{\alpha,\tau}(t)\| \leq C_{T,\tau} \frac{\alpha^{\frac{t+\tau}{T+\tau}}}{\left(W\left(\frac{(T+\tau)^2}{2\alpha}\right)\right)^{\frac{T-t}{T+\tau}}} \frac{(T+\tau)^{2\left(\frac{T-t}{T+\tau}\right)}}{\left(2 + W\left(\frac{(T+\tau)^2}{2\alpha}\right)\right)^{\frac{T-t}{T+\tau}}}, \tag{21}$$

where $u_{\alpha,\tau}$ is the solution of $QBVP$ (1),(3).

Proof. Let $\varepsilon > 0$. Suppose that the problem FVP (1),(2) has a unique solution u. Then u is given as

$$u(t) = \sum_{i=1}^{+\infty} b_i e^{\lambda_i(T-t)} \varphi_i.$$

Therefore

$$\|u(t) - u_{\alpha,\tau}(t)\|^2 = \sum_{i=1}^{+\infty} b_i^2 \alpha^2 \lambda_i^4 \left(\frac{e^{-\lambda_i(t-T)}}{e^{-\lambda_i(T+\tau)} + \alpha\lambda_i^2} \right)^2, \tag{22}$$

$$= \sum_{i=1}^{+\infty} b_i^2 \alpha^2 \lambda_i^4 e^{2\lambda_i(T+\tau)} \left(\frac{e^{-\lambda_i(t+\tau)}}{e^{-\lambda_i(T+\tau)} + \alpha\lambda_i^2} \right)^2. \tag{23}$$

Using (9), we get

$$\|u(t)-u_{\alpha,\tau}(t)\|^2 \leq \alpha^{2\left(\frac{t+\tau}{T+\tau}\right)} \left[\frac{(T+\tau)^2}{W\left(\frac{(T+\tau)^2}{2\alpha}\right)\left[2+W\left(\frac{(T+\tau)^2}{2\alpha}\right)\right]}\right]^{2\left(\frac{T-t}{T+\tau}\right)} \sum_{i=1}^{+\infty} b_i^2\lambda_i^4 e^{2\lambda_i(T+\tau)}.$$

Based on the condition $\sum_{i=1}^{+\infty} b_i^2\lambda_i^4 e^{2\lambda_i(T+\tau)} < +\infty$, we find

$$\|u(t)-u_{\alpha,\tau}(t)\| \leq C_{T,\tau}\frac{\alpha^{\frac{t+\tau}{T+\tau}}}{\left(W\left(\frac{(T+\tau)^2}{2\alpha}\right)\right)^{\frac{T-t}{T+\tau}}}\frac{(T+\tau)^{2\left(\frac{T-t}{T+\tau}\right)}}{\left(2+W\left(\frac{(T+\tau)^2}{2\alpha}\right)\right)^{\frac{T-t}{T+\tau}}},$$

as required.

Remark 2.2 Thus, new mixed Hölder-Lambert type of convergence rate estimates improves very much the Hölder type $\alpha^{\frac{t+\tau}{T+\tau}}$ known in the litterature. Clearly, from Theorem 2.4, it is of the from

$$\omega_c(\alpha,T,\tau) = \frac{\alpha^{\frac{t+\tau}{T+\tau}}}{W^2\left(\frac{(T+\tau)^2}{2\alpha}\right)^{\frac{T-t}{T+\tau}}},$$

where W^2 is the square of $W(x)$. From the asymptotic behaviour of the Lambert W function in (11), we have

$$\omega_c(\alpha,T,\tau) \ll \alpha^{\frac{t+\tau}{T+\tau}},$$

and $\omega_c(\alpha,T,\tau)$ tends to zero faster than $\alpha^{\frac{t+\tau}{T+\tau}}$ because of the new infinite term $W^2\left(\frac{(T+\tau)^2}{2\alpha}\right)$ in the denominator. This Hölder-Lambert type is more strong and exact than any Hölder type or Hölder-logarithmic rate known, and involves better precision for numerical computation and applications.

Theorem 2.5 *Let u and $u^\delta_{\alpha,\tau}$ be solutions of the FVP (1),(2) and QBVP (1),(3), respectively, in the case where $f \equiv f_\delta$ such that $\|f-f_\delta\| < \delta$.*
Suppose that $\left\|\sum_{i=1}^{+\infty} b_i\lambda_i^2 e^{\lambda_i T}\varphi_i\right\| \leq K$. Taking into account the fact that K is a positive constant, we have

$$\|u(t)-u^\delta_{\alpha,\tau}(t)\| \leq \frac{C_{k,\delta,\alpha}}{W\left(\frac{(T+\tau)^2}{2\alpha}\right)}.\frac{(T+\tau)^2}{\left(2+W\left(\frac{(T+\tau)^2}{2\alpha}\right)\right)}, \tag{24}$$

where $C_{k,\delta,\alpha} = (\frac{\delta}{\alpha}+K)$.

Proof. Let u and $u^\delta_{\alpha,\tau}$ be solutions of the FVP (1),(2) and QBVP (1),(3), respectively, in the case where $f \equiv f_\delta$ such that $\|f-f_\delta\| < \delta$.
Set

$$u^\delta_{\alpha,\tau}(t) = \sum_{i=1}^{+\infty} \frac{b_i^\delta e^{-\lambda_i(t+\tau)}}{e^{-\lambda_i(T+\tau)}+\alpha\lambda_i^2}\ \varphi_i\ ,\quad \forall t\in[0,T], \tau \geqslant 0, \tag{25}$$

where

$$b_i^\delta = (f_\delta, \varphi_i) \ , \quad \forall i \geq 1. \tag{26}$$

Substitute (7) and (25) into the following inequality:

$$\|u(t) - u_{\alpha,\tau}^\delta(t)\| \leq \|u(t) - u_{\alpha,\tau}(t)\| + \|u_{\alpha,\tau}(t) - u_{\alpha,\tau}^\delta(t)\|.$$

From (11), we obtain

$$\|u(t) - u_{\alpha,\tau}(t)\| \leq \frac{(T+\tau)^2}{W\left(\frac{(T+\tau)^2}{2\alpha}\right)\left(2 + W\left(\frac{(T+\tau)^2}{2\alpha}\right)\right)} K \tag{27}$$

and

$$\|u_{\alpha,\tau}(t) - u_{\alpha,\tau}^\delta(t)\| \leq \frac{(T+\tau)^2\delta}{\alpha W\left(\frac{(T+\tau)^2}{2\alpha}\right)\left(2 + W\left(\frac{(T+\tau)^2}{2\alpha}\right)\right)}, \tag{28}$$

once again, the use of (27) and (28) gives us

$$\|u(t) - u_{\alpha,\tau}^\delta(t)\| \leq \frac{(T+\tau)^2 K}{W\left(\frac{(T+\tau)^2}{2\alpha}\right)\left(2 + W\left(\frac{(T+\tau)^2}{2\alpha}\right)\right)} + \frac{(T+\tau)^2\delta}{\alpha W\left(\frac{(T+\tau)^2}{2\alpha}\right)\left(2 + W\left(\frac{(T+\tau)^2}{2\alpha}\right)\right)},$$

from which, by taking $\alpha = \delta$, we obtain

$$\|u(t) - u_{\alpha,\tau}^\delta(t)\| \leq \frac{(T+\tau)^2}{W\left(\frac{(T+\tau)^2}{2\delta}\right)\left(2 + W\left(\frac{(T+\tau)^2}{2\delta}\right)\right)}(1+K).$$

In the above theorem, α and δ are kept proportional; and the rate of convergence is of order $\frac{C_{k,\delta,\alpha}}{W^2\left(\frac{(T+\tau)^2}{2\alpha}\right)}$, where W^2 is the square of $W(x)$.

3 Numerical Experiments

In this section, we present numerical experiments to evaluate the performance of our two-parameter modified quasi-boundary regularisation method for an inverse heat conduction problem in a cylindrical domain. We consider the same example as that studied in [13] to allow for a direct comparison of results.

We begin by recalling the following initial-boundary value problem, which has been previously studied in [13]:

$$(3.1) \begin{cases} \frac{\partial u}{\partial t} = \frac{\partial^2 u}{\partial r^2} + \frac{1}{r}\frac{\partial u}{\partial r}, 0 < r < r_0, 0 < t < T, \\ u(r_0, t) = 0, 0 \leq t \leq T, \\ u(r,t) \ bounded \ as \ r \to 0 \ , \\ u(r,T) = f^{ex}(r), 0 \leq r \leq r_0. \end{cases}$$

Here, r is the radial coordinate, $f^{ex}(r) = e^T J_0(\frac{\mu_1}{r_0} r)$ represents the final temperature history of the cylinder. The objective is to reconstruct the temperature distribution $u(.,t)$ for $0 \leq t \leq T$, from noisy final-time data. The solution to problem (3.1) is given by

$$u^{ex}(r,t) = e^t e^{(\frac{\mu_1}{r_0})^2(T-t)} J_0(\frac{\mu_1}{r_0} r), \tag{29}$$

the function $J_0(x)$ is a Bessel function, where μ_n is its root. We will approximate (3.1) by the following regularised problem:

$$(3.2)\begin{cases} \frac{\partial u}{\partial t}=\frac{\partial^2 u}{\partial r^2}+\frac{1}{r}\frac{\partial u}{\partial r}, 0<r<r_0, 0<t<T,\\ u(r_0,t)=0, 0\le t\le T,\\ u(r,t)\ \textit{bounded as}\ r\to 0\ ,\\ u(r,T)=f^{\epsilon}(r), 0\le r\le r_0,\end{cases}$$

where

$$f^{\epsilon}(r)=e^{T}J_0(\frac{\mu_1}{r_0}r)+\sum_{p=1}^{p_0}\epsilon a_p J_0\left(\frac{\mu_p}{r_0}r\right),$$

where p_0 is a random natural number and a_p is a finite sequence of random normal numbers with mean 0 and variance A^2. It follows that the error in the measurement process is bounded by ϵ, $\parallel f^{\epsilon}-f^{ex}\parallel\le\epsilon$. The regularized solution, which is obtained by (8) and corresponds to the data f^{ϵ}, is

$$u_{\epsilon,\tau}(r,t)=\frac{e^{1-(\frac{\mu_1}{r_0})^2(t+\tau)}}{e^{-(\frac{\mu_1}{r_0})^2(T+\tau)}+\epsilon(\frac{\mu_1}{r_0})^4}J_0(\frac{\mu_1}{r_0}r)+\sum_{i=1}^{p_0}a_p\frac{\epsilon e^{-(\frac{\mu_p}{r_0})^2(t+\tau)}}{e^{-(\frac{\mu_p}{r_0})^2(T+\tau)}+\epsilon(\frac{\mu_p}{r_0})^4}J_0(\frac{\mu_p}{r_0}r). \quad (30)$$

For each point of time, the relative error is obtained by the following relationship:

$$RE(\epsilon,t)=\frac{\parallel u^{app}(.,t)-u^{ex}(.,t)\parallel}{\parallel u^{ex}(.,t)\parallel}.$$

Fix $T=1, r_0=2, p_0=1000, A^2=100$.

Case 01:

Fix $\tau=0.3$. We consider the discretizations $\epsilon_1=10^{-1}$, $\epsilon_2=10^{-2}$, $\epsilon_3=10^{-3}$, respectively. The results obtained are presented in the following figures.

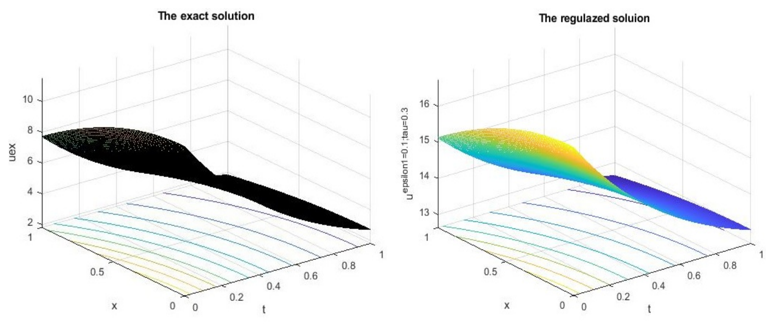

Figure 1: The exact solution and regularized solution with $\epsilon_1=10^{-1}$ and $\tau=0.3$.

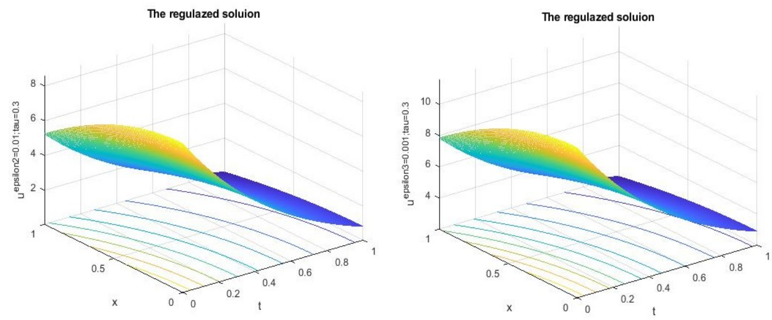

Figure 2: The approximate solution with $\tau = 0.3$, $\epsilon_2 = 10^{-2}$, and $\epsilon_3 = 10^{-3}$.

Case 02:
Fix $\epsilon = 10^{-3}$. We consider the discretizations $\tau_1 = 0$, $\tau_2 = 0.3$, respectively. The results obtained are presented in the following figures.

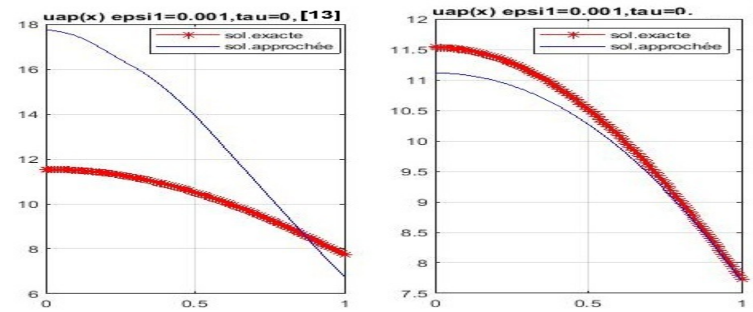

Figure 3: The comparison between the exact solution and the approximate solution in this paper and in [13] with $\epsilon = 10^{-3}$ for $\tau = 0$.

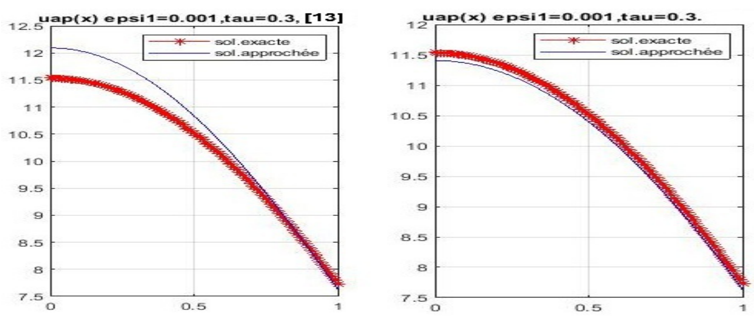

Figure 4: The comparison between the exact solution and the approximate solution in this paper and in [13] with $\epsilon = 10^{-3}$ for $\tau = 0.3$.

Furthermore, we provide comparison tables.

ε	$\|u_{\epsilon,\tau}(.,0) - u^{ex}(.,0)\|$	$RE(\varepsilon, 0)$
$\varepsilon = 10^{-3}$	1.89912372122484	0.0183775205270803
$\varepsilon = 10^{-4}$	0.370482962729477	0.00358510516002786
$\varepsilon = 10^{-5}$	0.0568432599456435	0.000550063255385745
$\varepsilon = 10^{-6}$	0.0508581110298997	0.000492145913915346
$\varepsilon = 10^{-7}$	0.0111367060795689	0.00010776814711647

Table 1: Error and relative error of the proposed method for $\tau = 0.3$ and various values of ε.

In paper [13], we have the same table as that we created with the same values ε, but with results different from our results. We notice that whenever we reduce the values ε, we find that the relative error and absolute error in the two tables decrease, but in our work it decreases better, which makes the regular solution closer to the exact solution and better than that found in [13], and this shows that our method is more effective. We note that our method improved accuracy and so our results are more accurate than in [13]. We also reduced the errors in the data. For comparison, we reproduce below the table presented in paper [13] (see p. 11)

ε	$\|u_{\epsilon,\tau}(.,0) - u^{ex}(.,0)\|$	$RE(\varepsilon, 0)$
$\varepsilon = 10^{-3}$	8.48702923827765	0.115626406608408
$\varepsilon = 10^{-4}$	5.84620043944197	0.079648028791562
$\varepsilon = 10^{-5}$	3.59734075211554	0.049009797519858
$\varepsilon = 10^{-6}$	0.723559578438893	0.009857700695156
$\varepsilon = 10^{-7}$	0.0550576642083171	0.000173396997915

Table 2: Error and relative error of the method by N.V. Hoa and T.Q. Khanh in [13] for $\tau = 0.3$ and various values of ε.

The numerical experiments confirm that our two-parameter regularisation method is accurate and stable. The solution improves as the noise level decreases, especially with $\tau = 0.3$. Our approach consistently achieves smaller errors than the method in [13]. These results validate the effectiveness of our method for inverse heat conduction problems with noisy data.

4 Conclusion

In this work, we proposed a two-parameter quasi-boundary regularisation method for solving the backward Cauchy problem commonly encountered in nonlinear dynamical systems. Our approach integrates the Lambert W function for the first time, significantly enhancing stability bounds and providing refined Hölder-Lambert-type convergence rates. Rigorous theoretical analysis established the well-posedness and stability of the regularised formulation. Numerical experiments demonstrated that our method achieves greater accuracy and robustness than existing techniques, particularly under high noise conditions. These results confirm our approach's effectiveness and practical applicability, especially for inverse problems involving noisy data in nonlinear dynamics and optimal control settings.

References

[1] R. T. Lattès and J. L. Lions. *Méthode de quasi-réversibilité et applications.* Dunod, Paris, 1967. (English translation by R. Bellman, Elsevier, New York, 1969.)

[2] L. E. Payne. Some general remarks on improperly posed problems for partial differential equations. In: *Lecture Notes in Mathematics* **316**. Springer, Berlin (1973), 1–30.

[3] K. Miller. Stabilized quasireversibility and other nearly best possible methods for non-well-posed problems. In: *Lecture Notes in Mathematics* **316**. Springer, Berlin (1973), 161–176.

[4] R. E. Showalter. The final value problem for evolution equations. *J. Math. Anal. Appl.* **47** (1974) 563–572.

[5] R. E. Showalter. *Cauchy Problem for Hyper-Parabolic Partial Differential Equations.* Elsevier, 1983.

[6] G. W. Clark and S. F. Oppenheimer. Quasireversibility methods for non-well-posed problems. *Electron. J. Diff. Eqns.* **8** (1994) 1–9.

[7] M. Denche and K. Bessila. A modified quasi-boundary value method for ill-posed problems. *J. Math. Anal. Appl.* **301** (2005) 419–426.

[8] K. Bessila. Regularization by a modified quasi-boundary value method of ill-posed differential-operator equations of first order. *J. Math. Anal. Appl.* **409** (1) (2014) 315–320.

[9] N. Teniou and S. Djezzar. An approximate solution for a class of ill-posed nonhomogeneous Cauchy problems. *Journal of Mathematics* **2021** (1) (2021).

[10] C. Wei and Y.-L. Liu. A quasi-boundary value regularization method for the spherically symmetric backward heat conduction problem. *Open Mathematics* **21** (2023) 20230171.

[11] D. D. Trong and N. H. Tuan. A nonhomogeneous backward heat problem: Regularization and error estimates. *Electron. J. Diff. Eqns.* **33** (2006) 1–14.

[12] M. Denche and A. Abdessemed. On regularization and error estimates for non-homogeneous backward Cauchy problem. *Arab. J. Math. Sci.* **18** (2) (2012) 149–164. DOI: 10.1016/j.ajmsc.2012.03.002.

[13] N. V. Hoa and T. Q. Khanh. Two-parameter regularization method for an axisymmetric inverse heat problem. *Bound. Value Probl.* **25** (2017).

[14] I. Mező. *The Lambert W Function, its Generalizations and Applications.* Chapman & Hall/CRC, New York, 2022.

[15] T. Dence. A brief look into the Lambert W function. *Appl. Math.* **4** (2013) 887–892.

[16] R. M. Corless, G. H. Gonnet, D. E. Hare, D. J. Jeffrey and D. E. Knuth. On the Lambert W function. *Adv. Comput. Math.* **5** (1996) 329–359.

[17] J. M. Borwein and S. B. Lindstrom. Meetings with Lambert W and other special functions in optimization and analysis. *Pure Appl. Funct. Anal.* **1** (2016).

Nonlinear Dynamics and Systems Theory, **25** (6) (2025) 656–668

Global Theoretical Investigation of Diffusion Driven Instability for Three Coupled Equations of a Reaction Diffusion System

Abid Abd Rraouf * and Kouachi Said

Departement of Mathematics, University of Abees Lagrour Khanchela, ICOSI Laboratory

Received: July 5, 2025; Revised: November 20, 2025

Abstract: In this paper, we investigate the mechanism called DDI (Diffusion Driven Instability) for a full three dimensional matrix of diffusion coefficients. We apply a linear approach in the neighborhood of an arbitrary equilibrium point using the Routh-Hurwitz stability criterion and we study the existence of at least one eigenvalue with positive real part of the matrix $A(k)$. Our main result is the proof of sufficient and necessary condition for the Turing instability. The research is extended to a reaction-diffusion system for three species.

Keywords: *reaction-diffusion system; Turing instability; cross diffusion; predator-prey.*

Mathematics Subject Classification (2020): 35K57, 35B36, 35B32, 92D25, 92D40, 37N25, 70K42.

1 Introduction

Back in the 1950s, Alan Turing published a paper under the title "The Chemical Basis of Morphogenesis". Turing demonstrated that under certain circumstances, chemicals can react and diffuse in a way that results in solutions that do not have concentration equilibrium. To study the process of morphogenesis, he took into account two coupled reaction-diffusion systems. Mathematically, Turing's idea was as follows:

$$\begin{cases} \dfrac{\partial u}{\partial t} = d_1 \Delta u + f(u,v), \quad t > 0 \quad x \in \Omega, \\ \dfrac{\partial v}{\partial t} = d_2 \Delta v + g(u,v), \quad t > 0 \quad x \in \Omega, \end{cases} \tag{E}$$

* Corresponding author: mailto:abid.abdrraouf@univ-khenchela.dz

and its corresponding kinetic equations was

$$\begin{cases} \dfrac{du}{dt} = f(u,v), \quad t>0, \\ \dfrac{dv}{dt} = g(u,v), \quad t>0. \end{cases} \tag{K}$$

The principal idea is that if there is no diffusion (regarding K), u and v converge to a linear stable uniform steady state, then the uniform stable steady state can be unstable due to the presence of diffusion and some other conditions (taking into account E) in certain instances. Turing realized that diffusions are the primary cause of the Turing instability in reaction-diffusion systems, which is referred to as Diffusion-Driven Instability. Qian and Murray [5] considered the case where the matrix of diffusion coefficients D is diagonal. Jia and Wang [6] considered the case

$$\begin{cases} \dfrac{\partial u_1(x,t)}{\partial t} - d_1(t)\,\Delta u_1(x,t) = u_1(x,t)\big[r_1(t) - a_{11}(t)\,u_1(x,t-\tau_1) - a_{12}(t)\,u_2(x,t)\big], \\ \dfrac{\partial u_2(x,t)}{\partial t} - d_2(t)\,\Delta u_2(x,t) = u_2(x,t)\big[-r_2(t) - a_{22}(t)\,u_2(x,t-\tau_2) + a_{21}(t)\,u_1(x,t-\tau_1)\big]. \end{cases}$$

Wu et al. [8] investigated the fractional-order predator-prey reaction-diffusion model

$$\begin{cases} \dfrac{\partial^\eta u}{\partial t^\eta} = d_1\Delta u + ru\Big(1-\dfrac{u}{k}\Big) - \dfrac{qu^2v}{u^2+a}, \\ \dfrac{\partial^\eta v}{\partial t^\eta} = d_2\Delta v - cv + \dfrac{pu^2v}{u^2+a}. \end{cases}$$

Didiharyono et al. [1] dealt with the kinetic equations

$$\begin{cases} \dfrac{dB}{dt} = r_1B\Big(1-\dfrac{B}{K}\Big) - \dfrac{\alpha NB}{(1+\eta B)(1+\mu N)} - \beta MB, \\ \dfrac{dN}{dt} = \dfrac{\delta\alpha NB}{(1+\eta B)(1+\mu N)} - r_2N + \theta M, \\ \dfrac{dM}{dt} = \vartheta MB - r_3M + \sigma N. \end{cases}$$

Also, in [7], Agus et al. considered the kinetic equations such that

$$\begin{cases} \dfrac{dx}{dt} = x\Big[(R-R_1x) - \dfrac{cx^2z}{c_1+x^2} - uy\Big] + \sigma_2 y, \\ \dfrac{dy}{dt} = y\big[(S-S_1y) - vx\big] + \sigma_1 x, \\ \dfrac{dz}{dt} = z\Big(\dfrac{g_1x^2}{c_1+x^2} - e - q_3z\Big). \end{cases}$$

Das K.P. and Said K. [2] handled

$$\begin{cases} \partial_t u - D_1\Delta u = u(1-u) - \dfrac{a_1uv}{1+b_1u}, \\ \partial_t v - D_2\Delta v = \dfrac{a_1uv}{1+b_1u} - \dfrac{a_2vw}{1+b_2v} - d_1v - dv^2, \qquad \text{in } \mathbb{R}^+\times\Omega, \\ \partial_t r - D_3\Delta r = \dfrac{a_2vw}{1+b_2v} - d_2w. \end{cases}$$

In this paper, we handle a more general situations, where D is a full matrix, and f, g and h are any continuously differentiable reaction terms. We focus only on a class of reaction-diffusion systems that fulfill the following hypotheses:

$$\operatorname{tr} A < 0, \quad \det A < 0, \quad \det A - \operatorname{tr} A \cdot \operatorname{tr} \operatorname{com} A > 0,$$

where A is the Jacobian matrix of linearization, and $\operatorname{com} A$ is the adjugate matrix of A.

2 Linearization and Stability of the Jacobian Matrix

Consider the reaction-diffusion system

$$\begin{cases} \dfrac{\partial u}{\partial t} = d_{11}\Delta u + d_{12}\Delta v + d_{13}\Delta w + f(u,v,w), \\ \dfrac{\partial v}{\partial t} = d_{21}\Delta u + d_{22}\Delta v + d_{23}\Delta w + g(u,v,w), \\ \dfrac{\partial w}{\partial t} = d_{31}\Delta u + d_{32}\Delta v + d_{33}\Delta w + h(u,v,w), \end{cases} \tag{1}$$

where f, g and h are nonlinear reaction terms and d_{ij}, $1 \le i, j \le 3$, represent diffusion coefficients of u, v and w, respectively. As discussed by Murray in 2003, see [3], system (1) is used to model predator-prey dynamics by blending local interactions (prey reproduce, predators eat prey) with space movement, resulting in patterns that demonstrate the evolution of predator-prey populations in time. A linear approach analysis of (1) near the steady state of its corresponding nonlinear ordinary differential equation yields

$$\frac{\partial y}{\partial t} = \left(A - k^2 D\right) y,$$

where

$$y = \begin{pmatrix} \widetilde{u} \\ \widetilde{v} \\ \widetilde{w} \end{pmatrix} \quad A = \begin{pmatrix} f_u & f_v & f_w \\ g_u & g_v & g_w \\ h_u & h_v & h_w \end{pmatrix} \quad D = \begin{pmatrix} d_{11} & d_{12} & d_{13} \\ d_{21} & d_{22} & d_{23} \\ d_{31} & d_{32} & d_{33} \end{pmatrix}$$

and k is the wave number of the Fourier Transform $\psi(x,t) = \int \widetilde{\psi}(k,t) e^{-ikx}\, dx$. The coefficients d_{ij} satisfy the conditions

$$\begin{cases} d_{11} > 0, \\ 4d_{11}d_{22} - (d_{12}+d_{21})^2 > 0, \\ d_{33} - \dfrac{(d_{13}+d_{31})^2}{d_{11}} - \dfrac{\left(2d_{11}(d_{23}+d_{32}) - (d_{12}+d_{21})(d_{13}+d_{31})\right)^2}{4d_{11}(4d_{11}d_{22} - (d_{12}+d_{21})^2)} > 0, \end{cases} \tag{P}$$

which reflects the parabolicity of the system (1) and implies at the same time that the matrix D is positive definite.

Definition 2.1 Diffusion-Driven Instability is the process of making conditions on A, k and D such that, with the presence of the diffusions $\left(d_{ij} \neq 0\right)$, the matrix $A(k) = A - k^2 D$ has at least one eigenvalue with a positive real part.

Remark 2.1 We assume that without the diffusion coefficients, i.e., $\big(d_{ij} = 0\big)$, the steady state is stable.

In what follows, we give some more details concerning the previous remark. We set:

$$A = \begin{pmatrix} f_u\big(U^*\big) & f_v\big(U^*\big) & f_w\big(U^*\big) \\ g_u\big(U^*\big) & g_v\big(U^*\big) & g_w\big(U^*\big) \\ h_u\big(U^*\big) & h_v\big(U^*\big) & h_w\big(U^*\big) \end{pmatrix} = \begin{pmatrix} a_{11} & a_{12} & a_{13} \\ a_{21} & a_{22} & a_{23} \\ a_{31} & a_{32} & a_{33} \end{pmatrix},$$

where $U^* = \big(u^*, v^*, w^*\big)$ denotes any equilibria of (1). The characteristic polynomial of A is given by

$$P(\lambda) = -\lambda^3 + \big(\mathrm{tr}A\big)\lambda^2 - \big(\mathrm{tr}\,\mathrm{com}\,A\big)\lambda + \big(\det A\big). \tag{2}$$

To determine if the matrix A is stable, we check that all its eigenvalues have a negative real part. For this purpose, we set

$$a = -\mathrm{tr}A, \quad b = \mathrm{tr}\,\mathrm{com}\,A, \quad c = -\det A,$$

and then P takes the form

$$\lambda^3 + a\lambda^2 + b\lambda + c = 0.$$

In order to get the roots of (2), i.e., all eigenvalues of A, with negative real parts, we apply the Routh-Hurwitz stability criterion. Hence,

$$a > 0, \quad c > 0, \quad \text{and} \quad ab - c > 0.$$

More precisely,

$$\mathrm{tr}A < 0, \tag{i}$$

$$\det A < 0, \tag{ii}$$

$$\det A - \mathrm{tr}A \cdot \mathrm{tr}\,\mathrm{com}\,A > 0. \tag{iii}$$

3 Explicit Conditions

For our main result, before we give the expression of the characteristic polynomial of the matrix $A\,(k)$, we first identify some tools. We set the submatrices

$$M_1 = \begin{pmatrix} a_{11} & a_{12} \\ d_{21} & d_{22} \end{pmatrix} \quad M_2 = \begin{pmatrix} a_{11} & a_{13} \\ d_{31} & d_{33} \end{pmatrix} \quad M_3 = \begin{pmatrix} a_{22} & a_{21} \\ d_{12} & d_{11} \end{pmatrix} \quad M_4 = \begin{pmatrix} a_{33} & a_{31} \\ d_{13} & d_{11} \end{pmatrix}$$

$$M_5 = \begin{pmatrix} a_{33} & a_{23} \\ d_{32} & d_{22} \end{pmatrix} \quad M_6 = \begin{pmatrix} a_{22} & a_{32} \\ d_{23} & d_{33} \end{pmatrix} \quad M_7 = \begin{pmatrix} a_{11} & d_{12} & d_{13} \\ a_{21} & d_{22} & d_{23} \\ a_{31} & d_{32} & d_{33} \end{pmatrix}$$

$$M_8 = \begin{pmatrix} d_{11} & a_{12} & a_{13} \\ d_{21} & a_{22} & a_{23} \\ d_{31} & a_{32} & a_{33} \end{pmatrix}.$$

We also define two constants σ_1 and σ_2 as follows:

$$\begin{aligned}\sigma_1 = &-d_{11}(a_{23}d_{32} + a_{32}d_{23} - a_{22}d_{33} - a_{33}d_{22}) + d_{21}(a_{13}d_{32} + a_{32}d_{13} - a_{12}d_{33} - a_{33}d_{12}) \\ &- d_{31}(a_{13}d_{22} + a_{22}d_{13} - a_{12}d_{23} - a_{23}d_{12}),\end{aligned}$$

$$\begin{aligned}\sigma_2 = &\ a_{11}(a_{23}d_{32} + a_{32}d_{23} - a_{22}d_{33} - a_{33}d_{22}) + a_{21}(a_{12}d_{33} + a_{33}d_{12} - a_{13}d_{32} - a_{32}d_{13}) \\ &+ a_{31}(a_{13}d_{22} + a_{22}d_{13} - a_{12}d_{23} - a_{23}d_{12}),\end{aligned}$$

then we have the following lemma.

Lemma 3.1 *The characteristic polynomial of $A(k)$ is*

$$\tilde{P}(\lambda) = -\lambda^3 + [\,\mathrm{tr}A - k^2\mathrm{tr}D\,]\,\lambda^2 + \Big[-\mathrm{tr}(\mathrm{com}D)\,k^4 + \Big(\sum_{i=1}^{6}\det M_i\Big)k^2 - \mathrm{tr}(\mathrm{com}A)\Big]\lambda$$
$$-\ (\det D)\,k^6 + (\sigma_1 + \det M_7)\,k^4 + (\sigma_2 - \det M_8)\,k^2 + \det A.$$

Proof. It suffices to apply the definition and use the above auxiliary tools.
We observe that $\tilde{P} = 0$ takes the form

$$\lambda^3 + \varphi_1\left(k^2\right)\lambda^2 + \varphi_2\left(k^2\right)\lambda + \varphi_3\left(k^2\right) = 0,$$

where

$$\begin{array}{lcl}
\varphi_1\left(k^2\right) & = & \mathrm{tr}(D)\,k^2 - \mathrm{tr}(A),\\
\varphi_2\left(k^2\right) & = & \mathrm{tr}\big(\mathrm{com}(D)\big)\,\left(k^2\right)^2 - \left(\sum\limits_{i=1}^{6}\det M_i\right)k^2 + \mathrm{tr}\big(\mathrm{com}(A)\big),\\
\varphi_3\left(k^2\right) & = & (\det D)\left(k^2\right)^3 - (\sigma_1 + \det M_7)\left(k^2\right)^2 + (\det M_8 - \sigma_2)\,k^2 - \det A.
\end{array}$$

We notice that the coefficients φ_1, φ_2, and φ_3 are polynomial functions in k^2. Now, we apply the Routh-Hurwitz stability criterion, see F. R. Gantmacher [2],

$$\varphi_1\left(k^2\right) > 0 \quad \textbf{and} \quad \varphi_3\left(k^2\right) > 0 \quad \textbf{and} \quad \left(\varphi_1\varphi_2 - \varphi_3\right)\left(k^2\right) > 0.$$

This means that all eigenvalues of $A\,(k)$ have a negative real part. In order to achieve our goal "Diffusion Driven Instability", we violate at least one of the above conditions, so

$$\begin{array}{c}
A\,(k)\ \text{ has at least one eigenvalue with positive real part}\\
\Leftrightarrow\\
\varphi_1\left(k^2\right) \le 0 \quad \textbf{or} \quad \varphi_3\left(k^2\right) \le 0 \quad \textbf{or} \quad \left(\varphi_1\varphi_2 - \varphi_3\right)\left(k^2\right) \le 0.
\end{array}$$

Remark 3.1 Since the functions we are dealing with, φ_1, φ_3, and $(\varphi_1\varphi_2 - \varphi_3)$, are even, we limit our study over $\mathbb{R}^+ = [0, +\infty)$.

At this point, we are now ready to establish the explicit conditions on k^2.

3.1 First condition

We have $\varphi_1\left(k^2\right) = \mathrm{tr}(D)\,k^2 - \mathrm{tr}(A)$, and since $\mathrm{tr}(D) > 0$, thanks to $d_{ii} > 0,\ i = 1, 2, 3$, and using the assumption $\mathrm{tr}(A) < 0$ (i), we get that $\forall\,k^2 \ge 0, \varphi_1\left(k^2\right) > 0$. This means we get nothing as a result.

Remark 3.2 The Routh-Hurwitz criterion implies that $\varphi_1\left(k^2\right) \le 0$, or $\varphi_3\left(k^2\right) \le 0$, or $(\varphi_1\varphi_2 - \varphi_3)\left(k^2\right) \le 0$, for some values of k^2, and because $\varphi_1\left(k^2\right) \le 0$ is impossible to to fulfil, the only option left is to deal with $\varphi_3\left(k^2\right) \le 0$ or $(\varphi_1\varphi_2 - \varphi_3)\left(k^2\right) \le 0$. Since we have the logical coordinator "**or",** it is much easier to handle $\varphi_3\left(k^2\right) \le 0$ instead of $(\varphi_1\varphi_2 - \varphi_3)\left(k^2\right) \le 0$. In other words, it suffices to focus on finding the values of k^2 such that $\varphi_3\left(k^2\right) \le 0$.

3.2 Second condition

The derivative of φ_3 with respect to k^2 is given by

$$\frac{\partial}{\partial k^2}\,\varphi_3\big(k^2\big) = 3\,\det D\,\big(k^2\big)^2 - 2\,\big(\sigma_1 + \det M_7\big)\,k^2 + \det M_8 - \sigma_2. \tag{3}$$

It appears that the derivative of φ_3 is a second degree polynomial in k^2. Set

$$\tilde{A} = 3\,\det D, \quad \tilde{B} = -2\,\big(\sigma_1 + \det M_7\big), \quad \tilde{C} = \det M_8 - \sigma_2.$$

The discriminant $\tilde{\Delta}$ of (3) is

$$\tilde{\Delta} = 4\Big[\,\big(\sigma_1 + \det M_7\big)^2 - 3\,\det D\,\big(\det M_8 - \sigma_2\big)\Big].$$

We denote by $\tilde{k}_i^2$ the roots of φ_3, and by k_i^2 the roots of $\dfrac{\partial}{\partial k^2}\,\varphi_3$. Following the signs of $\det D$ and $\tilde{\Delta}$, we give two propositions.

Proposition 3.1 *If the following conditions hold:*

$$\det D > 0, \quad \tilde{\Delta} > 0, \quad \tilde{B} < 0 \textit{ and } \tilde{C} > 0, \tag{4}$$

then $A\,(k)$ has at least one eigenvalue with positive real part. Furthermore,

$$\forall\, k^2 \in [\tilde{k}_1^2,\, \tilde{k}_2^2], \quad \varphi_3\,\big(k^2\big) \leq 0.$$

Proof. Since $\tilde{\Delta} > 0$, there exist two distinct roots, obviously with $k_1^2 < k_2^2$:

$$k_1^2 = \frac{-\tilde{B} - \sqrt{\tilde{\Delta}}}{2\,\tilde{A}}, \quad k_2^2 = \frac{-\tilde{B} + \sqrt{\tilde{\Delta}}}{2\,\tilde{A}}.$$

We must ensure that both roots are positive; otherwise, the analysis cannot proceed. So, the following conditions are required:

$$\tilde{B} < 0 \quad \text{and} \quad \tilde{C} > 0, \tag{5}$$

equivalently,

$$-2\,(\sigma_1 + \det M_7) < 0, \quad \det M_8 - \sigma_2 > 0.$$

Under the hypotheses given by (4), the behavior of φ_3 is determined as follows.

- The value $\varphi_3\big(k_1^2\big)$ must be positive:

$$\big(\det D\big)\left(\frac{-\tilde{B} - \sqrt{\tilde{\Delta}}}{2\tilde{A}}\right)^3 - \big(\sigma_1 + \det M_7\big)\left(\frac{-\tilde{B} - \sqrt{\tilde{\Delta}}}{2\tilde{A}}\right)^2 + \big(\det M_8 - \sigma_2\big)\left(\frac{-\tilde{B} - \sqrt{\tilde{\Delta}}}{2\tilde{A}}\right) - \det A > 0.$$

- Regarding $\varphi_3\big(k_2^2\big)$, there are two cases:

– If $\varphi_3(k_2^2) > 0$, then

$$\forall\, k^2 \geq 0, \quad \varphi_3(k^2) \geq 0.$$

– If $\varphi_3(k_2^2) < 0$, then there exist $\tilde{k}_1^2 \in [\,k_1^2,\, k_2^2]$ and $\tilde{k}_2^2 > k_2^2$ such that

$$\varphi_3(\tilde{k}_1^2) = \varphi_3(\tilde{k}_2^2) = 0.$$

Thus,

$$\forall\, k^2 \in [\,\tilde{k}_1^2,\, \tilde{k}_2^2], \quad \varphi_3(k^2) \leq 0.$$

Proposition 3.2 *If the following assumptions hold:*

$$\det D < 0 \quad \textit{and} \quad \tilde{\Delta} < 0, \tag{6}$$

then $A(k)$ has at least one eigenvalue with positive real part. Furthermore,

$$\forall\, k^2 \in [\,\tilde{k}_3^2, +\infty), \quad \varphi_3(k^2) \leq 0.$$

Moreover, if

$$\det D < 0, \quad \tilde{\Delta} > 0, \quad \varphi_3(k_3^2) > 0 \quad \textit{and} \quad \varphi_3(k_4^2) > 0,$$

then $A(k)$ has at least one eigenvalue with positive real part, and

$$\forall\, k^2 \in [\,\tilde{k}_4^2, +\infty), \quad \varphi_3(k^2) \leq 0.$$

If

$$\det D < 0, \quad \tilde{\Delta} > 0, \quad \varphi_3(k_3^2) < 0 \quad \textit{and} \quad \varphi_3(k_4^2) < 0,$$

then $A(k)$ has at least one eigenvalue with positive real part, and

$$\forall\, k^2 \in [\,\tilde{k}_5^2, +\infty), \quad \varphi_3(k^2) \leq 0.$$

Finally, if

$$\det D < 0, \quad \tilde{\Delta} > 0, \quad \varphi_3(k_3^2) < 0 \quad \textit{and} \quad \varphi_3(k_4^2) > 0,$$

then $A(k)$ has at least one eigenvalue with positive real part, and

$$\forall\, k^2 \in [\,\tilde{k}_6^2,\, \tilde{k}_7^2] \cup [\,\tilde{k}_8^2, +\infty), \quad \varphi_3(k^2) \leq 0.$$

Proof. We begin with the trivial case: if $\tilde{\Delta} < 0$, then there are no real roots of (3). The behavior of φ_3 under the hypotheses given by (6), ensures the existence of some $\tilde{k}_3^2 > 0$ such that $\varphi_3(\tilde{k}_3^2) = 0$. Hence,

$$\forall\, k^2 \in [\,\tilde{k}_3^2, +\infty), \quad \varphi_3(k^2) \leq 0.$$

Now, consider the case $\tilde{\Delta} > 0$. Then there exist two distinct real roots of (3), given by

$$k_3^2 = \frac{-\tilde{B} + \sqrt{\tilde{\Delta}}}{2\,\tilde{A}}, \quad k_4^2 = \frac{-\tilde{B} - \sqrt{\tilde{\Delta}}}{2\,\tilde{A}}, \quad \text{with} \quad k_3^2 < k_4^2.$$

Again, the roots must be positive and we require

$$\tilde{B} > 0 \quad \text{and} \quad \tilde{C} < 0. \tag{7}$$

Depending on the sign of $\varphi_3(k_3^2)$ and $\varphi_3(k_4^2)$, we have the following cases:
- If $\varphi_3(k_3^2) > 0$ and $\varphi_3(k_4^2) > 0$, then there exists $\tilde{k}_4^2 > k_4^2$ such that $\varphi_3(\tilde{k}_4^2) = 0$. Thus,

$$\forall\, k^2 \in [\,\tilde{k}_4^2, +\infty), \quad \varphi_3(k^2) \leq 0.$$

- If $\varphi_3(k_3^2) < 0$ and $\varphi_3(k_4^2) < 0$, then there exists $\tilde{k}_5^2 < k_3^2$ such that $\varphi_3(\tilde{k}_5^2) = 0$. Therefore,

$$\forall\, k^2 \in [\,\tilde{k}_5^2, +\infty), \quad \varphi_3(k^2) \leq 0.$$

- If $\varphi_3(k_3^2) < 0$ and $\varphi_3(k_4^2) > 0$, then there exist $\tilde{k}_6^2 \in (0, k_3^2)$, $\tilde{k}_7^2 \in (k_3^2, k_4^2)$, and $\tilde{k}_8^2 > k_4^2$ such that

$$\varphi_3(\tilde{k}_6^2) = \varphi_3(\tilde{k}_7^2) = \varphi_3(\tilde{k}_8^2) = 0.$$

In this case, we get

$$\forall\, k^2 \in [\,\tilde{k}_6^2,\, \tilde{k}_7^2] \cup [\,\tilde{k}_8^2, +\infty), \quad \varphi_3(k^2) \leq 0.$$

In addition, we discuss the sub-cases where $\det D = 0$. In this case, the function φ_3 takes the form

$$\varphi_3(k^2) = -(\sigma_1 + \det M_7)\,(k^2)^2 + (\det M_8 - \sigma_2)\,k^2 - \det A.$$

Suppose that $\sigma_1 + \det M_7 \neq 0$. Then φ_3 can be rewritten as

$$\varphi_3(k^2) = \tilde{A}_1\,(k^2)^2 + \tilde{B}_1\,k^2 + \tilde{C}_1, \tag{8}$$

where

$$\tilde{A}_1 = -(\sigma_1 + \det M_7), \quad \tilde{B}_1 = \det M_8 - \sigma_2, \quad \tilde{C}_1 = -\det A.$$

The discriminant of (8) is

$$\tilde{\Delta}_1 = \tilde{B}_1^2 - 4\,\tilde{A}_1\,\tilde{C}_1.$$

If $\tilde{\Delta}_1 > 0$ and $\tilde{A}_1 > 0$ (equivalently, $\sigma_1 + \det M_7 < 0$), then there exist two real roots

$$\tilde{k}_9^2 = \frac{-\tilde{B}_1 - \sqrt{\tilde{\Delta}_1}}{2\,\tilde{A}_1}, \quad \tilde{k}_{10}^2 = \frac{-\tilde{B}_1 + \sqrt{\tilde{\Delta}_1}}{2\,\tilde{A}_1}, \quad \text{with} \quad \tilde{k}_9^2 < \tilde{k}_{10}^2.$$

To ensure that both roots are positive, we require

$$\tilde{B}_1 < 0 \quad \text{and} \quad \tilde{C}_1 > 0. \tag{9}$$

That is,

$$\det M_8 - \sigma_2 < 0 \quad \text{and} \quad -\det A > 0.$$

In this case, we have

$$\forall\, k^2 \in [\,\tilde{k}_9^2,\, \tilde{k}_{10}^2], \quad \varphi_3(k^2) \leq 0.$$

Furthermore, if $\sigma_1 + \det M_7 = 0$, then φ_3 reduces to

$$\varphi_3(k^2) = (\det M_8 - \sigma_2)\,k^2 - \det A.$$

If $\det M_8 - \sigma_2 < 0$, then there exists $\tilde{k}_{11}^2 > 0$ such that $\varphi_3(\tilde{k}_{11}^2) = 0$. Hence,

$$\forall\, k^2 \in [\,\tilde{k}_{11}^2, +\infty), \quad \varphi_3(k^2) \leq 0.$$

4 Application

Consider the following reaction-diffusion system:

$$\begin{cases} \dfrac{\partial u}{\partial t} - d_u \Delta u = \alpha u - \beta uv + \delta v & \text{in } Q_t, \\ \dfrac{\partial v}{\partial t} - d_v \Delta v - d_{vw} \Delta w = \gamma uv - \mu v + \eta w & \text{in } Q_t, \\ \dfrac{\partial w}{\partial t} - d_w \Delta w = \tau w - \xi uw & \text{in } Q_t, \end{cases} \tag{10}$$

where $Q_t = \{t > 0\} \times \Omega$, Ω is an open bounded subset of $\mathbf{R}^n$.

This ecological system models the interactions of predator-prey dynamics, and the solutions $u(x,t), v(x,t)$ and $w(x,t)$ represent the concentrations of three interacting biological species. Now, we give the biological interpretation of constants.

Constant	Signification
α	Growth rate of species u
β	Interaction strength between u and v
γ	Production rate of v via interaction with u
μ	Natural decay rate of v
δ	Effect of v on u
η	Coupling term from w to v
τ	Growth rate of species w
ξ	Interaction term between v and w
d_{vw}	Cross-diffusion coefficient

Equating the left-hand side of (10) to 0, we get the equilibrium points:

- $E_0(0,0,0)$ exists always;
- $E_m\Big(\dfrac{\mu}{\gamma}, \dfrac{\alpha\mu}{\beta\mu - \delta\gamma}, 0\Big)$ exists under the conditions $\gamma \neq 0$ and $\beta\mu - \delta\gamma \neq 0$,
- $E_*\Big(\dfrac{\tau}{\xi}, \dfrac{\alpha\tau}{\beta\tau - \delta\xi}, \dfrac{\alpha\tau(\mu\xi - \gamma\tau)}{\eta\xi(\beta\tau - \delta\xi)}\Big)$ exists under the conditions $\xi \neq 0$, $\beta\tau - \delta\xi \neq 0$, and $\eta\xi(\beta\tau - \delta\xi) \neq 0$.

According to (P), the diffusion coefficients must satisfy

$$d_u > 0, \quad d_w > 0, \quad 4d_v d_w - d_{vw}^2 > 0,$$

so can they reflect the parabolicity of the system.

4.1 Turing instability

To obtain the Turing instability, we need find the values of k^2, for which the matrix $A(k^2) = A - k^2 D$ can be unstable; in other words, to define conditions on k^2 under which that the matrix $A(k)$ has at least one eigenvalue with positive real part. The discriminant D of the matrix is equal to $d_u d_v d_w > 0$, we apply only Proposition 3.1..

The Jacobian matrix of linearization in the neighborhood of the first equilibrium point E_0 is given by

$$A_0 = \begin{pmatrix} \alpha & \delta & 0 \\ 0 & -\mu & \eta \\ 0 & 0 & \tau \end{pmatrix}.$$

Note that this matrix is stable under the conditions (i), (ii) and (iii), respectively, hence

$$\begin{aligned} &\alpha - \mu + \tau < 0, \\ &-\alpha\mu\tau < 0, \\ &\alpha\mu\tau + \big(\alpha - \mu + \tau\big)\big(\alpha\tau - \mu\tau - \alpha\mu\big) < 0. \end{aligned}$$

To obtain the desired result, as we have mentioned earlier, the matrix $A_0\big(k^2\big) = A_0 - k^2 D$ must have an eigenvalue with positive real part.

By Proposition 3.1, if

$$\begin{aligned} &\tilde{A}_0 = 3d_u d_v d_w > 0, \\ &\tilde{B}_0 = 2\mu d_u d_w - 2\tau d_u d_v - 2\alpha d_v d_w < 0, \\ &\tilde{C}_0 = \alpha\tau d_v - \mu\tau d_u - \alpha\mu d_w > 0, \\ &\tilde{\Delta}_0 = \tilde{B}_0^2 - 4\tilde{A}_0\tilde{C}_0 > 0, \\ &\varphi_3\Big(\tfrac{-\tilde{B}_0 - \sqrt{\tilde{\Delta}_0}}{2\tilde{A}_0}\Big) > 0 \text{ and } \varphi_3\Big(\tfrac{-\tilde{B}_0 + \sqrt{\tilde{\Delta}_0}}{2\tilde{A}_0}\Big) < 0, \end{aligned}$$

it results in

$$\forall\, k^2 \in \left[\frac{-\tilde{B}_0 - \sqrt{\tilde{\Delta}_0}}{2\tilde{A}_0}, \frac{-\tilde{B}_0 + \sqrt{\tilde{\Delta}_0}}{2\tilde{A}_0}\right] \quad \varphi_3\big(k^2\big) \le 0,$$

where

$$\begin{aligned} \varphi_3(k^2) = \quad &\big(\det D\big)(k^2)^3 - \big(\sigma_1 + \det M_7\big)(k^2)^2 \\ &+\big(\det M_8 - \sigma_2\big)k^2 - \det A_0, \end{aligned}$$

and we get the Turing instability Move now to the second equilibrium point E_m, its associated matrix of linearization is given by

$$A_m = \begin{pmatrix} \alpha\Big(1 - \frac{\beta\mu}{\beta\mu - \gamma\delta}\Big) & \delta - \frac{\beta\mu}{\gamma} & 0 \\ \frac{\alpha\gamma\mu}{\beta\mu - \gamma\delta} & 0 & \eta \\ 0 & 0 & \tau - \frac{\xi\mu}{\gamma} \end{pmatrix}.$$

A_m is stable under the following conditions:

$$\begin{aligned} &\tau - \tfrac{\xi\mu}{\gamma} - \tfrac{\alpha\gamma\delta}{\beta\mu - \gamma\delta} < 0, \\ &\tfrac{\alpha\mu}{\delta}\big(\xi\mu - \gamma\tau\big) < 0, \\ &\tfrac{\alpha\mu}{\delta}\big(\xi\mu - \gamma\tau\big) - \Big(\tau - \tfrac{\xi\mu}{\gamma} - \tfrac{\alpha\gamma\delta}{\beta\mu - \gamma\delta}\Big)\Big(\alpha + \alpha\tfrac{\xi\mu - \gamma\tau}{\beta\mu - \gamma\delta}\Big) > 0. \end{aligned}$$

Following the same reasoning, we apply Proposition 3.1 under the following assumptions:

$$\begin{aligned}
&\tilde{A}_m = 3d_u d_v d_w > 0,\\
&\tilde{B}_m = 2\tfrac{\xi\mu-\gamma\tau}{\gamma} d_u d_v + 2\tfrac{\alpha\gamma\delta}{\beta\mu-\gamma\delta} d_v d_w < 0,\\
&\tilde{C}_m = \alpha\mu d_w - \tfrac{\alpha(\gamma\tau-\xi\mu)}{\beta\mu-\gamma\delta} d_v > 0,\\
&\tilde{\Delta}_m = \tilde{B}_m^2 - 4\tilde{A}_m\tilde{C}_m > 0,\\
&\varphi_3\Big(\tfrac{-\tilde{B}_m-\sqrt{\tilde{\Delta}_m}}{2\tilde{A}_m}\Big) > 0 \quad \text{and} \quad \varphi_3\Big(\tfrac{-\tilde{B}_m+\sqrt{\tilde{\Delta}_m}}{2\tilde{A}_m}\Big) < 0.
\end{aligned}$$

It results in

$$\forall\, k^2 \in \left[\frac{-\tilde{B}_m - \sqrt{\tilde{\Delta}_m}}{2\tilde{A}_m}, \frac{-\tilde{B}_m + \sqrt{\tilde{\Delta}_m}}{2\tilde{A}_m}\right] \quad \varphi_3\big(k^2\big) \leq 0,$$

where

$$\begin{aligned}
\varphi_3(k^2) = \quad & \big(\det D\big)(k^2)^3 - \big(\sigma_1 + \det M_7\big)(k^2)^2\\
& + \big(\det M_8 - \sigma_2\big)k^2 - \det A_m,
\end{aligned}$$

and we get the Turing instability. Finally, the matrix

$$A_* = \begin{pmatrix} \alpha\Big(1 - \frac{\beta\tau}{\beta\tau-\delta\xi}\Big) & \delta - \frac{\beta\tau}{\xi} & 0\\ \frac{\alpha\gamma\tau}{\beta\tau-\delta\xi} & \frac{\gamma\tau}{\xi} - \mu & \eta\\ \frac{\alpha\tau(\gamma\tau-\mu\xi)}{\eta(\beta\tau-\delta\xi)} & 0 & 0 \end{pmatrix}$$

is the Jacobian matrix of linearization around the final equilibrium point E_*, with the following conditions of stability:

$$\begin{aligned}
&\frac{\gamma\tau}{\xi} - \mu - \frac{\alpha\delta\xi}{\beta\tau-\delta\xi} < 0,\\
&\frac{\alpha\tau}{\xi}(\mu\xi - \gamma\tau) < 0,\\
&\frac{\alpha\tau}{\xi}(\mu\xi - \gamma\tau) - \alpha\Big(\frac{\gamma\tau}{\xi} - \mu - \frac{\alpha\delta\xi}{\beta\tau-\delta\xi}\Big)\Big(\frac{\gamma\tau}{\xi} - \delta\cdot\frac{\gamma\tau-\mu\xi}{\beta\tau-\delta\xi}\Big) > 0.
\end{aligned}$$

We apply Proposition 3.1 under the following assumptions:

$$\begin{aligned}
&\tilde{A}_* = 3d_u d_v d_w > 0,\\
&\tilde{B}_* = 2\tfrac{\mu\xi-\gamma\tau}{\xi} d_u d_w + 2\tfrac{\alpha\delta\xi}{\beta\tau-\delta\xi} d_v d_w < 0,\\
&\tilde{C}_* = \Big(\tfrac{\alpha\delta(\mu\xi-\gamma\tau)}{\beta\tau-\delta\xi} - \tfrac{\gamma\tau}{\xi}\Big)d_w + \tfrac{\alpha\tau(\gamma\tau-\mu\xi)}{\xi} d_{vw} > 0,\\
&\tilde{\Delta}_* = \tilde{B}_*^2 - 4\tilde{A}_*\tilde{C}_* > 0,\\
&\varphi_3\Big(\tfrac{-\tilde{B}_*-\sqrt{\tilde{\Delta}_*}}{2\tilde{A}_*}\Big) > 0 \quad \text{and} \quad \varphi_3\Big(\tfrac{-\tilde{B}_*+\sqrt{\tilde{\Delta}_*}}{2\tilde{A}_*}\Big) < 0,
\end{aligned}$$

this leads to

$$\forall\, k^2 \in \left[\frac{-\tilde{B}_* - \sqrt{\tilde{\Delta}_*}}{2\tilde{A}_*}, \frac{-\tilde{B}_* + \sqrt{\tilde{\Delta}_*}}{2\tilde{A}_*}\right] \quad \varphi_3(k^2) \leq 0,$$

where

$$\varphi_3(k^2) = \big(\det D\big)(k^2)^3 - \big(\sigma_1 + \det M_7\big)(k^2)^2 + \big(\det M_8 - \sigma_2\big)k^2 - \det A_*.$$

and we get the Turing instability.

5 Final Remarks

Corollary 5.1 *For $k = 0$, we recover the characteristic polynomial of the matrix A given by* (2).

Remark 5.1 We strongly recommend that the roots k_i^2 of $\frac{\partial}{\partial k^2}\varphi_3$ are positive. Otherwise, the analysis cannot proceed. We emphasize that conditions (5), (7) and (9) are necessary and sufficient.

Remark 5.2 The conditions

$$\operatorname{sign}\big(\varphi_3(k_i^2)\big) = -\operatorname{sign}\big(\varphi_3(k_{i+1}^2)\big)$$

for all $i \geq 1$ ensure the existence of $\tilde{k}_i^2$ for all $i \geq 1$.

Remark 5.3 The following cases do not ensure the existence of an eigenvalue with positive real part and lead to a contradiction.

- **Regarding φ_3:** If $\det D > 0$ and $\tilde{\Delta} < 0$, then $\varphi_3(k^2) > 0$ for all $k^2 \geq 0$, so no instability occurs.
- **Special case for φ_3 when it is reduced to**

  $$\varphi_3 = -(\sigma_1 + \det M_7)(k^2)^2 + (\det M_8 - \sigma_2)k^2 - \det A.$$

  If $\tilde{\Delta}_1 < 0$ and $(\sigma_1 + \det M_7) < 0$, then $\varphi_3(k^2) > 0$ for all $k^2 \geq 0$. If ($\tilde{\Delta}_1 < 0$ or $\tilde{\Delta}_1 > 0$) and $(\sigma_1 + \det M_7) > 0$, this contradicts hypothesis (ii).

6 Conclusion

This paper presents a detailed overview of a three-species reaction-diffusion system incorporating normal diffusion, cross-diffusion, and nonlinear interspecies interactions. It elucidates the role and significance of each model parameter, including growth rates, interaction strengths, decay rates and cross-diffusion coefficients. The system exhibits a wide range of complex dynamics such as the Turing pattern formation, oscillations, spatiotemporal chaos, and traveling wave phenomena. Such models are fundamental for advancing the understanding of chemical reactions, biological population dynamics, and natural pattern formation processes. The deep connection between reaction-diffusion systems and non-linear dynamical systems is highlighted by these phenomena, the equilibrium and stability of the system are determined by its local reaction kinetics, the driving force behind symmetry breaking and pattern selection is diffusion and crossdiffusion terms. The analysis of the Turing instability in this context reveals the process of small perturbations growing and evolving into rich spatiotemporal structures that bridge local dynamics and large-scale spatial organization.

References

[1] D. Didiharyono. Harvesting strategies in the migratory prey–predator model with a Crowley–Martin type response function and constant efforts. *Nonlinear Dyn. Syst. Theory* **23** (1) (2023) 14–23.

[2] K.P. Das and S. Kouachi, Effect of boundary conditions in controlling chaos in a tri-trophic food chain with density dependent mortality in intermediate predator. *Nonlinear Studies* **28** (1) (2021) 1–28.

[3] F.R. Gantmacher. *The Theory of Matrices*, Vol. 1, Chelsea Publ. Co., New York, 1964.

[4] J.D. Murray. *Mathematical Biology: Spatial Models and Biomedical Applications.* Springer, New York, 2003.

[5] H. Qian and J.D. Murray. A simple method of parameter space determination for diffusion-driven instability with three species. *Appl. Math. Lett.* **14** (4) (2001) 405–411.

[6] L. Jia and C. Wang. Stability of a nonautonomous delayed periodic reaction–diffusion predator–prey model. *J. Appl. Anal. Comput.* **15** (4) (2025) 1928–1944.

[7] S. Agus, S. Toaha and K. Khaeruddin. The dynamics and stability of prey–predator model of migration with Holling type-III response function and interspecific competition for prey. *Nonlinear Dyn. Syst. Theory* **25** (1) (2025) 1–12.

[8] Z. Wu, Z. Wang, Y. Cai, H. Yin and W. Wang. Pattern formation in a fractional-order reaction–diffusion predator–prey model with Holling-III functional response. *Adv. Contin. Discrete Models* **2025** (1) (2025) 1–13.

Nonlinear Dynamics and Systems Theory, **25** (6) (2025) 669–678

A Numerical Approach for Solving Delay Volterra Integral Equations with a Spatial Variable and Mixed Kernels

S. Saidane [1] and H. Laib [2*]

[1] *Laboratory of Mathematics and Its Interactions, University Center Abdelhafid Boussouf, Mila, Algeria.*
[2] *Ecole Normale Supérieure Echeikh Mohamed Elbachir Elibrahimi, Algiers, Algeria.*

Received: January 6, 2025; Revised: October 25, 2025

Abstract: We propose a numerical method based on Taylor polynomials to construct a collocation solution for approximating the solution of delay Volterra integral equations (DVIEs) with a spatial variable. The method effectively handles both time delay and spatial dependence, which are essential in modeling nonlinear dynamic systems. A rigorous convergence analysis establishes that the method is accurate and stable, with an $O((h+k)^p)$ error bound. Numerical experiments confirm its efficiency and demonstrate its applicability to nonlinear dynamical problems governed by delay integral equations. The proposed approach provides a reliable and computationally efficient tool for solving DVIEs arising in nonlinear dynamics, setting a foundation for further extensions to higher-dimensional problems.

Keywords: *delay Volterra integral equation with spatial variable; collocation method; Taylor polynomials.*

Mathematics Subject Classification (2020): 45D05, 65R20, 70K99, 93C15.

* Corresponding author: mailto:hafida.laib@gmail.com

1 Introduction

In this paper, we analyze a numerical method for solving delay Volterra integral equations (DVIEs) with a spatial variable and a time delay $\tau > 0$, given by

$$u(t,x) = \begin{cases} g(t,x) + A(t,x)u(t-\tau,x) + \displaystyle\int_0^t K_1(t,x,s)u(s,x)\,ds \\ \quad + \displaystyle\int_0^{t-\tau} K_2(t,x,s)u(s,x)\,ds, & t \in [0,T],\ x \in [0,X], \\ \Phi(t,x), & t \in [-\tau,0], \end{cases} \tag{1}$$

where the functions g, Φ, A, K_1, and K_2 are given smooth, real-valued functions defined on $D := [0,T] \times [0,X] \subset \mathbb{R}^2$ and $S := \{(t,x,s) : 0 \leq s \leq t \leq T,\ 0 \leq x \leq X\}$.

According to the classical theory of Volterra integral equations (VIEs), equation (1) admits a unique solution $u \in C(D)$ [6].

Delay Volterra integral equations (DVIEs) play a crucial role in modeling nonlinear dynamical systems where memory effects and delays significantly influence system behavior. Such systems arise in various disciplines, including population dynamics, epidemic models, viscoelastic materials, control systems, and financial modeling, where the future state of the system depends not only on its current state, but also on its past states. These delay effects often introduce nonlinearity and complexity, making analytical solutions difficult or impossible to obtain. Therefore, efficient and accurate numerical methods are essential for their analysis.

Several researchers have studied the numerical solutions of one-dimensional Volterra integral equations with time delays (see, for example, [1, 3, 5, 11, 12]). Ali et al. [1] proposed a spectral method for pantograph-type delay integral equations using the Legendre collocation method. Bellour and Bousselsal [3] constructed a collocation solution to approximate the solution of delay integral equations. Brunner and Yatsenko [11] investigated polynomial spline collocation methods for systems of VIEs with unknown delays. Zheng and Chen [12] developed spectral methods using Chebyshev bases and spectral collocation techniques to analyze VIEs with two types of delays.

While numerous studies have focused on two-dimensional Volterra integral equations [4, 7, 9, 10], fewer works have addressed delay Volterra integral equations with a spatial variable [13]. The primary challenge in solving such problems lies in handling both spatial dependence and time delay in the upper integral limit, distinguishing these equations from conventional two-dimensional Volterra integral equations.

To bridge this gap, we propose a Taylor collocation method, extending the approach in [3] to approximate the solution of equation (1). The main novelty of our work lies in:

1. The adaptation of the Taylor Collocation Method to DVIEs with spatial dependence, which is a relatively unexplored area in numerical analysis.

2. A computationally efficient framework, where the approximation coefficients are computed iteratively without requiring the solution of a system of algebraic equations.

3. A general numerical approach that can be extended to higher-dimensional delay integral equations encountered in physics, control theory, and engineering applications.

The paper is organized as follows. In Section 2, we partition the interval $[0,T] \times [0,X]$ into subintervals and approximate the solution of (1) in each subinterval using Taylor polynomials. Section 3 establishes the global convergence of the method. Section 4 presents numerical examples validating the method. Finally, the conclusion summarizes the main findings and potential future extensions.

2 Description of the Method

We assume, without loss of generality, that $T = r\tau$, where $r \in \mathbf{N}^*$. Let $\Pi_N^\epsilon = \{t_n^\epsilon = \epsilon\tau + nh,\ n = 0,1,...,N,\ \epsilon = 0,1,...,r\}$ and $\Pi_M = \{x_m = mk,\ m = 0,1,...,M\}$ denote uniform partitions of the intervals $[0,T]$ and $[0,X]$, respectively, with step sizes given by $h = \frac{\tau}{N}$ and $k = \frac{X}{M}$. These partitions define a grid for D:

$$\Pi_{N,M}^\epsilon = \Pi_N^\epsilon \times \Pi_M = \{(t_n^\epsilon, x_m) \mid 0 \le n \le N,\ 0 \le m \le M,\ \epsilon = 0,1,\dots,r\}.$$

Define the subintervals as follows:

$$\sigma_n^\epsilon = [t_n^\epsilon, t_{n+1}^\epsilon), \quad \sigma_{N-1}^\epsilon = [t_{N-1}^\epsilon, t_N^\epsilon], \quad n = 0,1,...,N-2, \quad \epsilon = 0,1,...,r-1.$$

$$\delta_m = [x_m, x_{m+1}), \quad m = 0,1,...,M-2, \quad \delta_{M-1} = [x_{M-1}, x_M].$$

The rectangular subdomains are given by

$$D_{n,m}^\epsilon := \sigma_n^\epsilon \times \delta_m, \quad \forall n = 0,1,...,N-1, \quad m = 0,1,...,M-1, \quad \epsilon = 0,1,...,r-1.$$

Moreover, let π_{p-1} denote the set of all real polynomials of degree at most $p-1$ in t and x. We define the real polynomial spline space of degree $p-1$ in t and x as follows:

$$\begin{aligned} S_{p-1}^{(-1)}(\Pi_{N,M}^\epsilon) = \{ & v \in D : v_{n,m}^\epsilon = v|_{D_{n,m}^\epsilon} \in \pi_{p-1}, \\ & n = 0,...,N-1; \quad m = 0,1,...,M-1; \quad \epsilon = 0,1,...,r-1\}. \end{aligned}$$

This represents the space of bivariate polynomial spline functions of degree at most $p-1$ in t and x. Its dimension is $rNMp^2$, which equals the total number of coefficients in the polynomials $v_{n,m}^\epsilon$, where $n = 0,...,N-1$, $m = 0,1,...,M-1$, and $\epsilon = 0,1,...,r-1$. To determine these coefficients, we apply the Taylor polynomial on each rectangle.

First, we approximate u in the rectangles $D_{0,m}^0$, where $m = 0,...,M-1$, using the polynomial

$$v_{0,m}^0(t,x) = \sum_{i+j=0}^{p-1} \frac{1}{i!j!} \partial_t^{(i)} \partial_x^{(j)} u(0,x_m) t^i (x-x_m)^j. \tag{2}$$

Here, $\partial_t^{(i)} \partial_x^{(j)} u(0,x_m)$ represents the exact value of $\partial_t^{(i)} \partial_x^{(j)} u$ at the point $(0,x_m)$.

To determine $\partial_t^{(i)} \partial_x^{(j)} u(t,x)$, we differentiate equation (1) j times with respect to x and i times with respect to t, obtaining

$$\begin{aligned} \partial_t^{(i)} \partial_x^{(j)} u(t,x) &= \partial_t^{(i)} \partial_x^{(j)} g(t,x) + \partial_t^{(i)} \partial_x^{(j)} \left(A(t,x)\Phi(t-\tau,x)\right) \\ &+ \sum_{q=0}^{i-1} \sum_{l=0}^{j} \sum_{\eta=0}^{q} \binom{j}{l} \binom{q}{\eta} \partial_t^{(q-\eta)} \left(\partial_t^{(i-1-q)} \partial_x^{(j-l)} K_1(t,x,s) \Big|_{s=t} \right) \partial_t^{(\eta)} \partial_x^{(l)} u(t,x) \\ &+ \int_0^t \sum_{l=0}^{j} \binom{j}{l} \partial_t^{(i)} \partial_x^{(j-l)} K_1(t,x,s)\, \partial_x^{(l)} u(s,x) ds \\ &- \partial_t^{(i)} \partial_x^{(j)} \left(\int_{t-\tau}^{0} K_2(t,x,s)\Phi(s,x)\, ds \right). \end{aligned}$$

Second, we approximate u in the rectangles $D^0_{n,m}$, where $n = 1, ..., N-1$ and $m = 0, ..., M-1$, using the polynomial

$$v^0_{n,m}(t,x) = \sum_{i+j=0}^{p-1} \frac{1}{i!j!} \partial_t^{(i)} \partial_x^{(j)} \hat{v}^0_{n,m}(t^0_n, x_m)(t-t^0_n)^i (x-x_m)^j. \tag{3}$$

Here, $\hat{v}^0_{n,m}(t,x)$ is the exact solution of the integral equation

$$\hat{v}^0_{n,m}(t,x) = g(t,x) + A(t,x)\Phi(t-\tau,x) + \sum_{\eta=0}^{n-1} \int_{t^0_\eta}^{t^0_{\eta+1}} K_1(t,x,s) v^0_{\eta,m}(s,x)ds$$
$$+ \int_{t^0_n}^{t} K_1(t,x,s)\hat{v}^0_{n,m}(s,x)ds - \int_{t-\tau}^{0} K_2(t,x,s)\Phi(s,x)ds. \tag{4}$$

To compute $\partial_t^{(i)}\partial_x^{(j)}\hat{v}^0_{n,m}(t,x)$, we differentiate equation (4) j times with respect to x and i times with respect to t, obtaining

$$\begin{aligned}
\partial_t^{(i)}\partial_x^{(j)}\hat{v}^0_{n,m}(t,x) &= \partial_t^{(i)}\partial_x^{(j)} g(t,x) + \partial_t^{(i)}\partial_x^{(j)} \left(A(t,x)\Phi(t-\tau,x)\right) \\
&+ \sum_{\eta=0}^{n-1} \int_{t^0_\eta}^{t^0_{\eta+1}} \sum_{l=0}^{j} \binom{j}{l} \partial_t^{(i)} \left(\partial_x^{(j-l)} K_1(t,x,s)\right) \partial_x^{(l)} v^0_{\eta,m}(s,x)ds \\
&+ \sum_{q=0}^{i-1}\sum_{l=0}^{j}\sum_{\eta=0}^{q} \binom{j}{l}\binom{q}{\eta} \partial_t^{(q-\eta)} \left(\partial_t^{(i-1-q)}\partial_x^{(j-l)} K_1(t,x,s)\right)\Big|_{s=t} \partial_t^{(\eta)}\partial_x^{(l)}\hat{v}^0_{n,m}(t,x) \\
&+ \int_{t^0_n}^{t} \sum_{l=0}^{j} \binom{j}{l} \partial_t^{(i)} \left(\partial_x^{(j-l)} K_1(t,x,s)\right) \partial_x^{(l)} \hat{v}^0_{n,m}(s,x)ds \\
&- \partial_t^{(i)}\partial_x^{(j)} \left(\int_{t-\tau}^{0} K_2(t,x,s)\Phi(s,x)\, ds\right).
\end{aligned}$$

Finally, we approximate u in the rectangles $D^\epsilon_{n,m}$, where $n = 0, ..., N-1$, $\epsilon = 1, ..., r$, and $m = 0, 1, ..., M-1$, using the polynomial

$$v^\epsilon_{n,m}(t,x) = \sum_{j+i=0}^{p-1} \frac{1}{i!j!} \partial_t^{(i)}\partial_x^{(j)} \hat{v}^\epsilon_{n,m}(t^\epsilon_n, x_m)(t-t^\epsilon_n)^i (x-x_m)^j. \tag{5}$$

Here, $\hat{v}^\epsilon_{n,m}(t,x)$ is the exact solution of the integral equation

$$\begin{aligned}
\hat{v}^\epsilon_{n,m}(t,x) &= g(t,x) + A(t,x) v^{\epsilon-1}_{n,m}(t-\tau,x) + \sum_{e=0}^{\epsilon-1}\sum_{\eta=0}^{N-1} \int_{t^e_\eta}^{t^e_{\eta+1}} K_1(t,x,s) v^e_{\eta,m}(s,x)ds \\
&+ \sum_{\eta=0}^{n-1} \int_{t^\epsilon_\eta}^{t^\epsilon_{\eta+1}} K_1(t,x,s) v^\epsilon_{\eta,m}(s,x)ds + \int_{t^\epsilon_n}^{t} K_1(t,x,s)\hat{v}^\epsilon_{n,m}(s,x)ds \\
&+ \sum_{e=0}^{\epsilon-2}\sum_{\eta=0}^{N-1} \int_{t^e_\eta}^{t^e_{\eta+1}} K_2(t,x,s) v^e_{\eta,m}(s,x)ds + \sum_{\eta=0}^{n-1} \int_{t^{\epsilon-1}_\eta}^{t^{\epsilon-1}_{\eta+1}} K_2(t,x,s) v^{\epsilon-1}_{\eta,m}(s,x)ds \\
&+ \int_{t^{\epsilon-1}_n}^{t-\tau} K_2(t,x,s) v^{\epsilon-1}_{n,m}(s,x)ds.
\end{aligned} \tag{6}$$

To compute $\partial_t^{(i)}\partial_x^{(j)}\hat{v}^{\epsilon}_{n,m}(t,x)$, we differentiate equation (6) j times with respect to x and i times with respect to t, obtaining

$$\begin{aligned}
&\partial_t^{(i)}\partial_x^{(j)}\hat{v}^{\epsilon}_{n,m}(t,x) = \partial_t^{(i)}\partial_x^{(j)}g(t,x)\\
&\quad+\sum_{l=0}^{j}\sum_{\eta=0}^{i}\binom{j}{l}\binom{i}{\eta}\partial_t^{(i-\eta)}\left(\partial_x^{(j-l)}A(t,x)\right)\partial_t^{(\eta)}\partial_x^{(l)}v^{\epsilon-1}_{n,m}(t-\tau,x)\\
&\quad+\sum_{e=0}^{\epsilon-1}\sum_{\eta=0}^{N-1}\int_{t^e_\eta}^{t^e_{\eta+1}}\sum_{l=0}^{j}\binom{j}{l}\partial_t^{(i)}\left(\partial_x^{(j-l)}K_1(t,x,s)\right)\partial_x^{(l)}v^{e}_{\eta,m}(s,x)ds\\
&\quad+\sum_{\eta=0}^{n-1}\int_{t^\epsilon_\eta}^{t^\epsilon_{\eta+1}}\sum_{l=0}^{j}\binom{j}{l}\partial_t^{(i)}\left(\partial_x^{(j-l)}K_1(t,x,s)\right)\partial_x^{(l)}v^{\epsilon}_{\eta,m}(s,x)\,ds\\
&\quad+\sum_{q=0}^{i-1}\sum_{l=0}^{j}\sum_{\eta=0}^{q}\binom{j}{l}\binom{q}{\eta}\partial_t^{(q-\eta)}\left[\partial_t^{(i-1-q)}\Big|_{s=t}\left(\partial_x^{(j-l)}K_1(t,x,s)\right)\right]\partial_t^{(\eta)}\partial_x^{(l)}\hat{v}^{\epsilon}_{n,m}(t,x)\\
&\quad+\int_{t^\epsilon_n}^{t}\sum_{l=0}^{j}\binom{j}{l}\partial_t^{(i)}\left(\partial_x^{(j-l)}K_1(t,x,s)\right)\partial_x^{(l)}\hat{v}^{\epsilon}_{n,m}(s,x)ds\\
&\quad+\sum_{e=0}^{\epsilon-2}\sum_{\eta=0}^{N-1}\int_{t^e_\eta}^{t^e_{\eta+1}}\sum_{l=0}^{j}\binom{j}{l}\partial_t^{(i)}\left(\partial_x^{(j-l)}K_2(t,x,s)\right)\partial_x^{(l)}v^{e}_{\eta,m}(s,x)ds\\
&\quad+\sum_{\eta=0}^{n-1}\int_{t^{\epsilon-1}_\eta}^{t^{\epsilon-1}_{\eta+1}}\sum_{l=0}^{j}\binom{j}{l}\partial_t^{(i)}\left(\partial_x^{(j-l)}K_2(t,x,s)\right)\partial_x^{(l)}v^{\epsilon-1}_{\eta,m}(s,x)\,ds\\
&\quad+\sum_{q=0}^{i-1}\sum_{l=0}^{j}\sum_{\eta=0}^{q}\binom{j}{l}\binom{q}{\eta}\partial_t^{(q-\eta)}\left[\partial_t^{(i-1-q)}\Big|_{s=t-\tau}\left(\partial_x^{(j-l)}K_2(t,x,s)\right)\right]\\
&\quad\times\partial_t^{(\eta)}\partial_x^{(l)}v^{\epsilon-1}_{n,m}(t-\tau,x).
\end{aligned}$$

3 Convergence Analysis

The following lemmas and theorems will be used in this section.

Theorem 3.1 (Taylor's Theorem for functions of two independent variables [8]) Let f be p times continuously differentiable on $D=[a,b]\times[c,d]$, and let $(x_0,y_0)\in D$. Then, for all $(x,y)\in D$, we have

$$\begin{aligned}
f(x,y) &= \sum_{i+j=0}^{p-1}\frac{1}{i!j!}\partial_t^{(i)}\partial_x^{(j)}f(x_0,y_0)(x-x_0)^i(y-y_0)^j\\
&\quad+\sum_{i+j=p}\frac{1}{i!j!}\partial_t^{(i)}\partial_x^{(j)}f(x_1,y_1)(x-x_0)^i(y-y_0)^j,
\end{aligned}$$

where

$$\begin{cases} x_1=\theta x+(1-\theta)x_0, & x_1\in[a,b],\\ y_1=\theta y+(1-\theta)y_0, & y_1\in[c,d],\end{cases}\qquad \theta\in(0,1).$$

Lemma 3.1 (Discrete Gronwall-type inequality [6]) Let $\{k_j\}_{j=0}^{n}$ be a given non-negative sequence, and suppose that the sequence $\{\varepsilon_n\}$ satisfies $\varepsilon_0 \leq p_0$ and $\varepsilon_n \leq p_0 + \sum_{i=0}^{n-1} k_i \varepsilon_i$, for $n \geq 1$, with $p_0 \geq 0$. Then ε_n is bounded by

$$\varepsilon_n \leq p_0 \exp\left(\sum_{j=0}^{n-1} k_j\right), \quad n \geq 1.$$

Lemma 3.2 (Bellman's inequality [2]) Let h and f be continuous and non-negative functions defined on $J = [\alpha, \beta]$, and let c be a non-negative constant. Then the inequality

$$h(t) \leq c + \int_\alpha^t f(s)h(s)ds, \quad t \in J,$$

implies that

$$h(t) \leq c \exp\left(\int_\alpha^t f(s)ds\right), \quad t \in J.$$

To establish the convergence of the proposed method, we require the following lemma. We work within the space $L^\infty(D)$ equipped with the norm

$$\|\varphi\|_{L^\infty(D)} = \inf\{C \in \mathbb{R} : |\varphi(t,x)| \leq C \quad \text{for a.e. } (t,x) \in D\} < \infty.$$

Lemma 3.3 Let g, Φ, A, K_1, and K_2 be p-times continuously differentiable on their respective domains. Then there exists a positive constant $\alpha(p)$ such that for all $n = 0, \ldots, N-1$, $m = 0, \ldots, M-1$, $\epsilon = 0, \ldots, r-1$, and $i + j = 0, \ldots, p$, we have

$$\left\| \frac{\partial^{i+j} \hat{v}_{n,m}^\epsilon}{\partial t^i \partial x^j} \right\|_{L^\infty(D_{n,m}^\epsilon)} \leq \alpha(p).$$

Proof. The lemma can be proved by directly generalizing the procedures used in Claim 1 of Theorem 3.3 in [3]. The following theorem establishes the convergence of the proposed method.

Theorem 3.2 Suppose that g, Φ, A, K_1, and K_2 are p-times continuously differentiable on their respective domains. Then the equations $(2), (3), (5)$ uniquely define an approximation $v \in S_{p-1}^{(-1)}(\Pi_{N,M}^\epsilon)$. Furthermore, the associated error function $E = u - v$ satisfies the following bound:

$$\|E\|_{L^\infty(D)} \leq C(h+k)^p,$$

where C is a finite constant independent of h and k.

Proof. Define the error function E on $D_{n,m}^\epsilon$ as

$$E_{n,m}^\epsilon = u - v_{n,m}^\epsilon, \quad \forall n \in \{0, \ldots, N-1\},\ m \in \{0, \ldots, M-1\},\ \epsilon \in \{0, \ldots, r-1\}.$$

Throughout this proof, the norm $\|\cdot\|$ refers to $\|\cdot\|_{L^\infty(D)}$.
Let $(t,x) \in D_{n,m}^\epsilon$. For $\epsilon = 0$, using Theorem 3.1 and equation (2), we write

$$|E_{0,m}^0(t,x)| \leq \sum_{i+j=p} \frac{1}{i!j!} \left\| \partial_t^{(i)} \partial_x^{(j)} u(0,x_m) \right\| h^i k^j.$$

According to Lemma 3.3, this implies

$$|E^0_{0,m}(t,x)| \le \alpha(p) \sum_{i+j=p} \frac{1}{i!j!} h^i k^j = \frac{\alpha(p)}{p!}(h+k)^p.$$

Define $C_1(p) = \frac{\alpha(p)}{p!}$. Thus,

$$\|E^0_{0,m}\| \le C_1(p)(h+k)^p.$$

For $\epsilon = 0$ and $n \in \{1, \dots, N-1\}$, using equation (4), we have

$$u(t,x) - \hat{v}^0_{n,m}(t,x) = \sum_{\eta=0}^{n-1} \int_{t^0_\eta}^{t^0_{\eta+1}} K_1(t,x,s)(u(s,x) - v^0_{\eta,m}(s,x))\, ds + \int_{t^0_n}^{t} K_1(t,x,s)(u(s,x) - \hat{v}^0_{n,m}(s,x))\, ds.$$

Taking the norm, we get

$$\|u - \hat{v}^0_{n,m}\| \le \sum_{\eta=0}^{n-1} hK\|E^0_{\eta,m}\| + K \int_{t^0_n}^{t} \|u - \hat{v}^0_{n,m}\|\, dt,$$

where $K = \max\{\|K_1\|, \|K_2\|\}$. By Lemma 3.2,

$$\|u - \hat{v}^0_{n,m}\| \le \sum_{\eta=0}^{n-1} hd_1\|E^0_{\eta,m}\|,$$

where $d_1 = K\exp(K\tau)$. On the other hand,

$$\|E^0_{n,m}\| \le \|u - \hat{v}^0_{n,m}\| + \|\hat{v}^0_{n,m} - v^0_{n,m}\|.$$

Substituting the bounds and applying Theorem 3.1 and Lemma 3.1, we get

$$\|E^0_{n,m}\| \le \frac{\alpha(p)}{p!}(h+k)^p \exp(\tau d_1).$$

Define $C_2(p) = \frac{\alpha(p)}{p!}\exp(\tau d_1)$.

For $\epsilon \in \{1, \dots, r-1\}$, using equation (6), we have

$$\|u - \hat{v}^\epsilon_{n,m}\| \le \|A\| \sum_{e=0}^{\epsilon-1} \|E^e\| + Kh \sum_{\eta=0}^{n-1} \|E^\epsilon_{\eta,m}\| + K \int_{t^\epsilon_n}^{t} \|u - \hat{v}^\epsilon_{n,m}\|\, ds.$$

According to Lemma 3.2, this implies

$$\|u - \hat{v}^\epsilon_{n,m}\| \le \widehat{A} \sum_{e=0}^{\epsilon-1} \|E^e\| + \widehat{K}h \sum_{\eta=0}^{n-1} \|E^\epsilon_{\eta,m}\|,$$

where $\widehat{A} = \|A\|\exp(K\tau)$ and $\widehat{K} = K\exp(K\tau)$.

On the other hand,

$$\|E^{\epsilon}_{n,m}\| \le \widehat{A}\sum_{e=0}^{\epsilon-1}\|E^e\| + \widehat{K}h\sum_{\eta=0}^{n-1}\|E^{\epsilon}_{\eta,m}\| + \frac{\alpha(p)}{p!}(h+k)^p.$$

Applying Lemma 3.1, we have

$$\|E^{\epsilon}\| \le \exp(\widehat{K}\tau)\frac{\alpha(p)}{p!}(h+k)^p + \exp(\widehat{K}\tau)\widehat{A}\sum_{e=0}^{\epsilon-1}\|E^e\|.$$

Using Lemma 3.1 again, we obtain

$$\|E^{\epsilon}\| \le \underbrace{\exp(\widehat{K}\tau)\frac{\alpha(p)}{p!}\exp((r-1)\exp(\widehat{K}\tau)\widehat{A})}_{C_3(p)}(h+k)^p.$$

Finally, setting $C = \max\{C_1(p), C_2(p), C_3(p)\}$, we conclude

$$\|E^{\epsilon}_{n,m}\| \le C(h+k)^p, \quad \forall n \in \{0,\dots,N-1\},\, m \in \{0,\dots,M-1\},\, \epsilon \in \{0,\dots,r-1\}. \square$$

4 Numerical Examples

In this section, we validate the theoretical results derived in the previous section through numerical examples. The exact solutions for all examples are known in advance. For each example, we compute the error between the exact solution u and the Taylor collocation solution v.

Example 4.1 Consider the DVIEs with a time delay $\tau = \frac{1}{5}$ of the form

$$u(t,x) = \begin{cases} g(t,x) + (t+x)u(t-\frac{1}{5},x) + \displaystyle\int_0^t s\cos(xt)u(s,x)ds \\ + \displaystyle\int_0^{t-\frac{1}{5}} (2\sin(t+x)+s)u(s,x)ds, \quad t \in [0,1], \quad x \in [0,1], \\ \Phi(t,x), \quad t \in [-\frac{1}{5}, 0]. \end{cases}$$

The exact solution of this problem is given by $u(t,x) = t + \sin(x)$. The function $g(t,x)$ is then computed using the exact solution. Numerical results were obtained by applying the proposed Taylor collocation method for different numbers of collocation points. The absolute error values are reported in Table 1, showing that the absolute errors decrease as the number of collocation points increases.

Example 4.2 Consider the two-dimensional Volterra integral equation from [10]

$$u(x,t) = x^2(-1 + e^{-t} + x^2 + e^t - x^2e^t) + \int_0^t (x^2 + e^{-2s})u(x,s)ds$$

for $x, t \in [0,1]$, which has the exact solution $u(x,t) = x^2e^t$. The numerical results for $p-1 = 2,4,6$ and $h = k = 0.1$ obtained using the Taylor collocation method (TCM) are compared with the numerical results obtained using a method based on expanding the solution in terms of bivariate shifted Legendre polynomials [10]. The comparison is presented in Table 2.

x \ t	0	0.2	0.4	0.6	0.8	1
0	0	$1.32e-12$	$1.15e-11$	$2.36e-11$	$2.92e-10$	$8.23e-10$
0.2	$3.8e-14$	$6.54e-11$	$2.30e-11$	$1.50e-10$	$3.45e-10$	$9.21e-10$
0.4	$2.66e-11$	$7.81e-12$	$7.20e-11$	$4.01e-10$	$1.24e-09$	$1.18e-10$
0.6	$4.38e-11$	$3.29e-11$	$1.99e-10$	$1.48e-10$	$3.99e-10$	$2.79e-10$
0.8	$8.73e-11$	$3.45e-10$	$2.61e-10$	$2.59e-10$	$1.00e-09$	$5.41e-09$

Table 1: Numerical results for Example 4.1.

	Present method (TCM)			Method in Ref. [10]		
(x,t)	$p-1=2$	$p-1=4$	$p-1=6$	$M=2$	$M=4$	$M=6$
$(0,0)$	0	0	0	0	0	0
$(0.1,0.1)$	$3.6e-08$	$7.3e-12$	$1.4e-11$	$2.9e-05$	$2.0e-07$	$1.3e-09$
$(0.2,0.2)$	$3.0e-07$	$9.8e-11$	$1.3e-11$	$1.6e-04$	$4.7e-07$	$5.8e-09$
$(0.3,0.3)$	$1.0e-06$	$2.5e-10$	$3.4e-10$	$4.9e-04$	$9.5e-07$	$1.3e-08$
$(0.4,0.4)$	$2.8e-06$	$1.1e-09$	$3.2e-10$	$5.8e-04$	$2.4e-06$	$2.3e-08$
$(0.5,0.5)$	$6.3e-06$	$2.1e-09$	$1.0e-10$	$1.5e-05$	$3.4e-07$	$3.6e-08$
$(0.6,0.6)$	$1.3e-05$	$3.9e-09$	$3.0e-10$	$1.3e-03$	$4.9e-06$	$5.2e-08$
$(0.7,0.7)$	$2.5e-05$	$7.8e-09$	$2.8e-09$	$3.0e-03$	$5.6e-06$	$7.0e-08$
$(0.8,0.8)$	$4.8e-05$	$1.5e-08$	$1.5e-09$	$3.4e-03$	$6.9e-06$	$9.1e-08$
$(0.9,0.9)$	$9.1e-05$	$3.0e-08$	$1.3e-09$	$6.2e-04$	$1.7e-05$	$1.1e-07$
CPU time	$56.17\,sec$	$253.82\,sec$	$997.32\,sec$	/	/	/

Table 2: Comparison of absolute errors for Example 4.2.

5 Conclusion

In this paper, we proposed a new numerical method based on Taylor polynomials to construct a collocation solution for approximating the solution of delay Volterra integral equations (DVIEs) with a spatial variable. Unlike existing approaches, our method efficiently handles the time delay and spatial dependence in the integral equation, which is a key challenge in solving such problems.

A rigorous convergence analysis confirms that the proposed method is accurate and stable, with an $O((h+k)^p)$ error bound. Numerical examples validate its effectiveness, demonstrating that it provides high-precision approximations while maintaining computational efficiency.

The novelty of our approach lies in the extension of the Taylor Collocation Method to DVIEs with spatial dependence, an area that has received limited attention in previous studies. Additionally, our method is computationally efficient as it computes the approximation coefficients iteratively without requiring the solution of any system of algebraic equations. Moreover, it can be adapted to various delay integral equations encountered in applied sciences and engineering.

These contributions make our method a powerful and efficient alternative for solving DVIEs with spatial variables, laying the groundwork for further extensions to higher-dimensional problems.

References

[1] I. Ali, H. Brunner and T. Tang. Spectral methods for pantograph-type differential and integral equations with multiple delays. *Frontiers of Mathematics in China* **4** (2009) 49–61.

[2] R. Bellman. The stability of solutions of linear differential equations. *Duke Mathematical Journal* **10** (1943) 643–647.

[3] A. Bellour and M. Bousselsal. A Taylor collocation method for solving delay integral equations. *Numerical Algorithms* **65** (2014) 843–857.

[4] F. Birem, A. Boulmerka, H. Laib and C. Hennous. An algorithm for solving first-kind two-dimensional Volterra integral equations using collocation method. *Nonlinear Dynamics and Systems Theory* **23** (2023) 475–486.

[5] H. Bouzeraieb, H. Laib and A. Boulmerka. Numerical solution of neutral double delay Volterra integral equations using Taylor collocation method. *Nonlinear Dynamics and Systems Theory* **24** (2024) 236–245.

[6] H. Brunner. *Collocation Methods for Volterra Integral and Related Functional Differential Equations*. Cambridge University Press, Cambridge, 2004.

[7] H. Brunner. The numerical solution of two-dimensional Volterra integral equations by collocation and iterated collocation. *IMA Journal of Numerical Analysis* **9** (1989) 47–59.

[8] S. R. Ghorpade and B. V. Limaye. *A Course in Multivariable Calculus and Analysis.* Springer, New York, 2010.

[9] S. McKee, T. Tang and T. Diogo. An Euler-type method for two-dimensional Volterra integral equations of the first kind. *IMA Journal of Numerical Analysis* **20** (2000) 423–440.

[10] S. Nemati, P. M. Lima and Y. Ordokhani. Numerical solution of a class of two-dimensional nonlinear Volterra integral equations using Legendre polynomials. *Journal of Computational and Applied Mathematics* **242** (2013) 53–69.

[11] H. Brunner and Y. Yatsenko. Spline collocation methods for nonlinear Volterra integral equations with unknown delay. *Journal of Computational and Applied Mathematics* **71** (1996) 67–81.

[12] W. Zheng and Y. Chen. Numerical analysis for Volterra integral equation with two kinds of delay. *Acta Mathematica Scientia* **39** (2019) 607–617.

[13] L. Zhang, J. Huang and H. Li. Splitting extrapolation algorithms for solving linear delay Volterra integral equations with a spatial variable. *Applied Numerical Mathematics* **178** (2022) 372–385.

Nonlinear Dynamics and Systems Theory, **25** (6) (2025) 679–690

Approximation of Invariant Solutions to the Nonlinear Filtration Equation by Modified Padé Approximants

S. Skurativskyi *, S. Mykulyak and I. Skurativska

Subbotin Institute of Geophysics of NAS of Ukraine,
Palladin av. 32, Kyiv, 03142, Ukraine

Received: November 20, 2024; Revised: October 27, 2025

Abstract: This paper deals with a mathematical model for oil filtration in a porous medium and its self-similar and traveling wave regimes. The model consists of the equation of mass conservation and dependencies of porosity, permeability, and oil density on pressure. The oil viscosity is considered to be the experimentally determined parabolic relationship with respect to pressure. To close the model, two types of the Darcy law are used: the classic one and the dynamic one describing the relaxation processes during filtration. In the former case, self-similar solutions are studied, while in the latter case, traveling wave solutions are the focus. Using the invariant solutions, the initial model is reduced to the nonlinear ordinary differential equations possessing the trajectories vanishing at infinity and representing the moving liquid fronts in porous media. To approximate these solutions, we elaborate the semi-analytic procedure based on modified Padé approximants. In fact, we calculate sequentially Padé approximants up to the 3-rd order for a two-point boundary value problem on the semi-infinite domain. A good agreement of evaluated Padé approximants and numerical solutions is observed. The approach provides relatively simple quasi-rational expressions of solutions and can be easily adapted for other types of model's nonlinearity.

Keywords: *nonlinear filtration; self-similar solution; relaxation; traveling wave; Padé approximant.*

Mathematics Subject Classification (2020): 35K55, 35L75, 35C06, 35C07, 41A21, 70K99, 93-10.

* Corresponding author: mailto:skurserg@gmail.com

1 Introduction

The filtration processes are studied in many branches of science, including geophysics, biology, ecology, medicine, etc. Control of the filtration processes is at the heart of technologies applied for enhancing oil and gas recovery [2, 5], cleaning polluted gas-liquid substances, and providing high-quality drugs in the biopharmaceutical industry. Due to the significance and prevalence of these processes in nature and technological developments, theoretical studies of filtration in porous media are relevant, especially regarding the deviation of filtration flow dynamics from linear patterns.

The complete formulation of filtration problems, incorporating process nonlinearity, high intensity, and multiphasicity of liquid flows, interacting effects, and complex initial and boundary conditions, presents significant challenges. This necessitates the development of new or improved tools for study.

In this research, we consider the oil filtration in a porous medium within the framework of continuous mechanics [2], taking into account several nonlinear effects. The filtration model consists of the equation of motion representing the conservation of mass, the equation of state for oil, the dependencies of porosity and permeability on pressure, and finally, the Darcy law, which is considered in its classical or generalized form. Model nonlinearity originates from the nonlinear dependence of oil viscosity on pressure which is discovered experimentally. Note that the viscosity of reservoir oil is an important characteristic that affects the proper functioning of producing wells [4,10]. Other fluid dynamics problems in porous media also seek to determine the influence of variable viscosity and permeability of filtrating liquids on flow behavior [15].

In the case of the classic Darcy law, the model in the one-dimensional case is reduced to the nonlinear filtration equation, which can be regarded as a weakly nonlinear diffusion equation [11,19,20] $p_t = (k(p)p_x)_x$, where the function $k(p)$ is the diffusion coefficient or hydraulic conductivity. A vast number of studies concern the boundary value problem (BVP) on a semi-infinite domain when the model admits self-similar regimes.

Another interesting class of filtration models known as relaxation models or models with memory [8, 14] has been formed when considering the filtration processes with a relatively rapid change in parameters, the flows of non-Newtonian liquids (heavy oil, solutions of polymers, mixtures, emulsions, multiphase liquids with mass exchange between phases), and filtration in layers with a particularly complex structure (crack-porous media) [2]. In such conditions, a delay is observed in the response of the filtration flow; in other words, there is a local nonequilibrity of the filtration process accompanied by the relaxation of pressure and velocity. To incorporate process nonequilibrity, the classical Darcy law is generalized by adding the terms with the first temporal derivatives [5,12,18] describing the approach of pressure and velocity to their equilibrium values. As a rule, the nonequilibrium (or relaxation) filtration models do not admit the same self-similar solutions as the classical Darcy-type models. Instead, the relaxation models possess the traveling wave solutions, the structure of which is richer.

Despite an immense number of research on the nonlinear diffusion-type equations, they rarely succeed in obtaining a general exact solution of equations, especially their hyperbolic generalizations. Therefore, there is still a need to improve existing and develop more general methods of derivation of solutions, including the development of the asymptotic approach [1] in combination with the extensive involvement of numerical methods [13].

Thus, we aim to develop a semi-analytic approach based on the Padé approximants, which were proven to be effective in many applications [1,3,17], and use it for calculating the invariant solutions describing the filtration of oil with variable viscosity.

2 The Model of Oil Filtration and Its Reduction to a Single Equation

The mathematical model for the elastic mode of filtration reads as follows:

$$\begin{aligned} (m\rho)_t + (\rho v)_x = 0, \qquad & \rho = \rho_0\left(1 + C_f\left(p - p_0\right)\right), \\ m = m_0\left(1 + C_m\left(p - p_0\right)\right), \quad & k = k_0\left(1 + C_k\left(p - p_0\right)\right). \end{aligned} \tag{1}$$

Here, the system (1) consists of the continuity equation expressing the mass conservation law, equation of state for a fluid, and dependencies of porosity and permeability on pressure. The traditional designations used are: ρ is the fluid density, p is the pressure, v is the filtration velocity, C_f, C_m, and C_k are the compression coefficients of the fluid, porosity, and permeability.

To close the system, we used the generalized Darcy law containing the description of the nonequilibrium (or relaxation) filtration process [5,12,18]

$$\tau\left(v + K_\infty p_x\right)_t + v + K_0 p_x = 0, \tag{2}$$

where the hydraulic conductivity functions $K_0 = \frac{k}{\mu}$ and $K_\infty = \theta K_0$ are related to the equilibrium and frozen diffusion coefficients, τ and θ are constants. In this research, we pay more attention to the oil viscosity μ, assuming that it varies significantly with pressure, which prompts the consideration of nonlinear pressure dependencies for the function $\mu(p)$.

It is obvious that by dropping the relaxing terms in (2), we arrive at the classical Darcy law

$$v = -K_0 p_x. \tag{3}$$

To simplify the problem, we reduce the model of filtration to a single equation with respect to p.

Let us start with considering the model using the classic Darcy law while justifying the quadratic pressure dependence of oil viscosity μ.

To specify the function μ, we consider the process of oil filtration in a reservoir in the range of pressures when the oil is close to the phase transition zone which can form during depletion away from a wellbore ([4], p.42). We are interested in the vicinity of the phase transition point, where a single phase of oil transforms into a gas-liquid mixture. Assume that in this zone, the amount of gas phase is not enough to influence the filtration dynamics, but the oil viscosity undergoes significant changes, which are taken into account in the model.

We consider the experimental data concerning the measurements of the viscosities of oils under reservoir conditions [10]. Several experimental points from the paper [10] (see Fig.3, curve 4) are depicted in Fig.1. These data confidently show the convex character of the graph of oil viscosity at pressure variations.

In this study, we pay attention to the vicinity of the point of minimum known as a bubble point and describe the oil viscosity μ as a quadratic function of pressure,

$$\mu = \mu_0\left(1 + a\left(p - p_0\right)^2\right), \tag{4}$$

where μ_0 is the viscosity at $p = p_0$, a is a positive constant.

To specify the function μ, we approximate the experimental data in Fig.1 by the parabola (4) whose vertex coincides with the minimum value of the data (Fig.1). The coordinates of the parabola vertex $(p_0; \mu_0)$ are evaluated from the experimental data quite accurately providing that $\mu_0 = 0.005$ Pa·s and $p_0 = 41.6855$ bar (or 4.169 MPa). The evaluation of the parameter a leads to the following value $a = 1.507 \cdot 10^{-14}$ Pa^{-2}.

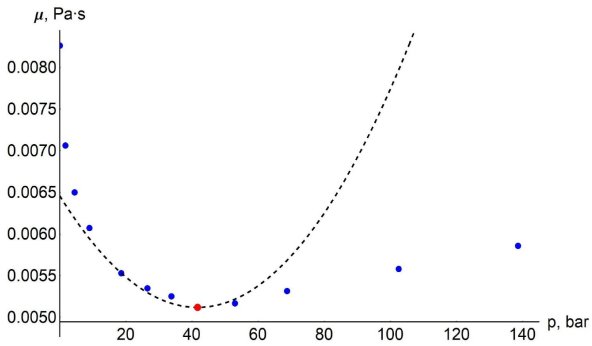

Figure 1: The approximation of viscosity by the parabola $\mu = \mu_0 \left(1 + a\,(p - p_0)^2\right)$ with the vertex $(p_0; \mu_0) = (4.16855 \cdot 10^6, 0.005)$ and $a = 1.507 \cdot 10^{-14}$ Pa^{-2}. The experiment of Hocott et al. [10] is marked with filled circles, while their parabolic approximation is drawn with the dashed line.

Applying the auxiliary constraints $C_f C_m \ll 1$, the filtration model (1) closed by the dynamic Darcy law (2) is reduced to the single partial differential equation

$$\tau p_{tt} - \tau\theta[D(p)p_x]_{xt} + p_t - [D(p)p_x]_x = 0, \tag{5}$$

where

$$D(p) = \kappa \frac{1 + C_k\,(p - p_0)}{1 + a\,(p - p_0)^2} \text{ and } \kappa = \frac{k_0}{\mu_0 m_0 (C_f + C_m)}.$$

When $\tau = 0$, that is, the classic Darcy law (3) is used, it follows from (5) that

$$p_t = (D(p)p_x)_x\,. \tag{6}$$

Next, we consider the invariant solutions of equations (5) and (6) and develop the semi-analytical procedure for their approximation using Padé approximations. Let us start from the more straightforward equation (6) and solve a BVP possessing the self-similar invariant solutions.

3 BVP for the Filtration Model with the Classical Darcy Law and Its Self-Similar Solutions

When equation (6) is subject to the following initial and boundary conditions:

$$p(x, t = 0) = p_1, \quad p(x = 0, t) = p_2, \qquad p_{1,2} = \text{const}, \tag{7}$$

we arrive at the classical BVP [2, 7, 16] that admits self-similar solutions. To continue the theoretical studies, let us perform the substitution

$$p(x,t) = \Omega(P + y_1), \tag{8}$$

where $\Omega = 1/\sqrt{a}$ and $p_{0,1,2} = \Omega y_{0,1,2}$.

Then equation (6) and conditions (7) can be written in the form of the dimensionless BVP

$$\begin{gathered} P_t = \left(D(P)P_x\right)_x, \\ P(x,t=0) = 0, \qquad P(x=0,t) = y_2 - y_1, \end{gathered} \tag{9}$$

where

$$D(P) = D(0)G(P), \qquad G(P) = \frac{1+\beta_1 P}{1+2\beta_3 P + \beta_2 P^2}, \qquad D(0) = \kappa \frac{1 + C_k\Omega\,(y_1 - y_0)}{1 + (y_1 - y_0)^2},$$

$$\beta_1 = \frac{C_k\Omega}{1 + C_k\Omega\,(y_1 - y_0)}, \qquad \beta_2 = \frac{1}{1 + (y_1 - y_0)^2}, \qquad \beta_3 = \frac{(y_1 - y_0)}{1 + (y_1 - y_0)^2}.$$

Further studies do not require the value of $D(0)$ due to the special selection of the solution form, while β_j affects the solution characteristics.

Since $a \sim 10^{-14}$ Pa^{-2}, one has $\Omega \sim 10^7 = 10$ MPa. The values of C_f and C_k are of order $10^{-10} - 10^{-8}$ Pa^{-1} [2], therefore, β_1 may not be small, especially if we take into account the possibility of a negative value of $y_1 - y_0$.

The remarkable feature of the model (9) is that this problem possesses the well-known self similar solution

$$P(x,t) = P(\xi), \quad \xi = \frac{x}{2\sqrt{D(0)t}}, \tag{10}$$

reducing (9) to the ordinary differential equation

$$\frac{d}{d\xi}\left(\frac{1+\beta_1 P}{1+2\beta_3 P+\beta_2 P^2}\frac{dP}{d\xi}\right) = -2\xi\frac{dP}{d\xi} \tag{11}$$

subjected to the conditions

$$P(\xi = 0) = y_2 - y_1, \qquad P(\xi = \infty) = 0. \tag{12}$$

Equation (11) has a long history that can be traced through the works [7, 16]. Here, we briefly remark that the construction of the solution of (11) depends on the form of hydraulic conductivity function $D(P)$. It is known [7, 16] that the analytical representation of the solution can be obtained for the cases $\beta_1 = \beta_2 = 0$, $\beta_3 = -q, \beta_2 = q^2$, and $\beta_1 = 0$. In other cases, equation (11) is analyzed by alternative methods.

In what follows, we develop the semi-analytic procedure for the evaluation of solutions to BVP (11) – (12) utilizing the Padé approximants.

4 The Padé Approximant Construction for the BVP Self-Similar Solutions

To do this, we need the integral relations representing a certain type of conservation laws for equation (11). In particular, integrating (11) over the interval $(0;\infty)$, we obtain

$$\frac{dP}{d\xi}(0) = -2\frac{1+2\beta_3 P(0)+\beta_2 P(0)^2}{1+\beta_1 P(0)}\int_0^\infty P d\xi. \tag{13}$$

In essence, the procedure is the adaptation of the approaches developed in [1,17]. The direct application of the procedures outlined in the above-mentioned papers encounters massive symbolic calculations that do not allow to obtain desired results or significantly exploit the peculiarities of the model. In this research, we use the specific conservation laws and quasi-fractional Padé approximants [1].

Thus, we are looking for the solution of the problem in the form of the Taylor series

$$P = \sum_{i=0}^{N} r_i \xi^i, \tag{14}$$

where $P(0) = r_0$ is evaluated from the initial condition at $\xi = 0$.

Inserting it into equation (11), we derive the coefficients r_i, $i \geqslant 2$, as the functions of $r_1 = P'(0)$ only. As ξ increases, series (14) diverges and does not describe the solution properly. Therefore, we approximate it by a Padé approximant, i.e., the rational approximation for a series. To specify the form of the Padé approximant, we use the additional information on the solution's behavior at infinity.

Assume that $P(\xi)$ is vanishing as ξ tends to infinity. Then, from equation (11), it follows that asymptotics is defined by the equation $\frac{d^2P}{d\xi^2} = -2\xi\frac{dP}{d\xi}$, whose vanishing solution is $P(\xi) = const \cdot \mathrm{erfc}(\xi) \equiv const \cdot \int_\xi^\infty \exp(-z^2)dz$. In turn, the asymptotics of the function $\mathrm{erfc}(\xi) \sim Q(\xi)\exp(-\xi^2)$ is also valid.

Thus, to construct the solution valid for all ξ, we approximate the Taylor series (14) by the quasi-fractional Padé approximant [1] combining the rational Padé approximant and the asymptotics $\sim \exp(-\xi^2)$

$$PA_{[M/M]} = \frac{\sum_{i=0}^{M} A_i \xi^i}{\sum_{j=0}^{M} B_j \xi^j} e^{-\xi^2}, \tag{15}$$

where M is the order of the Padé approximant; A_i and B_j are constants.

Let us recall that A_i and B_j depend on r_1 only. To evaluate M coefficients of A_i and B_j, we need to derive $N = 2M$ coefficients of the Taylor series (14). Relation (15) is inserted in integral relations (13) which are solved with respect to r_1. Note that the form of $PA_{[M/M]}$ can be modified further by incorporating the polynomial $\sum_k^L C_k \xi^k$ into the exponent of the exponential function. The constants C_k can be calculated by the auxiliary integral equations deduced from the starting equation by multiplying by ξ^n and integration over $(0; \infty)$ [1].

4.1 Application of the procedure of BVP solving

To apply the procedure developed above, we consider BVP (11) – (12) at a and p_0 evaluated for the parabola of Fig. 1. We choose the value $p_1 = 2$MPa, which lies to the left of the point $p = p_0$ in Fig. 1. Then we obtain $\Omega = 1/\sqrt{a} = 0.81 \cdot 10^7$; $(y_1 - y_0) = (20 \cdot 10^5 - p_0)/\Omega = -0.2677$. To evaluate β_1, we fix the product $C_k\Omega$ that varies in a wide range due to the significant variations of C_k as mentioned above. Then, for instance, when $C_k\Omega = 0.001$, then $\beta_1 = 0.001$, while at $C_k\Omega = 0.4$, we have $\beta_1 = 0.447973$. Therefore, let us consider two cases. The former when β_1 is small enough to be neglected and the latter when β_1 is not small. For the sake of simplicity, the initial condition $y_2 - y_1$ is assumed to be 1. Thus, $P(0) = r_0 = 1$ in (14) for all further studies.

Thus, the coefficients r_i of series (14) are as follows:

$$r_2 = r_1^2 \frac{\beta_1(\beta_2 - 1) + 2(\beta_2 + \beta_3)}{2(1+\beta_1)(1+\beta_2+2\beta_3}, \qquad r_3 = -r_1 \frac{1+\beta_2+2\beta_3}{3(1+\beta_1)} +$$
$$r_1^3 \frac{\beta_1^2(3+\beta_2^2+4\beta_3) + 2(\beta_2 + 3\beta_2^2 + 6\beta_2\beta_3 + 2\beta_3^2) + 4\beta_1(\beta_2^2 - \beta_2 - 2\beta_3(1+\beta_3))}{6(1+\beta_1)^2(1+\beta_2+2\beta_3)^2}, \ldots$$

The coefficients r_i, $i \geqslant 2$, depend only on r_1. However, they quickly become cumbersome when the number i increases.

Next, by relation (15), we construct the expression $PA_{[M/M]}$ for the Taylor series (14) in a conventional way taking into account in addition the expansion $\exp(-\xi^2) = \sum_{n=0}^{\infty}(-1)^n \xi^{2n}/n!$. Let us start from the simplest case when $M = 1$ and $PA_{[1/1]} = (1 + A_1\xi)\exp(-\xi^2)/(1 + B_1\xi)$. Then the relation for specifying A_1 and B_1 reads as follows:

$$(1 + r_1\xi + r_2\xi^2 + \ldots)(1 + B_1\xi) - (1 - \xi^2 + \xi^4/2 + \ldots)(1 + A_1\xi) = 0.$$

Nullifying the coefficients at ξ and ξ^2, we obtain a pair of equations whose roots are as follows:

$$A_1 = -\frac{1 + r_2 - r_1^2}{r_1}, \qquad B_1 = -\frac{1 + r_2}{r_1}. \tag{16}$$

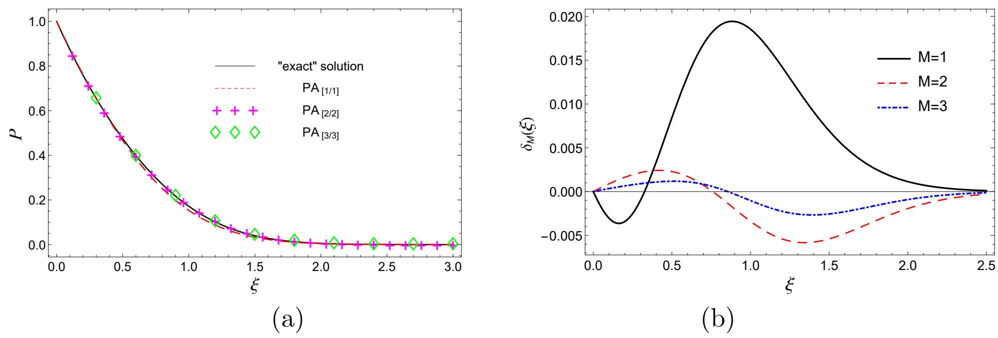

Figure 2: a: The $P(\xi)$ profiles for the solutions of BVPs (11) – (12) evaluated numerically (regarded as the "exact" solution and marked by the solid curve) and corresponding $PA_{[M/M]}$. b: The differences $\delta_M(\xi) = P - PA_{[M/M]}$ vs. ξ for the profiles from the left panel.

Let the parameter values be as follows:

$$\beta_1 = 0.447973; \qquad \beta_2 = 0.933119; \qquad 2\beta_3 = -0.249816. \tag{17}$$

Using the *Mathematica* commands NDSolve[Equation (11), P[0]==1, P[5]==0}, P, ξ, Method $\to$ {"Shooting", "StartingInitialConditions" $\to$ {P[0] == 1, P'[0] == −2}, we calculate the trajectory $P(\xi)$ (Fig.2a, solid curve) and its derivative at zero $(r_1)_{ex} = -1.32175$, which is regarded as exact. The coefficients r_i of the series (14) are as follows:

$$\begin{aligned} &r_0 = 1, \qquad r_1 - \text{unknown}, \qquad r_2 = 0.3254 r_1^2, \qquad r_3 = -0.3875 r_1 + 0.1883 r_1^3, \\ &r_4 = -0.3783 r_1^2 + 0.0608 r_1^4, \ldots \end{aligned} \tag{18}$$

M	1	2	3
$(r_1)_M$ by (13)	-1.28324	-1.33149	-1.32556
$\eta = \left\| \frac{(r_1)_M-(r_1)_{ex}}{(r_1)_{ex}} \right\|$	0.0291	0.0073	0.0028

Table 1: Values of $(r_1)_M$ and their relative errors depending on M ($(r_1)_{ex} = -1.32175$).

We construct $PA_{[M/M]}$ using the coefficients (18) and insert the resulting Padé approximants into the integral law (13). Solving the resulting equations with respect to r_1, we obtain the successive approximations for r_1 shown in Table 1, the second row.

Then, using the evaluated values of r_1 and inserting them into (18), we write the corresponding Pade approximants (it is especially easy to obtain $PA_{[1/1]}$ by evaluating (16))

$$PA_{[1/1]} = \frac{1 - 0.0863411x}{1 + 1.1969x}e^{-x^2}, \qquad PA_{[2/2]} = \frac{1 + 0.141081x + 0.414061x^2}{1 + 1.47257x + 0.797799x^2}e^{-x^2},$$

$$PA_{[3/3]} = \frac{1 + 0.0632479x + 0.632533x^2 - 0.0548591x^3}{1 + 1.38881x + 0.901649x^2 + 0.207737x^3}e^{-x^2}.$$

To find out the quality of the approximation, we compare the numerically derived profile $P(\xi)$ and the profiles $PA_{[M/M]}$ (Fig. 2a). For convenience, we depict the differences $\delta_M(\xi) = P(\xi) - PA_{[M/M]}$ in Fig.2b. Obviously, the deviations of the profiles from zero decrease when the order M grows. In particular, at $M = 3$, the difference $\delta_3(\xi)$ varies in the interval $[-0.0026; 0.0012]$, i.e., $P(\xi)$ and $PA_{[M/M]}$ are almost indistinguishable.

The convergence of the iteration procedure of the Padé approximant evaluation is monitored by calculating the relative error $\eta = |\{(r_1)_M - (r_1)_{ex}\}/(r_1)_{ex}|$, where $(r_1)_M = dPA_{[M/M]}/d\xi$ is the derivative of the Padé approximant at $\xi = 0$ and $(r_1)_{ex} = -1.32175$. The results of the calculations are presented in Table 1, the third row. Analyzing the behavior of relative errors, we see that η decreases when M grows. This allows one to conclude that the iteration process converges to the value $(r_1)_{ex}$.

5 Traveling Wave Solutions of the Filtration Model with the Relaxation Darcy Law and Their Padé Approximants

Now, consider equation (5), assuming that the pressure approaches p_1 as $x \to \infty$, and transform it using the substitution $p = \Omega P + p_1 \equiv \Omega(P + y_1)$ similar to (8). The resulting equation is as follows:

$$\tau P_{tt} - \tau\theta[D(P)P_x]_{xt} + P_t - [D(P)P_x]_x = 0, \tag{19}$$

where $D(P) = D(0)G(P)$ is defined in (9). For our studies, we can further put $D(0) = 1$ without loss of generality.

Equation (19) does not admit the self-similar regimes (10), instead, among invariant solutions, there are traveling wave regimes. Therefore, in what follows, we consider the traveling wave solution

$$p = P(\xi), \qquad \xi = x - ct, \tag{20}$$

where c is the phase velocity.

Inserting (20) into (19), we get the ordinary differential equation of the third order. After integration under the condition $P \to 0$ when ξ tends to infinity, we get the second order differential equation

$$\tau c^2 P' + c\tau\theta[G(P)P']' - cP - G(P)P' = 0. \tag{21}$$

Thus, the problem is to approximate the forward semi-trajectory starting from $P(0)$ and approaching zero at infinity by the Padé approximant. Note that such solutions can be helpful for the description of moving fronts in models for heat and mass transfer [6].

To develop the Padé approximations for this solution, the conservation law is required. To derive it, we integrate equation (21) from 0 to infinity and arrive at the resulting relation

$$\int_0^\infty P d\xi = \left(-\tau c^2 - c\theta G(1)P'(0) + \int_0^1 G(x)dx\right)/c \equiv \Delta. \tag{22}$$

Using the approach described in Section 4, in the vicinity of the point $\xi = 0$, we look for the Taylor series expansion $P = 1 + \sum_{j=1}^N r_j\xi^j$ inserting it into relation (21). All coefficients r_j, $j \geq 2$, are the functions of $r_1 = P'(0)$ only. The Padé approximant now is written in the following form:

$$PA_{[M/M]} = \frac{\sum_{i=0}^M A_i\xi^i}{\sum_{j=0}^M B_j\xi^j} e^{H\xi},$$

where the multiplier $e^{H\xi}$ describes the asymptotic solution's behavior as $\xi \to \infty$. To evaluate H, we linearize equation (21) arriving to

$$\tau\theta P'' + (\tau c^2 - 1)P' - cP = 0,$$

and then the simplest solution vanishing at infinity is $e^{H\xi}$, where $H = (1 - \tau c^2 - \sqrt{(\tau c^2-1)^2 + 4\tau\theta c})/(2\tau\theta) < 0$.

The coefficients of the $PA_{[M/M]}$ nullify the relation for all ξ,

$$\sum_{j=0}^{2M} \frac{(H\xi)^j}{j!}\left(1 + \sum_{j=1}^M A_j\xi^j\right) - \left(1 + \sum_{j=1}^{2M} r_j\xi^j\right)\left(1 + \sum_{j=1}^M B_j\xi^j\right) = 0.$$

From this relation, the system of equations with respect to $2M$ variables A_j and B_j can be extracted. For instance, when $M = 1$, we obtain

$$A_1 - B_1 = r_1 - H, \qquad HA_1 - r_1B_1 = r_2 - H^2/2, \tag{23}$$

and at $M = 2$,

$$\begin{aligned} &A_1 - B_1 = r_1 - H, \qquad A_2 - r_1B_1 - B_2 + A_1H = r_2 + H^2/2, \\ &-r_2B_1 - r_1B_2 + A_2H + A_1H^2/2 = r_3 + H^3/6, \\ &-r_3B_1 - r_2B_2 + A_2H^2/2 + A_1H^3/6 = r_4 + H^4/24. \end{aligned} \tag{24}$$

Systems (23) and (24) are linear and consistent. Thus, they possess unique solutions.

After identifying Padé approximant (15), we insert it into the conservation law (22), where $P'(0) = r_1$, $G(1) = \frac{1+\beta_1}{1+2\beta_3+\beta_2}$ = const, and $\int_0^1 G(x)dx$ = const. The resulting integral equation serves for the evaluation of the unknown quantity r_1. It is hard to solve such an equation even numerically.

To overcome this, we use the analytical representations for the integral term. Specifically, for $M = 1$ or $M = 2$, the expression $\int_0^\infty P dx = \int_0^\infty PA_{[M/M]} dx$ can be derived analytically. Using the *Mathematica* command, we obtain

$$\int_0^\infty PA_{[1,1]} dx = \int_0^\infty e^{Hx} \frac{1 + A_1 x}{1 + B_1 x} dx = -\frac{A_1}{B_1 H} + \frac{A_1 - B_1}{B_1^2} \operatorname{Ei}\left(\frac{H}{B_1}\right) e^{-H/B_1}, \quad (25)$$

where Ei(·) is the exponential integral function. A similar, but a bit cumbersome expression can also be computed for $M = 2$. In this case, it is hard to derive the improper integral. Instead, the definite integral on the interval $[0, L]$ (L is large enough, $L = 4$ is used in this case) fits well.

5.1 Padé approximant construction

Now, consider the application of the approach we developed at the fixed parameters $\tau = 1$, $\theta = 1.5$, $c = 2.7$, and the initial condition $P(0) = 1$. The parameters $\beta_{1,2,3}$ for the function $G(p)$ coincide with (17).

To justify the existence of a trajectory vanishing at infinity, let us integrate equation (21) under the second initial condition for the derivative $P'(0)$, which varies in the range $[-2.218, -2.215]$ with the step 0.0005. The resulting bundle of solutions, depicted in the inset of Fig.3a, contains the trajectories unbounded from above and others – from below. Then we can conclude that a unique trajectory exists, vanishing at infinity at a certain $P'(0)$. To control the conservation law implementation, we also attach the equation $dY/d\xi = P(\xi)$ with the initial condition $Y(0) = 0$ to equation (21) and calculate the trajectory $Y(\xi)$ which approaches to Δ as $\xi \to \infty$, as shown in Fig. 3b.

The numerically evaluated trajectory is regarded as an "exact" solution with which we will compare its Padé approximant. Using the *Mathematica* command `NDSolve[·, Method → {"Shooting", "StartingInitialConditions" → {P[0] == 1, P'[0] == -1.7}`, the trajectory we are looking for is estimated with good accuracy (Fig.3a) providing $P'(0) = -2.21658 \equiv (r_1)_{ex}$.

Finally, when the coefficients of the Taylor series $r_{1,2,3,4}$ and Padé approximant A_1, B_1, and relation (25) are inserted into the conservation law (22), we arrive at the equation with respect to r_1 possessing the root $r_1 = -2.18753$. The corresponding Padé approximant is as follows:

$$PA_{[1/1]} = \frac{0.17637 + 0.94988\xi}{0.17637 + \xi} e^{H\xi}, \qquad H = -1.90335. \quad (26)$$

Proceeding in the same manner, we calculate the next $r_1 = -2.22365$ and the corresponding Padé approximant

$$PA_{[2/2]} = \frac{1 + 2.00241\xi + 1.16097\xi^2}{1 + 2.32541\xi + 0.28312\xi^2} e^{H\xi}. \quad (27)$$

Figure 3a exhibits the comparison of $PA_{[1/1]}$ (dashed line), $PA_{[2/2]}$ (crosses), and "exact" solution (solid curve). It is obvious that $PA_{[2/2]}$ is indistinguishable from the "exact" solution.

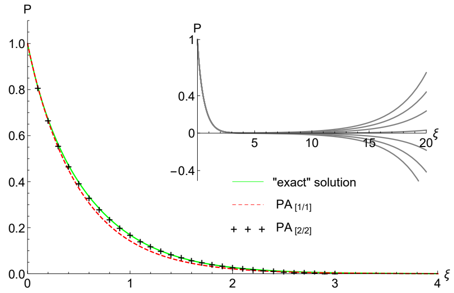

(a)

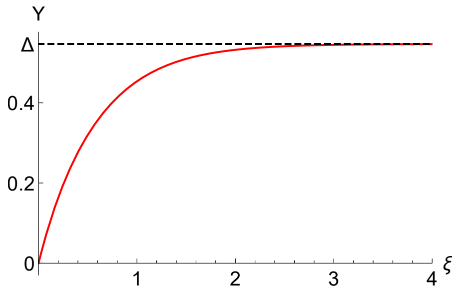

(b)

Figure 3: (a) The profiles of the solution of equation (21) and Padé approximants $PA_{[1/1]}$ and $PA_{[2/2]}$, defined by (26) and (27), respectively. The inset shows the bundle of trajectories starting from the initial conditions $P(0) = 1$ and $P'(0)$ from the range $[-2.218, -2.215]$. (b) The profile of $Y(\xi)$ describing the approach of a conservative quantity to its limit value Δ.

6 Conclusion

Thus, this research considered the nonlinear model describing the filtration of oil with variable viscosity in the semi-infinite domain. Model's nonlinearity was mostly determined by the quadratic pressure dependence of oil viscosity, the parameters of which were estimated from experimental data. The model incorporating the classical Darcy law possesses self-similar invariant solutions, which allow one to reduce the initial BVP to the nonlinear BVP for an ODE on a semi-infinite domain. The traveling wave solutions are considered when the filtration model is closed by the relaxation Darcy law. The research focused on the solutions vanishing at infinity. We developed the semi-analytical procedure for approximating the self-similar and traveling wave solutions utilizing the modified Padé approximant approach. The results of the procedure's application were compared with numerical solutions. It was shown that excellent results of approximation can be achieved even when using the low-order Padé approximations (up to the 3-rd order) in contrast to the use of conventional rational Padé approximations. Note also that the proposed procedure can be applied to the filtration equation with another form of hydraulic conductivity $D(p)$. Note also that the low order modified Padé approximants represent relatively simple and useful expressions for the model's solutions, which are preferable to use even when the exact but cumbersome solution exists. Moreover, quasi-rational approximations are indispensable when further manipulations on solutions are performed. Specifically, this is important for modeling well operation and liquid front propagation in porous media. Similar models and their solutions are also encountered in heat transfer theory [7, 16], demonstrating the multidisciplinary nature of the research.

Acknowledgment

The research is partly supported by the NAS of Ukraine, Project 0123U100183.

References

[1] I. Andrianov and A. Shatrov. Padé approximation to solve the problems of aerodynamics and heat transfer in the boundary layer. In: *Mathematical Theorems - Boundary Value*

Problems and Approximations (Ed.: L. Alexeyeva), Ch. 2. IntechOpen, 2020, 1–21.

[2] G. I. Barenblatt, V. M. Entov and V. M. Ryzhik. *The motion of fluids and gases in natural strata*. Moscow, Nedra Publishing House, 1984. [Russian]

[3] J. P. Boyd. Padé approximant algorithm for solving nonlinear ordinary differential equation boundary value problems on an unbounded domain. *Computers in Physics* **11** (3) (1997) 299 –303.

[4] A. Danesh. PVT tests and correlations. In: *PVT and Phase Behaviour of Petroleum Reservoir Fluids* (Ed.: A. Danesh), **47** Developments in Petroleum Science. Elsevier, 1998, 33–104.

[5] I. I. Denysiuk, I. A. Skurativska and I. M. Hubar. Attenuation of velocity fields during non-equilibrium filtration in a half-space medium for harmonic action on it. *J. Phys. Stud.* **27** (3) (2023) 3801.

[6] N. T. Fadai and M. J. Simpson. New travelling wave solutions of the porous–fisher model with a moving boundary. *J. Phys. A-Math.* **53** (2020) 095601.

[7] H. Fujita. The exact pattern of a concentration-dependent diffusion in a semi-infinite medium. Part III. *Textile Research Journal* **24** (3) (1954) 234–240.

[8] C. Guenoune, A. Bachmar and S. Boutechebak. A dynamic problem with wear involving thermoviscoelastic materials with a long memory. *Nonlinear Dyn. Syst. Theory* **24** (5) (2024) 473–484.

[9] D. F. Hays and H. N. Curd. Concentration-dependent diffusion in a semi-infinite medium. *J. Frank. Inst.* **283** (4) (1967) 300–307.

[10] C. R. Hocott and S. E. Buckley. Measurements of the viscosities of oils under reservoir conditions. *Transactions of the AIME* **142** (01) (1941) 131–136.

[11] K. Huber, J. Nowack and D. Göritz. Pervaporation of alcohols in PBT near the glass temperature: An analysis of the concentration-dependent diffusion. *J. Appl. Polym. Sci.* **68** (9) (1998) 1503–1515.

[12] J. Jäckle and H. L. Frisch. Properties of a generalized diffusion equation with a memory. *J. Chem. Phys.* **85** (1986) 1621–1627.

[13] A. M. Jasim, A. A. Ali, I. H. Halil, F. Z. Ahmed and M. A. Shallal. Numerical solution for Benjamin-Bona-Mahony-Burgers equation using septic b-spline Galerkin method *Nonlinear Dyn. Syst. Theory* **24** (3) (2024) 267–274.

[14] B. Khuzhayorov, J. Auriault and P. Royer. Derivation of macroscopic filtration law for transient linear viscoelastic fluid flow in porous media. *Int. J. Engineering Science* **38** (5) (2000) 487–504.

[15] N. A. Kudryashov, M. B. Kochanov and V. L. Savatorova. Approximate self-similar solutions for the boundary value problem arising in modeling of gas flow in porous media with pressure dependent permeability. *Appl. Math. Model.* **37** (7) (2013) 5563–5573.

[16] A. V. Lykov. *Theory of Heat Conduction.* Moscow, Vysshaya Shkola, 1967. [Russian]

[17] Y. V. Mikhlin and G. V. Manucharyan. Construction of homoclinic and heteroclinic trajectories in mechanical systems with several equilibrium positions. *Chaos, Solitons and Fractals* **16** (2) (2003) 299–309.

[18] S. Skurativskyi and I. Skurativska. Solutions of the model of liquid and gas filtration in the elastic mode with dynamic filtration law. *Ukr. J. Phys.* **64** (1) (2019) 19–26.

[19] J. Philip. General method of exact solution of the concentration-dependent diffusion equation. *Aust. J. Phys.* **13** (1960) 1–12.

[20] L. F. Shampine. Exact solutions for concentration dependent diffusion and the inverse complementary error function. *J. Frank. Inst.* **295** (3) (1973) 239–247.

Nonlinear Dynamics and Systems Theory, **25** (6) (2025) 691–704

Fokker-Planck Equation and Its Application in Production Function

S. Sutrima [1*], S. Siswanto [1], S. Wibowo [1] and C.R. Indrati [2]

[1] *Department of Mathematics, Sebelas Maret University, Surakarta, Indonesia,*
[2] *Department of Mathematics, Gadjah Mada University, Yogyakarta, Indonesia.*

Received: February 17, 2025; Revised: November 11, 2025

Abstract: The one-dimensional Fokker-Planck equation (FPE) with drift and diffusion coefficients depending on the space variable is identified by a semigroup approach. The stationary solution u_s of the FPE induces a Hilbert space X, i.e., $L^2(a,b)$ with an inner product weighted by u_s. The backward Fokker-Planck operator A generates a C_0-semigroup in X. The well-posedness for the FPE follows the well-posedness for the Cauchy problem generated by A. The solution u is asymptotically stable with respect to u_s as $t \to \infty$. Furthermore, if the ratio of the drift to diffusion coefficients is nondecreasing, then u is a nonnegative classical solution. As an application, the backward Fokker-Planck operator A confirms the well-posedness for production function equations. In case $X = L^2(0,\infty)$, the operator A has a continuous spectrum generating the Gaus-Weierstrass semigroup.

Keywords: *Fokker-Planck equation; stationary solution; C_0-semigroup; well-posed; production function.*

Mathematics Subject Classification (2020): 35K57, 35Q84, 47D07, 70K20,93-10.

1 Introduction

The Fokker-Planck equation (FPE) which originally describes a Brownian motion of a particle has wide applications leading to many interdisciplinary studies, for example, in solid state physics, quantum optics, chemical physics, theoretical biology, circuit theory, plasma waves, finance and economics. Concretely, the applications of the FPEs are found in differential equations and stochastic processes [1, 2], bilinear control systems

* Corresponding author: mailto:sutrima@mipa.uns.ac.id

and chaotic systems [3, 4], production and generation of entropies [5–7], plasma physics, protein folding and fluid [8–10].

There has been a lot of theoretical and numerical research discussing the FPE for various cases and applications. Bluman [11] proposed to construct the exact solutions for the one-dimensional FPE corresponding to a class of non-linear forcing functions using group theoretic methods. A particle approach to solve variational formulation of the FPE with decay was considered in [12]. The analytical solution of the FPE with logarithmic, decreasing and bistable drifts has been investigated in [13–15]. See also the numerical research of the FPE using He's variational iteration method [16], the differential transform method [17], the cubic B-spline scaling functions [18], the Adomian decomposition method [19], and the homotopy perturbation method [20].

The generic form of the one-dimensional FPE for the probability density $u(x,t)$ depending on the space variable x and time t is given by

$$\frac{\partial u}{\partial t} = -\frac{\partial}{\partial x}\left[f(x,t)u\right] + \frac{\partial^2}{\partial x^2}\left[\frac{D(x,t)}{2}u\right] \tag{1}$$

with the initial condition

$$u(x,0) = u_0(x), \quad x \in \mathbb{R},$$

where $u(x,t)$ is the unknown function, $f(x,t)$ is the drift coefficient or force, and $D(x,t) > 0$ is the diffusion coefficient [21]. Equation (1) describes a motion for the distribution function $u(x,t)$ and is called the forward Kolmogorov equation. Also, a similar equation, the backward Kolmogorov equation, is given by

$$\frac{\partial u}{\partial t} = -f(x,t)\frac{\partial u}{\partial x} + \frac{D(x,t)}{2}\frac{\partial^2 u}{\partial x^2}. \tag{2}$$

The special case of FPE (1) provides the distribution function $W(v,t)$ for a small particle of mass m immersed in a fluid satisfying

$$\frac{\partial W}{\partial t} = \gamma\frac{\partial(vW)}{\partial v} + \gamma\frac{KT}{m}\frac{\partial^2 W}{\partial v^2},$$

where v is the velocity for the Brownian motion of a particle, t is the time, γ is the fraction constant, K is Boltzmann's constant and T is the temperature of fluid [21]. In this case, the drift coefficient is linear and the diffusion coefficient is a constant.

We note that the partial differential equations in (1) and (2) are nonlinear-parabolic. This nonlinearity affects the difficulties in solving the equations, either theoretically or numerically. For the linear case, the well-posedness for the equations follows Theorems 12, 15 and 16 in Chapter I of [22]. However, we can not explicitly find the sufficiency and necessity of the well-posedness from the theorems. We see that the linearities of the FPE depend on the type of drift and diffusion coefficients. In the fact, if the drift and diffusion coefficients do not depend on u, the equations are linear. The FPE of this type are involved in the advection-diffusion equations, see [23, 24]. This allows us to formulate the FPE as an autonomous or non-autonomous abstract Cauchy problem. In this context, the C_0-semigroup or C_0-quasi semigroup approach has proven to be reliable for solving the problems, which have not been discussed in previous studies. Therefore, the infinitesimal generator of the C_0-semigroup or C_0-quasi semigroup can characterize the well-posedness and the properties of solution of the problems.

In this paper, we focus on the well-posedness and the properties of solution of FPE (1), where the drift and diffusion coefficients depend only on the space variable x, and the use of C_0-semigroup approach and its application in the product function given in [23]. The organization of the results is as follows. Section 2 provides the well-posedness and some properties of the solution of FPE (1) equipped with the boundary values. In Section 3, we apply the FPE to solve the product function in two cases of the spectrum of the infinitesimal generator of the related semigroup.

2 Solution of Fokker-Planck equation

In this paper, we study the Fokker–Planck equation in one dimension in a bounded interval with boundary conditions. Let X_t be a diffusion process in the interval $[0,\ell]$ with the drift and diffusion coefficients $f(x)$ and $D(x)$, respectively. We assume that $D(x)$ is positive in $[0,\ell]$. The transition probability density $u(x,t)$ is the solution of an initial and boundary value problem of the FPE

$$\frac{\partial u}{\partial t} = -\frac{\partial}{\partial x}\left[f(x)u\right] + \frac{\partial^2}{\partial x^2}\left[\frac{D(x)}{2}u\right], \quad 0 < x < \ell, \tag{3a}$$

with the boundary and initial conditions

$$J(u(0)) = J(u(\ell) = 0, \tag{3b}$$

$$u(x,0) = u_0(x), \quad 0 \le x \le \ell, \tag{3c}$$

where

$$J(u) := f(x)u(x) - \frac{1}{2}\frac{d}{dx}\left[D(x)u(x)\right], \quad 0 \le x \le \ell.$$

We can rewrite problem (3) as a Cauchy problem and use a strongly continuous semigroup (C_0-semigroup) to solve. Indeed, problem (3) is the Cauchy problem

$$\dot{u}(t) = \mathcal{A}u(t), \quad t \ge 0, \qquad u(0) = u_0, \tag{4}$$

where $\mathcal{A}$ is a generator of the Fokker–Planck (forward Kolmogorov) equation (3) that is defined by

$$\mathcal{A}u := -\frac{d}{dx}\left[f(x)u\right] + \frac{1}{2}\frac{d^2}{dx^2}\left[D(x)u\right] \tag{5}$$

on a domain

$$\mathcal{D}(\mathcal{A}) := \{u \in C^2(0,\ell) : J(u(0)) = J(u(\ell)) = 0\}.$$

Henceforth, we call the generator $\mathcal{A}$ the Fokker-Planck operator.

To solve the Fokker–Planck problem (3), we first transform the equation into the backward Kolmogorov equation generated by an operator A. Note that the boundary conditions for the operator A are simpler than those for the operator $\mathcal{A}$. Due to this fact, we first find the stationary solution of problem (3). Let $u_s(x)$ be the stationary solution of (3), i.e., the long-time limit of $u(x,t)$ as $t \to \infty$, which follows from the equation

$$-\frac{d}{dx}\left[f(x)u_s(x) - \frac{1}{2}\frac{d}{dx}\left[D(x)u_s(x)\right]\right] = 0.$$

Integrating the both sides with respect to x yields $J(u_s) = C$ for some constant C. However, the boundary conditions give a zero flux

$$J(u_s) = f(x)u_s(x) - \frac{1}{2}\frac{d}{dx}\left[D(x)u_s(x)\right] = 0. \tag{6}$$

Therefore, we have

$$\frac{2f(x)}{D(x)}dx = \frac{du_s(x)}{u_s(x)} + \frac{dD(x)}{D(x)}$$

that gives the stationary solution

$$u_s(x) = N^{-1}Y(x), \quad x \in [0, \ell], \tag{7}$$

where

$$Y(x) = \frac{1}{D(x)} \exp\left(2\int_0^x \frac{f(\tau)}{D(\tau)}d\tau\right)$$

and N is the normalization constant,

$$N = \int_0^\ell \frac{1}{D(x)} \exp\left(2\int_0^x \frac{f(\tau)}{D(\tau)}d\tau\right) dx.$$

Further, from (6), if $u = vu_s$, we have

$$J(u) = J(vu_s) = -\frac{1}{2}D(x)u_s(x)\frac{dv}{dx}.$$

This confirms that if $J(u(0)) = J(u(\ell)) = 0$, then $v'(0) = v'(\ell) = 0$. Therefore, when setting $u(x,t) = v(x,t)u_s(x)$, the problem (3) leads to the Cauchy problem

$$\dot{v}(t) = Av(t), \quad t \geq 0, \qquad v(0) = v_0(x) = u_s^{-1}(x)u_0(x), \tag{8}$$

where A generates the backward Kolmogorov equation given by

$$Av := f(x)\frac{dv}{dx} + \frac{D(x)}{2}\frac{d^2v}{dx^2} \tag{9}$$

on the domain $\mathcal{D}(A) = \{v \in C^2(0,\ell) : v'(0) = v'(\ell) = 0\}$. In other words, solving problem (3) is sufficient to solve problem (8). The sufficiency for the Cauchy problem (8) is well-posed is that A is the infinitesimal generator of a C_0-semigroup.

Lemma 2.1 *If $u(x) = v(x)u_s(x)$ for $v \in \mathcal{D}(A)$, then $\mathcal{A}u = u_sAv$ and both have common eigenvalues.*

Proof. For $u(x) = v(x)u_s(x)$ and from (6), we obtain

$$\begin{aligned}
\mathcal{A}u &= \frac{d}{dx}\left[-f(x)v(x)u_s(x) + \frac{1}{2}\frac{d}{dx}\left[D(x)v(x)u_s(x)\right]\right] \\
&= \frac{d}{dx}\left[\left[-f(x)u_s(x) + \frac{1}{2}\frac{d}{dx}[D(x)u_s(x)]\right]v(x) + \frac{1}{2}[D(x)u_s(x)]\frac{dv}{dx}\right] \\
&= \frac{1}{2}\frac{d}{dx}[D(x)u_s(x)]\frac{dv}{dx} + \frac{1}{2}[D(x)u_s(x)]\frac{d^2v}{dx^2} \\
&= u_s(x)\left[f(x)\frac{dv}{dx} + \frac{D(x)}{2}\frac{d^2v}{dx^2}\right] = u_sAv.
\end{aligned}$$

Therefore, if λ is an eigenvalue of $\mathcal{A}$ corresponding to the eigenfunction u, then λ is the eigenvalue of A with the eigenfunction v.

Henceforth, let X be the Hilbert space $L^2(0,\ell)$, the space of square-integrable functions in the interval $(0,\ell)$, with respect to the weighted inner product

$$\langle v, w\rangle_{u_s} := \int_0^\ell v(x)w(x)u_s(x)\,dx.$$

The operator A in the Hilbert space X gives the following.

Lemma 2.2 *The operator A has the following properties:*

(a) $-A$ is a positive operator on X.

(b) The null space of A consists of constants.

(c) A is self-adjoint with a discrete spectrum in the Hilbert space X.

Proof. (a) Using an integration by parts and the fact that the stationary solution u_s is positive, for $v \in \mathcal{D}(A)$, we obtain

$$\langle -Av, v\rangle_{u_s} = \int_0^\ell (-Av)vu_s\,dx = \int_0^\ell -\mathcal{A}(u_s)v\,dx = \frac{1}{2}\int_0^\ell |v'|^2 Du_s\,dx. \tag{10}$$

Therefore, $-A$ is positive.

(b) Let v be in the null space of A. From (10), we deduce that

$$\int_0^\ell |v'|^2 Du_s\,dx = 0.$$

Since $u_s, D > 0$, this implies that v is a constant.

(c) For all $v, w \in \mathcal{D}(A)$, again using the integration by parts and the stationary solution, we obtain

$$\int_0^\ell v\mathcal{A}(wu_s)\,dx = \left[\frac{Du_s}{2}\left(vw' - wv'\right)\right]_0^\ell + \int_0^\ell \left(fv' + \frac{D}{2}v^{''}\right)wu_s\,dx = \int_0^\ell Avwu_s\,dx.$$

Therefore, Lemma 2.1 gives the self-adjointness of A,

$$\langle Av, w\rangle_{u_s} = \int_0^\ell Avwu_s\,dx = \int_0^\ell v\mathcal{A}(wu_s)\,dx = \int_0^\ell vAwu_s\,dx = \langle v, Aw\rangle_{u_s}.$$

Since A is self-adjoint in the Hilbert space $L^2(0,\ell)$, where $[0,\ell]$ is a bounded interval, A has a discrete spectrum [28]. Moreover, the eigenvalues λ_n of $-A$ are real and nonnegative such that $0 = \lambda_0 < \lambda_1 < \lambda_2 < \cdots$. Also, the eigenfunctions ϕ_n corresponding to the eigenvalues λ_n form an orthonormal basis in X. From (b), we obtain that $\lambda_0 = 0$ corresponds to $\phi_0 = 1$.

As a consequence of Lemma 2.2, the Fokker-Planck operator $\mathcal{A}$ is nonpositive, self-adjoint with discrete spectrum and its null space is the one-dimensional space with the basis $\{u_s\}$.

Theorem 2.1 *The operator A generates a contraction of C_0-semigroup $T(t)$ given by*

$$[T(t)v](x) = \sum_{n=0}^{\infty} e^{-\lambda_n t}\langle v, \phi_n\rangle_{u_s}\phi_n(x), \quad v \in L^2(0,\ell). \tag{11}$$

Proof. Since A is self-adjoint, A is a closed operator. Thus, A is the Riesz spectral operator with real eigenvalues $-\lambda_n$ such that $\sup\{-\lambda_n : n \in \mathbb{N}_0\} = 0 < \infty$, where $\mathbb{N}_0 = \mathbb{N} \cup \{0\}$. Therefore, A is the infinitesimal generator of the C_0-semigroup $T(t)$ given by (11), Theorem 2.3.5 of [25]. Furthermore, since $\{\phi_n\}$ are orthonormal, for $v = \phi_n$, (11) gives

$$T(t)\phi_n = e^{-\lambda_n t}\phi_n \qquad \text{or} \qquad \|T(t)\| \leq 1, \quad t \geq 0,$$

i.e., $T(t)$ is a contraction.

Theorem 2.2 *The Fokker-Planck problem* (3) *is well-posed. Moreover, for any initial condition u_0, the solution $u(x,t)$ satisfies*

$$\lim_{t\to\infty} u(x,t) = \gamma_0 u_s(x),$$

where $\gamma_0 = \int_0^\ell u_0(x)\,dx$.

Proof. Since the operator A generates a C_0-semigroup in X, the Cauchy problem (8) is well-posed with a solution $v(x,t) = T(t)v_0(x)$. This implies the well-posedness of the Fokker-Planck problem (3) with the solution

$$u(x,t) = u_s(x)[T(t)u_s^{-1}u_0](x). \tag{12}$$

Moreover, the equations (11) and (12) give

$$u(x,t) = \gamma_0 u_s(x) + \sum_{n=1}^{\infty} e^{-\lambda_n t}\left[\int_0^\ell u_0(\tau)\phi_n(\tau)\,d\tau\right] u_s(x)\phi_n(x),$$

where $\gamma_0 = \int_0^\ell u_0(x)\,dx$. Since all $\lambda_n > 0$ for $n \geq 1$, this implies that $u(x,t)$ converges to $\gamma_0 u_s(x)$ as $t \to \infty$.

Theorem 2.3 *If $u_0(x) \geq 0$ and the ratio of the drift and diffusion $r(x) = \frac{f(x)}{D(x)}$ is nondecreasing in $(0,\ell)$, then the Fokker-Planck problem* (3) *has a uniquely nonnegative classical solution.*

Proof. The uniqueness follows the uniqueness of the solution of the Cauchy problems. To prove the nonnegativity of the solution, we set $u = \exp(\int_0^x \frac{f-2D'}{2D})v$ and substitute in equation (3), which leads to

$$v_t - Dv_{xx} + \frac{D}{2}\left[\frac{d}{dx}\left(\frac{f}{D}\right) + \frac{1}{2}\left(\frac{f}{D}\right)^2\right] v \equiv 0. \tag{13}$$

The nondecreasing of the ratio r implies that $r'(x) \geq 0$ for all $x \in (0,\ell)$. This imposes the coefficient of v in (13) is nonnegative. Consequently, by the maximum principle (Lemma 4.1, p. 19 of [26]), the solution v is nonnegative. The nonnegativity of u follows.

Corollary 2.1 *If f and D are constants, the solution of* (3) *is*

$$u(x,t) = \gamma_0 u_s(x) + \sum_{n=1}^{\infty} e^{\lambda_n t + \frac{f}{D}x}\left[\alpha_n \cos\frac{n\pi}{\ell}x + \beta_n \sin\frac{n\pi}{\ell}x\right], \tag{14}$$

where

$$\alpha_n = \frac{2N_0}{\ell}\int_0^\ell [u_0(\tau) - \gamma_0 u_s(\tau)] \exp\left(-\frac{f}{D}\tau\right) \cos\frac{n\pi}{\ell}\tau \, d\tau,$$
$$\beta_n = \frac{2N_0}{\ell}\int_0^\ell [u_0(\tau) - \gamma_0 u_s(\tau)] \exp\left(-\frac{f}{D}\tau\right) \sin\frac{n\pi}{\ell}\tau \, d\tau.$$

If f and D are constants, the stationary solution of (3) is $u_s(x) = N_0^{-1}\exp\left(\frac{2f}{D}x\right)$, where $N_0 = \int_0^\ell \exp\left(\frac{2f}{D}x\right) dx$ and the eigenvalues and eigenfunctions of A are given by

$$\lambda_0 = 0, \qquad \lambda_n = -\frac{1}{2}\left(\frac{n^2\pi^2 D}{\ell^2} + \frac{f^2}{D}\right),$$
$$\phi_0(x) = 1, \qquad \phi_n(x) = e^{-\frac{f}{D}x}\left[A_n \cos\frac{n\pi}{\ell}x + B_n \sin\frac{n\pi}{\ell}x\right], \quad n \geq 1,$$

respectively, where A_n and B_n are constants such that $\int_0^\ell \phi_n(x)\, dx = 1$. By solving the Fourier coefficients, the solution (12) gives the solution (14). Moreover, we verify that Theorems 2.2 and 2.3 are valid for this solution.

3 An Application to Production Function

In micro economics, a technical relationship between physical inputs (land, labour, capital) and physical outputs (quantity produced) is described by the production function. The relationship is not an economic relationship, but only studies the relationship of material inputs on one side and material outputs on the other side. The production function is denoted by $F = F(L(\tau), K(\tau))$, where $L(\tau)$ and $K(\tau)$ are the quantities of labour and capital at time τ in the time interval $[0, \mathrm{T}]$, respectively. Henceforth, we assume that the production function F is homogenous of degree one. Let $x(\tau) = K(\tau)/L(\tau)$ and $y = u(x(\tau), \tau)$, and we also assume that $x(\tau)$ is the solution to the following stochastic differential equation:

$$dx(\tau) = x(\tau)[a d\tau + b d\omega(\tau)], \tag{15}$$

where $\omega(\tau)$ is a standard Brownian motion, a and b are constants. Let $u(x, \tau)$ denote the value of the production function at any instant τ, $\tau \geq 0$. Using Ito's lemma [27], we have

$$du = \frac{\partial u}{\partial \tau}d\tau + \frac{\partial u}{\partial x}dx + \frac{1}{2}\frac{\partial^2 u}{\partial x^2}dx^2. \tag{16}$$

Putting (15) and (16) together, we find that

$$du = \left[\frac{\partial u}{\partial \tau} + ax\frac{\partial u}{\partial x} + \frac{b^2}{2}x^2\frac{\partial^2 u}{\partial x^2}\right] d\tau + bx\frac{\partial u}{\partial x}d\omega(\tau). \tag{17}$$

We assume that the production function can be written as

$$u(x, \tau) = u_d(x, \tau) + \Delta x(\tau), \tag{18}$$

where Δ is unknown to be determined such that

$$du_d(x, \tau) = r u_d(x, \tau) d\tau$$

and r is a real positive constant. If $\Delta = \frac{\partial u}{\partial x}$, then the stochastic term vanishes, and we obtain

$$\frac{\partial u}{\partial \tau} + ax\frac{\partial u}{\partial x} + \frac{b^2}{2}x^2\frac{\partial^2 u}{\partial x^2} - ru = 0.$$

This is a linear second-order partial differential equation. Under the change of variable $t = \frac{b^2(\mathrm{T}-\tau)}{2}$ and equipped an initial value, it becomes

$$\begin{aligned} \frac{\partial u}{\partial t} &= x^2\frac{\partial^2 u}{\partial x^2} + \gamma x\frac{\partial u}{\partial x} - \gamma u, \\ u(x,0) &= u_0(x), \end{aligned} \tag{19}$$

where $\gamma := \frac{2r}{b^2}$.

Let $\mathcal{L}$ be a linear operator defined on the Hilbert space $X = L^2(a,b)$ by

$$(\mathcal{L}u)(x) := x^2u^{''}(x) + \gamma xu'(x) - \gamma u(x) \tag{20}$$

on the domain

$$\mathcal{D}(\mathcal{L}) = \{u \in X : u, u' \text{ are absolute continuous and } u', u^{''} \in X\}.$$

The initial problem (19) can be written as a Cauchy problem in X

$$\begin{aligned} u_t &= \mathcal{L}u,\ t > 0, \\ u(0) &= u_0, \qquad u_0 \in X. \end{aligned} \tag{21}$$

The sufficient condition for well-posedness for the Cauchy problem (21) is that $\mathcal{L}$ is the infinitesimal generator of a C_0-semigroup in X. We note that the operator $\mathcal{L}$ is composed to be

$$\mathcal{L} = A - \gamma I,$$

where A is the backward Fokker-Planck operator given in (9) with $f(x) = \gamma x$ and $D(x) = 2x^2$. The main aim is to prove the operator $\mathcal{L}$ defined in (20) generates a C_0-semigroup. The form of the semigroup depends on the type of the spectrum of $\mathcal{L}$ or A, i.e., discrete or continuous spectrum.

3.1 The infinitesimal generator with discrete spectrum

We see that if the initial problem (19) works on the finite boundary values, then $\mathcal{L}$ has the discrete spectrum [28]. In this case, we assume the dynamics of production $u(x,t)$ is described by the Dirichlet boundary problem on $X = L^2(1,\ell)$, $\ell > 1$,

$$\begin{aligned} u_t &= \mathcal{L}u, \quad 1 < x < \ell,\ t > 0, \\ u(1,t) &= u(\ell,t) = 0,\ t > 0, \\ u(x,0) &= u_0(x), \quad 1 \le x \le \ell. \end{aligned} \tag{22}$$

In this subsection, we assume $\gamma \neq 1$. First, we consider the Cauchy problem generated by the backward Fokker-Planck operator A in X

$$\begin{aligned} u_t &= Au, \quad 1 < x < \ell,\ t > 0, \\ u(1,t) &= u(\ell,t) = 0,\ t > 0, \\ u(x,0) &= u_0(x), \quad 1 \le x \le \ell. \end{aligned} \tag{23}$$

In this case, the stationary solution of the forward Fokker-Planck equation is

$$u_s(x) = \frac{1}{2N} x^{\gamma-2}, \quad 1 \le x \le \ell, \tag{24}$$

where $N = (\ell^{\gamma-1} - 1)/2(\gamma - 1)$. We can find out that the eigenvalues and eigenfunctions of A are

$$\begin{aligned} \lambda_n &= -\left(\frac{n\pi}{\ln \ell}\right)^2 - \left(\frac{\gamma-1}{2}\right)^2, \\ \phi_n(x) &= 2x^{-(\gamma-1)/2} \sqrt{\frac{N}{\ln \ell}} \sin\left(\frac{n\pi}{\ln \ell} \ln x\right), \quad n \in \mathbb{N}, \end{aligned} \tag{25}$$

respectively. Therefore, the C_0-semigroup $T(t)$ generated by A in (11) is given by

$$(T(t)v)(x) = \sum_{n=1}^{\infty} e^{\lambda_n t} \langle v, \phi_n \rangle_{u_s} \phi_n(x), \quad v \in L^2(1, \ell), \tag{26}$$

where λ_n and ϕ_n are the eigenvalues and eigenfunctions, respectively, given in (25) and the weighted inner product $\langle \cdot, \cdot \rangle_{u_s}$ in $L^2(1, \ell)$ with respect to u_s is given in (24).

By the theorem on the perturbation for the semigroups and the fact that $\mathcal{L} = A - \gamma I$, the operator $\mathcal{L}$ is the infinitesimal generator of the C_0-semigroup $S(t)$ given by

$$S(t) = e^{-\gamma t} T(t),$$

where $T(t)$ is given in (26). Theorem 3.6 of [29] implies that the dynamics of production inducted by $\mathcal{L}$ has a unique solution

$$u(x,t) = (S(t)u_0)(x) = \sum_{n=1}^{\infty} e^{(\lambda_n - \gamma)t} \langle u_0, \phi_n \rangle_{u_s} \phi_n(x).$$

Therefore, we have the following result.

Theorem 3.1 *The dynamics of production $u(x,t)$ described by the Cauchy problem* (22) *is well-posed.*

Remark 3.1 The forward Fokker-Planck problem corresponding to the operator A is

$$\begin{aligned} &\frac{\partial u}{\partial t} = -\frac{\partial}{\partial x}\left[\gamma x u\right] + \frac{\partial^2}{\partial x^2}\left[x^2 u\right], \quad 1 < x < \ell, \\ &J(u(1)) = J(u(\ell)) = 0, \\ &u(x,0) = u_0(x), \quad 1 \le x \le \ell, \end{aligned} \tag{27}$$

where

$$J(u(x)) = \gamma x u(x) - \frac{d}{dx}\left[x^2 u(x)\right], \quad 1 \le x \le \ell.$$

In particular, if we choose $\ell = e$ and $u_0(x) = \delta x^\alpha$, $\alpha \in (0,1)$, $\delta > 0$, Theorem 2.2 confirms that the solution of problem (27) is

$$u(x,t) = \gamma_0 u_s(x) + \sum_{n=1}^{\infty} \gamma_n e^{\lambda_n t} u_s(x) \phi_n(x), \quad 1 \le x \le e,$$

where u_s is given in (24) and

$$\gamma_0 = \frac{\delta(e^{\alpha-1}-1)}{\alpha-1},$$
$$\gamma_n = \frac{[1-(-1)^n e^{\nu}]\delta n\pi}{(\nu^2+n^2\pi^2)\sqrt{N}}, \qquad \nu = \frac{\gamma-1}{2}+\alpha,$$
$$\lambda_n = -n^2\pi^2 - \left(\frac{\gamma-1}{2}\right)^2,$$
$$\phi_n(x) = 2x^{-(\gamma-1)/2}\sqrt{N}\sin(n\pi\ln x).$$

Therefore, since $\lambda_n < 0$ for all $n \geq 1$, we have

$$\lim_{t\to\infty} u(x,t) = \gamma_0 u_s(x).$$

3.2 The infinitesimal generator with a continuous spectrum

Now, we consider the dynamics of production $u(x,t)$ of the Cauchy problem (19) in the Hilbert space $X = L^2(0,\infty)$,

$$\begin{aligned} u_t &= \mathcal{L}u, \quad x \geq 0,\ t > 0, \\ u(x,0) &= u_0(x) = \begin{cases} \delta e^{\alpha x}, & 0 \leq x \leq \ell \\ 0, & x > \ell, \end{cases} \end{aligned} \tag{28}$$

where $\alpha \in (0,1)$, $\delta > 0$, and $\ell > 0$. As before, we must prove that the operator $\mathcal{L}$ generates a C_0-semigroup. However, in this context, the spectrum of A in the form $\mathcal{L} = A - \gamma I$ is not discrete. Also, the corresponding forward Fokker-Planck equation does not have the stationary solution since the integral in (7) diverges. Indeed, the operator A has a continuous spectrum, so we can not apply the method used in the above section. For this purpose, first, we define the linear operator

$$(Vu)(x) := xu'(x) + \mu u(x), \qquad \mu = \tfrac{1}{2}(\gamma-1)$$

on the domain

$$\mathcal{D}(V) = \{u \in X : u \text{ is absolute continuous and } u' \in X\}.$$

We can check that
$$A = V^2 - \mu^2 I = (V-\mu I)(V+\mu I).$$

This implies that the spectrum of A depends on the spectrum of operators $(V-\mu I)$ and $(V+\mu I)$.

Lemma 3.1 *The operator A in* (20) *has a continuous spectrum in* $\mathbb{R}$.

Proof. We see that the resolvent operator $\mathcal{R}(\lambda, V+\mu I)$ exists only if the equation $(\lambda I - (V+\mu I))u = f$ has a unique solution. By the variation of constants formula, we find the resolvent operator given by $H : X \to X$,

$$(Hu)(x) := x^{\lambda-\gamma+1}\int_x^\infty \frac{u(s)}{s^{\lambda-\gamma+2}}ds, \quad u \in X, \quad \lambda > \gamma.$$

We need to show that the operator H is well-defined and bounded. We note that

$$
\begin{aligned}
|(Hu)(x)|^2 &\le x^{2(\lambda-\gamma+1)} \left(\int_x^\infty \frac{|u(s)|}{s^{\lambda-\gamma}} \frac{s^{\lambda-\gamma}}{s^{\lambda-\gamma+2}} \right)^2 \\
&\le x^{2(\lambda-\gamma+1)} \int_x^\infty \frac{|u(s)|^2}{s^{2(\lambda-\gamma)}} ds \int_x^\infty \frac{s^{2(\lambda-\gamma)}}{s^{2(\lambda-\gamma)+4}} ds = \frac{1}{3} \int_x^\infty \frac{|u(s)|^2}{s^{2(\lambda-\gamma)}} x^{2(\lambda-\gamma)-1} ds.
\end{aligned}
$$

Therefore,

$$
\begin{aligned}
\|Hu\|_2^2 &= \int_0^\infty |(Hu)(x)|^2 dx \\
&\le \frac{1}{3} \int_0^\infty \int_x^\infty \frac{|u(s)|^2}{s^{2(\lambda-\gamma)}} x^{2(\lambda-\gamma)-1} ds dx \\
&= \frac{1}{3} \int_0^\infty \int_0^s \frac{|u(s)|^2}{s^{2(\lambda-\gamma)}} x^{2(\lambda-\gamma)-1} dx ds = \frac{1}{6(\lambda-\gamma)} \|u\|_2^2.
\end{aligned}
$$

Thus H is well-defined and bounded when $\lambda > \gamma$. Moreover, we have $Hu \in \mathcal{D}(V)$ and

$$((V + \mu I)Hu)(x) = x(Hu)'(x) + 2\mu(Hu)(x) = -u(x) + \lambda(Hu)(x)$$

for all $u \in X$, and

$$(H(V + \mu I)u)(x) = (H(xu'))(x) + 2\mu(Hu)(x) = -u(x) + \lambda(Hu)(x)$$

for all $u \in \mathcal{D}(V)$. This proves that the resolvent operator $\mathcal{R}(\lambda, V + \mu I)$ exists and equals to H with $\rho(V + \mu I) = (\gamma, \infty)$.

Similarly, we can show that $\rho(V - \mu I) = (0, \infty)$. Therefore, the resolvent set $\rho(A) = (\tau, \infty)$, where $\tau = \max\{0, \gamma\}$. Thus, the spectrum $\sigma(A) = \mathbb{R} - \rho(A)$ is not discrete.

Since the spectrum $\sigma(A)$ is not discrete, we can not use the expansion of the eigenfunctions to solve the Cauchy problem (28). Using the concept of the fundamental solution for the diffusive equations, we can construct the Gaus-Weierstrass semigroup for the Cauchy problem (28), see [30].

Theorem 3.2 *The operator $\mathcal{L}$ is the infinitesimal generator of the C_0-semigroup $T(t)$ given by $T(0) = I$ and*

$$(T(t)u)(x) = \frac{e^{-\gamma t}}{\sqrt{4\pi t}} \int_{-\infty}^\infty \exp\left(-\frac{(\ln x + (\gamma - 1)t - s)^2}{4t} \right) u(s)\, ds, \quad t > 0. \tag{29}$$

Moreover, the Cauchy problem (28) is well-posed in X.

Proof. Substitution $x = e^\xi$ reduces the operator A to be the differential operator with constant coefficients

$$A_0 u := u_{\xi\xi} + (\gamma - 1)u_\xi.$$

Following Example 1.8 of [30] and returning the substitution, we see that the operator A generates a C_0-semigroup $T_0(t)$ given by $T_0(0) = I$ and

$$(T_0(t)u)(x) = \frac{1}{\sqrt{4\pi t}} \int_{-\infty}^\infty \exp\left(-\frac{(\ln x + (\gamma - 1)t - s)^2}{4t} \right) u(s)\, ds, \quad t > 0. \tag{30}$$

Thus, the operator $\mathcal{L}$ is the infinitesimal generator of the C_0-semigroup $T(t)$ given by

$$T(t) = e^{-\gamma t} T_0(t), \quad t \geq 0.$$

Further, from Theorem 3.6 of [29], the Cauchy problem (28) is well-posed with the solution $u(x,t) = (T(t)u_0)(x)$, $u_0 \in X$. Indeed,

$$\begin{aligned} u(x,t) &= \frac{\delta e^{-\gamma t}}{\sqrt{4\pi t}} \int_{-\infty}^{\infty} \exp\left(-\frac{(\ln x + (\gamma-1)t - s)^2}{4t} + \alpha s \right) ds, \\ &= \frac{\delta x^{\alpha} e^{-(\alpha+(1-\alpha)\gamma)t}}{\sqrt{\pi}} \int_{-\infty}^{\infty} e^{-(z^2+2\alpha\sqrt{t}z)} dz, \qquad z = \frac{\ln x + (\gamma-1)t - s}{2\sqrt{t}} \\ &= \frac{\delta x^{\alpha} e^{-(1-\alpha)(\alpha+\gamma)t}}{\sqrt{\pi}} \int_{-\infty}^{\infty} e^{-(z+\alpha\sqrt{t})^2} dz, \\ &= \delta x^{\alpha} e^{-(1-\alpha)(\alpha+\gamma)t}. \end{aligned}$$

Remark 3.2 (a) Theorem 3.2 gives an alternative way for solving the Fokker-Planck operator with the mixed eigenvalue spectrum of [31]. Furthermore, Theorem 3.2 can also be applied to solve the problem of the Fokker-Planck equation and Kramers' reaction rate theory [15].

(b) The FPE is also applicable to some advection-diffusion equations. As an example, we consider the advection-diffusion of the transport equation of open channels and river flows [32]

$$\frac{\partial C}{\partial t} = -U\frac{\partial C}{\partial x} + \frac{1}{A}\frac{\partial}{\partial x}\left(KA\frac{\partial C}{\partial x} \right). \tag{31}$$

Equation (31) describes the evolution of contaminant concentration $C(x,t)$ in a one-dimensional flow in a channel of cross-sectional area $A(x,t)$, with a mean flow velocity $U(x,t)$ and a diffusion coefficient $K(x,t)$. In cases where U and K depend only on x and A is a constant, equation (31) is the backward Kolmogorov equation with the drift coefficient $f(x) = \frac{\partial K}{\partial x} - U(x)$ and the diffusion coefficient $D(x) = 2K(x)$. Therefore, the methods used in the previous sections can be implemented to solve the equation.

(c) The FPE can also be used to solve the advection diffusion equation of larval dispersal alongshore [24]

$$\frac{\partial C}{\partial t} = -\frac{\partial}{\partial x}\left(U(x,t)C - K(x,t)\frac{\partial C}{\partial x} \right) + g(x,t), \tag{32}$$

where $C(x,t)$ is larval concentration at alongshore position x and time t, $U(x,t)$ is the mean advection velocity on a given time interval, $K(x,t)$ is the local dispersion coefficient and $g(x,t)$ is the 'reaction' term, which represents a source or sink. We see that equation (32) is the nonhomogenous perturbated backward Kolmogorov equation with the drift coefficient $f(x,t) = \frac{\partial K}{\partial x} - U$, the diffusion coefficient $D(x,t) = 2K(x,t)$ and the perturbation coefficient $-\frac{\partial U}{\partial x}$. Thus, the solution method for the FPE together with the Duhamel principle gives the solution of (32).

4 Conclusion

A semigroup approach is applicable for the Fokker-Planck equation with the drift and diffusion coefficients of a space variable. The stationary solution u_s of the FPE inducted a Hilbert space $X = L^2(a,b)$ with an inner product weighted by u_s. The corresponding backward Fokker-Planck operator A generates a C_0-semigroup $T(t)$ in X. The well-posedness of the Fokker-Planck equation follows the well-posedness of the Cauchy problem generated by A. The solution u of the FPE is asymptotically stable with respect to u_s as $t \to \infty$. As an application, the backward Fokker-Planck operator A confirms the well-posedness of product function equations.

Acknowledgements
The authors would like to thank the referees for valuable comments improving this paper and Sebelas Maret University for supporting and funding through Fundamental Research under Grant No.194.2/UN27.22/PT.01.03/2024.

References

[1] D. Liberzon and R.W. Brockett. Spectral analysis of Fokker-Planck and related operators arising from linear stochastic differential equations. *SIAM J. Control Optim.* **38** (5) (2000) 1453—1467.

[2] G.A. Pavliotis. *Stochastic Processes and Applications.* Springer Science Business Media, New York, 2014.

[3] T. Breiten, K. Kunisch and K. Pfeiffer. Control strategies for the Fokker-Planck equation. *ESAIM: Control Optim. Calc. Var.* **24** (2) (2018) 741-–763.

[4] J.M. Heninger, D. Lippolis and P. Cvitanović. Perturbation theory for the Fokker-Planck operator in chaos. *Commun. Nonlinear Sci. Numer. Simul.* **55** (2018) 16–28.

[5] J. Chandrasegaran and P. Sharma. A Short Review on Fokker-Planck equations, entropy production and entropy generation. *Bioinfo. Proteom. Img. Anal.* **4** (1) (2020) 21–24.

[6] U. Lucia. Entropy generation and the Fokker–Planck equation. *Physica A* **393** (2014) 256-–260.

[7] T. Tome. Entropy production in nonequilibrium systems described by a Fokker-Planck equation. *Braz. J. Phys.* **36** (4A) (2006) 1285–1289.

[8] F. Flandoli, M. Leocata and C. Ricci. The Navier–Stokes–Vlasov–Fokker–Planck system as a scaling limit of particles in a fluid. *J. Math. Fluid Mech.* (2021) 23-–40.

[9] A.G. Peeters and D. Strintzi. The Fokker-Planck equation, and its application in plasma physics. *Ann. Phys.* **17** (2-3) (2008) 142—157.

[10] L. Philipp and B.D. Shizgal. A pseudospectral solution of a bistable Fokker–Planck equation that models protein folding. *Physica A* **522** (2019) 158—166.

[11] G.W. Bluman. Similarity solutions of the one-dimensional Fokker-Planck equation. *Int. J. Non Linear Mech.* **6** (1971) 143–153.

[12] M.A. Peletier and D.R.M. Renger. Variational formulation of the Fokker-Planck equation with decay: a particle approach. *Commun. Contemp. Math.* **15** (5) (2013) 1350017.

[13] F. Guarnieri, W. Moon and J.S. Wettlaufer. Solution of the Fokker-Planck equation with a logarithmic potential and mixed eigenvalue spectrum. *J. Math. Phys.* **58** (093301) (2017) 1–22.

[14] R. Novak and X.R. Wang. On the Kramers–Fokker–Planck equation with decreasing potentials in dimension one. *J. Spectr. Theory* **10** (1) (2020) 1–32.

[15] Y. Zhan and B.D. Shizgal. Diffusion in a bistable system: The eigenvalue spectrum of the Fokker-Planck operator and Kramers' reaction rate theory. *Phys. Rev. E* **99** (042101) (2019) 1–12.

[16] M. Dehghan and M. Tatari. The use of He's variational iteration method for solving a Fokker–Planck equation. *Phys. Scr.* **74** (2006) 310-–316.

[17] S. Hesam, A.R. Nazemi and A. Haghbin. Analytical solution for the Fokker–Planck equation by differential transform method. *Sci. Iran. B* **19** (4) (2012) 1140—1145.

[18] M. Lakestani and M. Dehghan. Numerical solution of Fokker-Planck equation using the cubic B-spline scaling functions. *Numer. Methods Partial Differ. Equ.* **25** (2009) 418-–429.

[19] M. Tatari, M. Dehghan and M. Razzaghi. Application of the Adomian decomposition method for the Fokker–Planck equation. *Math. Comput. Model.* **45** (2007) 639-–650.

[20] A. Yildrim. Application of the homotopy perturbation method for the Fokker–Planck equation. *Int. J. Numer. Meth. Biomed. Eng.* **26** (2010) 1144-–1154.

[21] H. Risken. *The Fokker–Planck Equation Method of Solution and Applications*. Springer Verlag, Berlin, 1989.

[22] A. Friedman. *Partial Differential Equations of Parabolic Type*. Robert E. Krieger Publishing Company, Floria, 1983.

[23] C. Chilarescu and N. Vaneecloo. A Stochastic approach to the Cobb-Douglas production function. *Econ. Bull.* **3** (9) (2007) 1–9.

[24] J.L. Largier. Conssierations in estimating larval dispersial distances from oceanographic data. *Ecol. Appl.* **13** (1) (2003) S71-–S89.

[25] R. Curtain and H. Zwart. *An introdution to Infinite-Dimensional Linear System Theory*. Springer-Verlag, New York, 1995.

[26] C.V. Pao. *Nonlinear Parabolic and Elliptic Equations*. Plenum Press C.V, New York, 1992.

[27] I. Karatzas and S. Shreve. *Brownian Motion and Stochastic Calculus*. Springer-Verlag, Berlin, 1991.

[28] R.T. Lewis. The Discreteness of the spectrum of self-adjoint, even order, one-term, differential operators. *Proc. Am. Math. Soc.* **42** (2) (1974) 480–482.

[29] S. Sutrima, M. Mardiyana, R. Setiyowati and R. Respatiwulan. A new approach on the well-posedness of nonautonomous Cauhy problems: An application in population growth. *J. Nonlinear Funct. Anal.* **2021** (2021), Article ID 29.

[30] A.C. McBride. *Semigroups of Linear Operators: An Introduction*. John Wiley& Sons, Inc., New York, 1987

[31] M. Brics, J. Kaupuž and R. Mahnke. How to solve Fokker-Planck equation treating mixed eigenvalue spectrum?. *Condens. Matter Phys.* **16** (1) (2013) 1–13.

[32] B.H. Devkota and J. Imberger. Lagrangian modeling of advection-diffusion transport in open channel flow. *Water Resour. Res.* **45** (12406) (2009), doi:10.1029/2009WR008364.

Nonlinear Dynamics and Systems Theory, **25** (6) (2025) 705–708

Contents of Volume 25, 2025

Volume 25 **Number 1** **2025**

Volume 25 **Number 2** **2025**

WORLD SCIENTIFIC PUBLISHING

Series on Advances in Mathematics for Applied Sciences - Vol 96

Integral Methods in Nonlinear Dynamics of Systems
by
Anatoliy A. Martynyuk *(S. P. Timoshenko Institute of Mechanics, Ukraine)*

This monograph presents an integral method for analyzing the dynamic behavior of nonlinear non-stationary and controlled systems. The method is based on the application of nonlinear integral inequalities in obtaining new estimates for the norms of solutions and Lyapunov functions on solutions of the corresponding systems of differential equations of perturbed motion. The monograph consists of a preface, seven chapters, two appendices, a bibliography, and a subject index.

CONTENTS

Integral Methods in Nonlinear Dynamics of Systems have significant potential for application in pure and applied mathematics, applied physics, and by industrial engineers, operations researchers, and undergraduate and graduate students studying ordinary differential equations, polynomial equations, affine systems and equations with fractional-like derivatives of the state vector, time-scale equations, generalized Richardson arms race models, and their applications**.**

272 pp. December 2025, 978-981-98-1799-3 (hardback) - US$88 / £80,
978-981-98-1800-6 (eBook for institution) - US$141 / £130,
978-981-98-1801-3 (eBook for individual) - US$70 / £65

NAUKOVA DUMKA

MATRIX METHODS FOR THE ANALYSIS AND SYNTHESIS OF DYNAMICAL SYSTEMS

Kyiv: Naukova dumka, 2023, 320 pp. [Ukrainian]
ISBN 978-966-00-1892-1
https://doi.org/10.37863/6103136622-55

A. G. Mazko

Institute of Mathematics, National Academy of Sciences of Ukraine, Kyiv, Ukraine

The book outlines constructive methods for the analysis and synthesis of dynamical systems based on the application of matrix equations and inequalities. The generalizations of the Lyapunov equation are presented in the framework of stability and spectrum localization theory of linear systems. Classical methods for motion stability analysis, modern methods for robust stabilization and optimization of dynamical systems, as well as new approaches to solving generalized H_∞-control problems for continuous and discrete time systems with controllable and observable outputs are presented. Algorithms for estimating and minimizing the weighted damping level of bounded perturbations in standard and descriptor control systems are proposed. The stability theory of positive and monotone dynamical systems is developed. The book is intended for scientists, engineers, PhD students and senior students of the corresponding specialties.

CONTENTS (8 chapters):

For more information please check:
https://imath.kiev.ua/monographs/?id=4
https://imath.kiev.ua/monographs/4/monograph.pdf
Contents & Abstract (pdf)